METEOR -Berichte

The Benguela System under climate change Effects of variability in physical forcing on carbon and oxygen budgets

Cruise No. M157

04.08.2019 – 16.09.2019
Mindelo (Cape Verde) – Walvis Bay (Namibia)
BUSUC 1

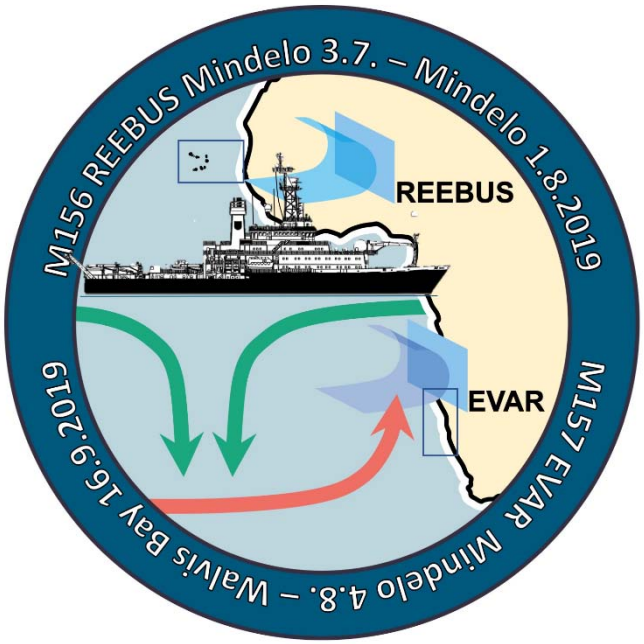

Matthias Zabel, Volker Mohrholz, Heide Schulz-Vogt, Stefan Sommer, Michael Zettler

Chief Scientist: Matthias Zabel
MARUM – Center for Marine Environmental Sciences

2019

Table of Contents

1 Cruise Summary ... 3
1.1 Summary in English ... 3
1.2 Zusammenfassung ... 3
2 Participants ... 4
2.1 Principal Investigators ... 4
2.2 Scientific Party ... 4
2.3 Participating Institutions ... 5
3 Research Program ... 5
3.1 Description of the Work Area ... 5
3.2 Aims of the Cruise ... 6
3.2 Agenda of the Cruise ... 7
4 Narrative of the Cruise ... 9
5 Preliminary Results ... 11
5.1 Environmental Chemistry ... 11
5.2 Hydrography ... 12
5.3 Marine Chemistry ... 22
5.4 Microbial Ecology ... 27
5.5 Geomicrobiology ... 32
5.6 Macrobenthic Ecology ... 35
5.7 In Situ Flux Measurements and Experiments ... 38
5.8 Sediment Geochemistry ... 43
6 Ship's Meteorological Station ... 46
7 Station List M157 ... 48
8 Data and Sample Storage and Availability ... 56
9 Acknowledgements ... 56
10 References ... 57
11 Abbreviations ... 58

1 Cruise Summary

1.1 Summary in English

R/V METEOR expedition M157 was directly connected with the collaborative research project EVAR (*The Benguela Upwelling System under Climate Change – Effects of Variability in Physical Forcing on Carbon and Oxygen Budgets*), which is funded by the Ministry of Education and Research (BMBF). The major goal of this expedition was to obtain high-resolution data and samples from shelf and upper slope to document and to understand the variability of the geochemical environment and the present day physical forcing of the Benguela Upwelling System (BUS). For this purpose, comprehensive, multidisciplinary investigations were conducted along three transects perpendicular to the coast of Namibia at about 17,3°S, 23°S and 25°S. The work concentrated in particular on four selected locations, two on each of the southern transects, at which almost all devices could be deployed and all planned measuring methods and sub-sampling could be carried out. This program was complemented by comparative studies at numerous other stations along the three transects, as well as profiling measurements in the water column between all stations and on the transit from Cape Verde Islands to the working area. The geochemical measurements showed that, as expected at this time of year, the oxygen content in the bottom water was not completely depleted. A total of 330 deployments of different devices at 49 individual stations with water depth between 32 m and 2078 m were used to collect and gained extremely valuable samples and sensor data.

1.2 Zusammenfassung

Die FS METEOR-Expedition M157 stand in direktem Zusammenhang mit dem Verbundforschungsprojekt EVAR (*The Benguela Upwelling System under Climate Change - Effects of Variability in Physical Forcing on Carbon and Oxygen Budgets*), das vom Bundesministerium für Bildung und Forschung (BMBF) finanziert wird. Das Hauptziel dieser Expedition war es, hochauflösende Daten und Proben von Schelf und oberem Hang zu erhalten, um die Variabilität der geochemischen Umweltbedingungen und den heutigen physikalischen Antrieb des Benguela-Auftriebssystems (BUS) zu dokumentieren und zu verstehen. Zu diesem Zweck wurden umfassende, multidisziplinäre Untersuchungen entlang dreier Transekte senkrecht zur Küste Namibias auf etwa 17,3°S, 23°S und 25°S durchgeführt. Die Arbeiten konzentrierten sich insbesondere auf vier ausgewählte Standorte, je zwei auf beiden südlichen Schnitte, an denen fast alle Geräte eingesetzt und alle geplanten Messmethoden durchgeführt und alle Unterproben genommen werden konnten. Ergänzt wurde dieses Programm durch vergleichende Studien an zahlreichen anderen Stationen entlang der genannten Transekte sowie durch Profilmessungen in der Wassersäule zwischen allen Stationen und auf der Anreise von den Kapverdischen Inseln in das Arbeitsgebiet. Die geochemischen Messungen zeigten, dass der Sauerstoffgehalt im Bodenwasser, wie zu dieser Jahreszeit erwartet, nicht vollständig erschöpft war. Insgesamt 330 Einsätze verschiedener Geräte an 49 Einzelstationen mit Wassertiefen zwischen 32 und 2078 m wurden zur Gewinnung äußerst wertvoller Proben und Messdaten eingesetzt.

2 Participants

2.1 Principal Investigators

Name	Institution
Mohrholz, Volker, Dr.	IOW
Schulz-Vogt, Heide, Prof.	IOW
Sommer, Stefan, Dr.	GEOMAR
Zabel, Matthias, Dr.	MARUM
Zettler, Michael, Dr.	IOW

2.2 Scientific Party

Name	Discipline	Institution
Amorim, Katherine [B]	Biological Oceanography	IOW
Anderson, Chloe, Dr. [B]	Sediment Geochemistry	MARUM
Beck, Antje [B]	Technician	GEOMAR
Beier, Sebastian [B]	Technician	IOW
Burmeister, Christian [A+B]	Technician	IOW
Dangl, Gabriela [B]	Biological Oceanography	IOW
Fabian, Jenny, Dr. [B]	Biological Oceanography	IOW
Glockzin, Michael [A+B]	Technician	IOW
Heene, Toralf [B]	Technician	IOW
Herrán, Natalia, Dr. [B]	Physical Oceanography	IOW
Kolbe, Martin [A+B]	Technician	IOW
Kossak, Michael [B]	Sediment Geochemistry	MARUM
Langeloh, Hendrik [B]	Technician	IOW
Meckelnburg, Isabelle [B]	Technician	GEOMAR
Meeske, Christian [B]	Technician	IOW
Mohrholz, Volker, Dr. [A+B]	Physical Oceanography	IOW
Otto, Stefan, Dr. [A+B]	Technician	IOW
Nolte, Gabriel [B]	Technician	GEOMAR
Sabbaghzadeh, Bita, Dr. [A+B]	Marine Chemistry	IOW
Scholz, Florian, Dr. [B]	Sediment Geochemistry	GEOMAR
Schulz-Vogt, Heide, Prof. [B]	Biological Oceanography	IOW
Sommer, Stefan, Dr. [B]	Marine Biogeochemistry	GEOMAR
Stelzner, Martin [A+B]	Technician	DWD
Tambo, Munyaradzi, Dr. [B]	Geomicrobiology	IOW
Tewes, Simon [A]	Oceanography	BSH
Türk, Matthias [B]	Engineer	GEOMAR
Wäge, Janine, Dr. [B]	Microbial Ecology	IOW
Wiezoreck, Marco [A]	Chemistry	MPI-C
Zabel, Matthias, Dr. [B]	Sediment Geochem. / Chief Scientist	MARUM

Name	Discipline	Institution
Zettler, Michael, Dr. [B]	Biological Oceanography	IOW

A – Leg/Transit 04.-18.08.2019; B – Leg 18.08.-16.09.2019

2.3 Participating Institutions

BSH	Bundesanstalt für Seeschifffahrt und Hydrographie Hamburg
DWD	Deutscher Wetterdienst, Geschäftsfeld Seeschifffahrt
GEOMAR	Helmholtz-Zentrum für Ozeanforschung Kiel
IOW	Leibniz-Institut für Ostseeforschung Warnemünde
MARUM	Zentrum für Marine Umweltwissenschaften, Universität Bremen
MPI-C	Max-Planck-Institut für Chemie Mainz

3 Research Program

3.1 Description of the Work Area

The Benguela Upwellig System (BUS) belongs to the eastern boundary current systems, which are among the most productive areas of the world`s oceans. It is driven by upwelling of nutrient-rich intermediate waters as a result of atmospheric forcing and oceanographic circulation. Yet, upwelling intensity is not constant, and can vary on time scales from days to millennia. In the northern BUS a number of high quality field data and time series are available from recent research projects (NAMIBGAS, GENUS, SACUS, PREFACE) and the environmental monitoring of the Ministry of Fisheries and Marine Resources of Namibia. Based on the available data, that also display decadal variability, a significant long-term trend in upwelling intensity cannot be detected (Junker et al., 2017). Accordingly, the Bakun hypothesis of intensification of upwelling with global warming (Bakun, 1990) has not been verified for the BUS so far (Rykaczewski et al., 2015). However, paleo-studies based on sediment archives indicate that the productivity in the BUS has been subject to strong fluctuations in the geological past (Little et al., 1997).

It is well-recognized that the feedback of benthic and pelagic communities to upwelling variability can lead to changes in extent and intensity of oxygen minimum zones (OMZ). Benthic communities further control the burial of detritus sinking to the seafloor and the flux of dissolved and gaseous compounds across the sediment water interface. In the BUS, the benthic contribution to the pelagic nutrient budget is considered to be of local or temporal importance only (Neumann et al., 2016). However, this assessment is based on diffusive fluxes determined ex situ from pore water profiles during low upwelling intensity. Studies in other upwelling areas instead show that total fluxes determined in situ using flux chambers can greatly exceed diffusive fluxes (e.g. Noffke et al., 2012) and are further modulated by seasonal variability of bottom water redox conditions (e.g. Sommer et al., 2016). A systematic investigation of benthic fluxes as a function of bottom water redox-variability is so far lacking for the BUS. Upwelling also fosters the release of the greenhouse gases methane, nitrous oxide and carbon dioxide to the atmosphere. Several investigations have addressed methane biogeochemistry in the BUS, in particular on the shelf, mostly due to “gas eruptions” or sulfidic events that frequently occur in the late summer (Emeis et al., 2004). In contrast, the exact nature of the interaction between microbial nitrous oxide production and the variability of oxygen and sulfide distribution has not been investigated so far.

The collaborative BMBF project EVAR pursues three very interdependent goals: a) to decipher the interrelationships between macrobenthic diversity and microbial transformation processes in the

water column and in surface sediments as a function of the environmental conditions (i.e. oxic-suboxic-anoxic-sulfidic), b) to identify indicators of paleo-anoxia in sediment archives for assessing past variability in upwelling intensity, and c) to develop a comprehensive coupled, regional ecosystem model on the basis of our new analytical and experimental results to allow reliable predictions of future scenarios of OMZ intensity and extent. Through an innovative multi-disciplinary approach, EVAR will in particular gain new information on specific, essential processes such as the plasticity and feedback mechanisms of macrobenthic and microbiological communities to fluctuations in oxygen, sulfide and nutrient concentrations. EVAR will identify crucial parameters and concentrations that most likely dictate tipping points with positive or negative feedback for OMZ intensity such as the release of N_2O to the atmosphere, build up of toxic sulfide concentrations in the water column as well as the detoxification potential of microbial communities, extinction of benthic macro-organisms and decline of bioturbation.

3.2 Aims of the Cruise

The major goal of this expedition, and a second cruise within the EVAR project scheduled in spring 2021, was to obtain high-resolution data and samples to document and to understand the variability of the geochemical environment and the present day physical forcing of the Benguela Upwelling System (BUS). For this purpose, comprehensive, multidisciplinary investigations were conducted along three transects perpendicular to the coast of Namibia at about 17,3°S, 23°S and 25°S. The work concentrated in particular on 4 selected locations at which all planned measuring methods and sampling could be carried out. This program was complemented by comparative studies at numerous other stations along the mentioned transects, as well as profiling measurements in the water column between all stations. Specific aims of the different working groups were as follows:

Hydrographic Regime

- Detection of short term upwelling peaks by recording standard hydrographic parameters
- Exchange the long-term mooring at 23°S and deployment of similar sensors at 25°S

Assessing variability in past upwelling intensity

- Recovering of high resolution sediment archives to investigate the history of geochemical environmental conditions during the Holocene

Fluxes and turnover in response to variable redox conditions

- Estimate the pelagic microbial potential to react towards changes in abiotic parameters such as a sudden increase in sulfide or decrease in oxygen, and how this is related to trace gas production and sulfide oxidation. Identification of specific biogeochemical transformation zones and the involved microbial key organisms. Investigation of the effect of sulfide accumulation in the water column on the phosphorus cycling.
- Elucidation of the magnitude and pathways of benthic fluxes of nutrient (N-species, phosphate, Fe), dissolved gases (CH_4, $_pCO_2$, N_2/Ar) as well as dissolved inorganic carbon (DIC), sulfide and silicate in response to fluctuating and shifting regimes of the bottom water availability of O_2 and NO_3^-. Determine microbial controls and tipping points of the sequestration and release of phosphate, as well as of the benthic N and S cycling. Investigation of the tolerance of distinct microbenthic species to oxygen availability

- Determination of the timing and magnitude of sulfidic events after stepwise depletion of O_2 and NO_3^- in the bottom water
- Determination of the contribution of the macro- and microbenthic communities to the overall solute turnover in sediments at the upper and lower boundary of the OMZ

Trace gases

- Determination of sea surface concentration and fluxes of trace gases and relation to upwelling intensity and chemical physicochemical signature of the feed waters. Linking trace gas transformations to the microbial key players. Determination of the key depth horizons and processes for trace gas transformations and sensitivity of the underlying processes to variations in redox conditions (O_2 and H_2S levels).

3.3 Agenda of the Cruise

Figure 3.1 shows the detailed station map and the route of the cruise. Additionally to the program on the three transects at 25°S, 23°S and 17,3°S water column profiling with different sensors was done on some sites along the 18°S latitude, which are regularly measured by the Namibian partner institute (NatMIRC) as part of a joint monitoring program.

The time and work planning of the proposal did not include a very long transit to the actual work area. In addition to preparatory work, the transit could also be used for important, additional measurements. These include, among others, continuous, on-the-go measurements of the concentration of various trace gases in surface water, or the measurement of persistent organic pollutants (POPs) in the atmosphere.

Within the working area, the unexpected, extremely soft, not to say soupy consistency of the surface sediments within the coastal mud belt, which initially presented us with greater difficulties. Especially the multicorer, but also the core catcher of the gravity corer and the bottom water trace profiler had to be modified several times to ensure the ultimately very successful sampling.

Due to the very high suspension load close to the seafloor, the planned use of the Ocean Floor Observation System (OFOS) for visual examination of the seafloor to find the most promising sites for the benthic lander deployments proved to be useless. In addition, no significant structures, such as bacterial mats, could be observed during the only 3, instead of at least 5 OFOS missions as planned. In the end, we based our choice of stations mainly on the sampling scheme of the NatMIRC monitoring program. This also ensured that our measurement results from the water column can be integrated into the corresponding long-term data sets.

In general, this cruise made very high demands on the timing of the equipment deployment. For example, contamination of the water column with sediment particles had to be prevented. Due to the usually very shallow water depth and the resulting high frequency of sample collection and the time required to process the samples, many stations had to be visited several times. This was especially true for the stations where the benthic landing systems were used (see below).

A major difference compared to the previous planning concerned the time requirements of the two Biogeochemical Observatories (lander systems) BIGO-1/-2. The complicated preparation of the instruments required that this work, the deployments and recoveries should be carried out in daylight only. Additionally, the necessary processing of the samples obtained forced the deployment of the systems on different consecutive days. The conception of the in-situ measurements and experiments required several missions of the systems at all of the so-called main stations, where also all other devices were used and profiling measurements were carried out. This meant that the ship has to go at

all respective stations 4 times within 7 days, a very time-limited procedure with an unexpected large number of transits. Consequently, the observatories could only be used at 4 instead of 5 stations and there only with 2 instead of 3 missions, an inevitability which could have been taken into account when planning the expedition with a better exchange of information between the working groups. All these constraints allowed only 8 of the 15 initially planned deployments could be conducted within the 28 days of the cruise. On the other hand, it were precisely the relatively short transits between stations, that brought some necessary recovery for the whole crew in the densely and ambitiously packed work program. Nevertheless, on the second EVAR expedition, a significant optimization of these critical points should be implemented. One aim here is to ensure that work with the BIGO systems can also take place during night times. In the same context, the frequent repositioning of the wires, particularly with regard to telemetry (necessary for the launcher, but to be disconnected for the GCs), meant that deployments of the gravity corer had be carried out in very small time frames, which, with a limited number of scientists, were actually too short for careful processing.

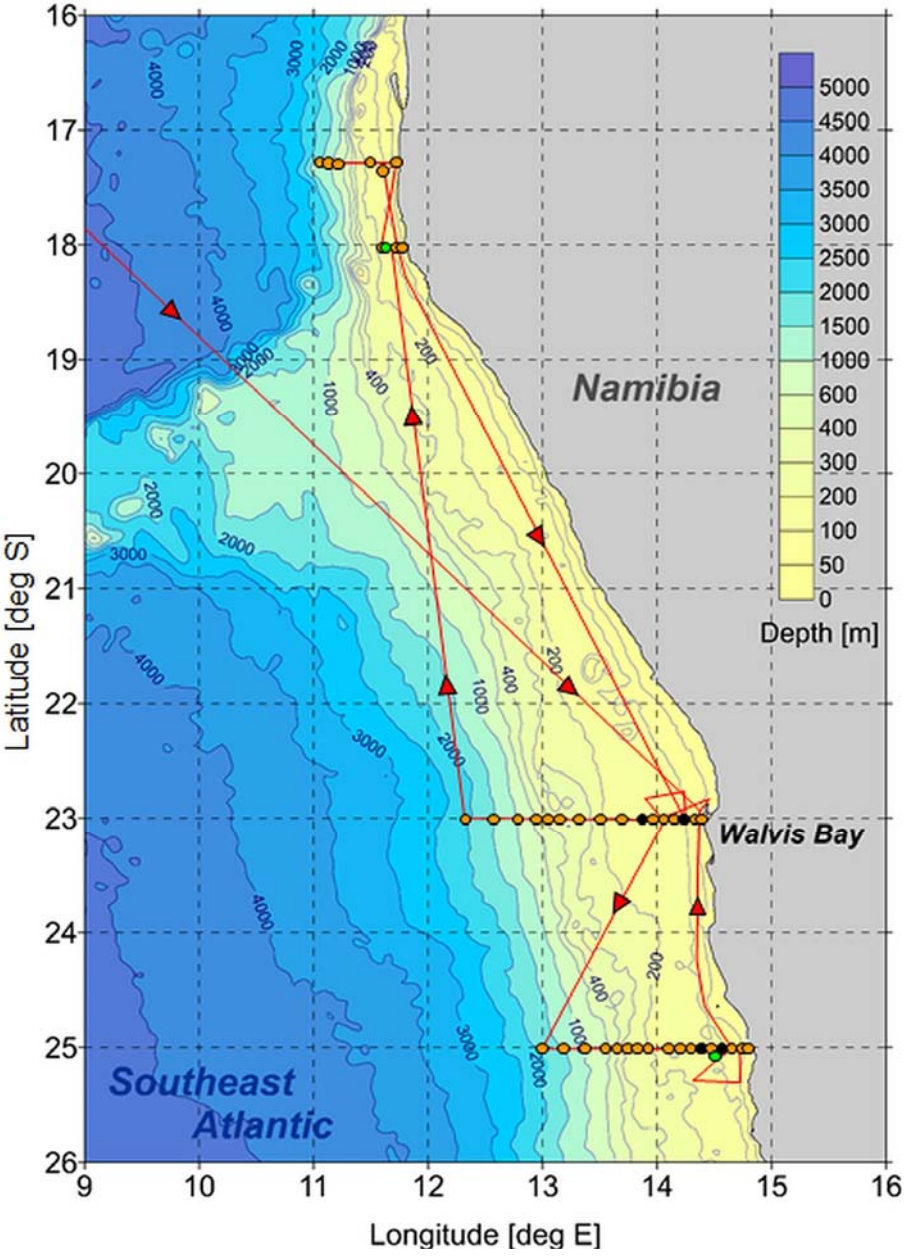

Fig. 3.1 Track chart of R/V METEOR Cruise M157 with locations of sampling along the three transects.

Furthermore, minor defects occurred, e.g. on the hose of the Pump CTD, or the sensors of the ScanFish. However, these could all be repaired with own resources in relatively short times, so that the number of uses of the affected devices was not significantly endangered. In the end there was only one total failure. Two drifters could not be used due to a non-functioning satellite connection.

In summary, some of our plans were too ambitious to be implemented 100% in the given time. However, thanks to the great mutual support of all groups involved and the excellent interaction with the ship's crew, so much new data were measured and valuable samples were obtained that this expedition can be described as very successful in terms of its objectives.

4 Narrative of the Cruise

The expedition M157 was divided into two parts. The official start was on August 8th with the departure from the port of Mindelo on the Cape Verde Islands. The scientific crew on the transit to the working area off Namibia consisted of 6 scientists from the Leibniz Institute for Baltic Sea Research Warnemünde (IOW) and two secondary users, one from the Federal Maritime and Hydrographic Agency (BSH) and one from the Max-Planck-Institute for Chemistry (MPI-C). The transit was interrupted only by a few short stops to test different instruments. The first 14 days were be used very effectively for unloading the scientific equipment, setting up the different laboratories and first test measurements, like on-the-go measurements of the flow field, surface water properties and trace substances as well as air pollutants. For the latter, concentration of persistent organic pollutants (POPs) was of particular interest. Despite their negative effects on the environment and human health, the proliferation of many of these pollutants is still insufficient or in areas far from primary sources almost not described at all in the literature. While valuable samples for the analysis of POPs were taken from the air and from the surface waters, the second, accompanying mission was unfortunately not successful. As the ordered Argo floats were not delivered in time to the Vessel in Mindelo, the floats could not be deployed as planned. On the morning of 18 August, the first transit leg of expedition M157 ended with the arrival of R/V METEOR at the port of Walvis Bay.

The two secondary users disembark and 22 scientific participants, mostly members of the EVAR cluster project, boarded. Unfortunately, none of the Namibian partners was able to participate in the cruise. At least one place was reserved until the last moment, but our hope was dashed just before the departure in the evening of August 18th. We are not aware of any reasons for the cancellations. According to our working plan in the proposal, investigations in the following four weeks concentrated on the coastal region off Namibia and here on three transects at 17.3°S, 23°S and 25°S respectively. Already 2 hours after leaving the port of Walvis Bay, the first profiling oceanographic measurements could be started along the 23°S transect. The excellent preparatory work during the transits from Mindelo to Walvis Bay for the laboratory setup and the instrumentation proved to be extremely important. In order to get a first impression of the current chemical and physical conditions in the water column, especially the distribution and concentration of oxygen, a towed measuring device (the so-called ScanFish) was used together with the vessel mounted ADCP 38kHz and 75kHz ocean surveyors along a profile lines from the coast line up to about 75 nautical miles offshore. At the same time, the ship's sediment acoustic systems were used to explore the bathymetry and the internal structure of the sediments on the seabed. The profiling observations with the ScanFish were supplemented by the multiple use of a profiler for turbulence and mixing study (MSS), which provided high-resolution measurements of the characteristics of the water mass structure. For the selection of the individual sampling locations, we followed the monitoring scheme of the National

Marine Information and Research Centre (NatMIRC) in Swakopmund. On the base of the new sensor data from the water column, locations were determined where we expect to gain the most promising results to answer our questions by using the other devices. The first successful sampling of the seabed surface by means of a large box grab was carried out in 2071 m water depth in the late evening of August 19. In rapid succession, we frequently used all our sampling devices. In addition, long-term measuring systems (moorings) placed on previous expeditions were recovered at two stations and one could be newly deployed. The different needs of the individual investigation devices and methods (e.g. clean ship during CTD operations), as well as the short distances between neighboring investigation stations (max. 20 nautical miles) required the repeated visiting of the individual stations.

In the night of August 28-29, the investigations on the 23°S transect were completed for the time being and the RV METEOR steamed to the northern section of the working area. In addition to standard measurements in the water column by CTD, MSS and an in situ absorption spectrophotometer (AC-S), as well as the exchange of an anchored oceanographic mooring, from August 30th onwards mainly sampling of the surface sediments with Dredge, Van-Veen-Grab, boxcorer and multicorer took place. The latter serve investigations on the species distribution of macro-benthos, which can be used among others as an indicator for the oxygen concentration in the bottom water. In the evening of September 1st we left the northern working area between 17.3°S and 18°S. On the transit to the transect at 25°S the vessel stopped for two more CTD missions about 10 and 20 nautical miles off Walvis Bay.

On the evening of 3 September, work began on the southern Transect at 25°S. We applied the same observation and sampling strategy, which was successful already along the 23°S transect, starting the measurements using CTD, AC-S and MSS and acoustic sediment observations from deeper waters to near the coast. Due to technical problems that could be solved later, a profile with the ScanFish could only be created 5 days later. The different requirements of the individual instrument operations, measurements and laboratory work required a high degree of flexibility for all participants also on this transect. After about 8.5 days, on the morning of September 12, the investigations in the southernmost working area were completed. One last time the 23°S transect was approached in order to obtain further sample material for incubation experiments at one station and to use the meanwhile repaired Pump-CTD at two other stations.

Despite the difficult conditions due to the very soft sediment surface in the area of the coastal mud belt (cf. 3.3), almost all planned samples could be obtained. In total, R/V METEOR expedition M157 covered 6,300 nautical miles, half of which was the transit from Mindelo to Walvis Bay. We were able to collect extremely valuable samples and measurement data at 49 individual stations and along different transit routes. 330 instrument operations were carried out in water depth between 32 and 2078 m.

On the morning of September 16 the cruise ended in Walvis Bay. As promised when applying for the work permit, a workshop was held at the NatMIRC on the following two days, where the first, preliminary results could be presented to Namibian colleagues and discussed with them.

5 Preliminary Results

5.1 Environmental Chemistry

(M. Wiezoreck)

During the transit from Mindelo to Walvis Bay air and surface water sample were taken in order to determine the concentration of persistent organic pollutants (POPs) on the Atlantic off the coast of West and Central Africa. This work was carried out as part of the ITTWIA project "Intercontinental transport of persistent organic pollutants from Western and Central Africa".

Despite their negative effects on the environment and human health, the proliferation of many of these pollutants is still insufficient or in areas far from primary sources almost not described at all in the literature. This campaign aims to determine the concentrations of these pollutants in the tropical Atlantic off the West and Central African coasts during the West African rainy season and the slash-and-burn season on agricultural land in Central Africa. In addition, the transatlantic transport of the substances was investigated by simultaneous sampling on the coast of French Guyana. Due to the trade winds in the tropics, air masses with the pollutants were transported from West and Central Africa to South America.

For this purpose, air samples were collected 24 hours a day using a high volume air sampler. In this collector, particles up to a size of 10 µm (PM_{10}) were collected separately on quartz fiber filters and the pollutants in the gas phase on two sequential polyurethane foams. In order to prevent contamination with exhaust gases from the own ship, the sample collector was set up in the front part of the ship on the 2nd deck, the so-called "heli deck", at the railing (see Fig. 5.1). The loaded samples were then wrapped in aluminium foil in the laboratory, minimizing any contamination, and stored in the refrigeration room at -20 °C. The offline analysis including extraction with organic solvent, purification and subsequent analysis with gas chromatography coupled to a mass spectrometer is currently done at the Research Centre for Toxic Compounds in the Environment in Brno (Czech Republic).

Pollutants in surface water were collected using a passive sampling device. Thin silicone rubber plates were continuously exposed to the surface water of the Atlantic Ocean. This passive sampling of POPs in surface water was running several days before the samples were collected and stored in the cold store at -20°C, minimizing any further contamination during packing. Also these samples were sent by air freight to the laboratory in Brno for further analysis.

Fig. 5.1.1 Marco Wietzoreck from MPI for Chemistry in Mainz exchanging the filter at the air sampler.

5.2 Hydrography

(V. Mohrholz, S. Beier, T. Heene, M. Kolbe)

The focus of hydrographic investigations during the cruise was on the impact of short term upwelling variability on oxygen and nutrient supply to the shelf, and on the response of primary production to short term upwelling peaks.

Standard hydrographic parameters were gathered with a Seabird CTD along three transects. The transects at 23°S and 25°S were be covered with 12-13 hydrographic stations each. The northernmost transect included 4 hydrographic stations. At stations deeper than 200 m a LADCP was be used at the CTD to obtain full depth current profiles. The along transect station distances range from 5 to 10 nm to resolve mesoscale structures. A microstructure profiler (MSS) was deployed after the CTD cast at all stations. The MSS provides data about diapycnal mixing and turbulent eddy diffusivity. In combination with high resolution profiles of oxygen and nutrients the MSS data allow the estimation of vertical fluxes. Since the CTD stations cannot resolve the expected spatial variability of phytoplankton distribution a towed undulating CTD (ScanFish) was deployed along the transects.

On the main stations the Pump-CTD was used to obtain nutrient profiles and biological sampling with high vertical resolution (see below). To relate the spatial distribution data gathered along the transects to the temporal change and evolution on a seasonal scale two long term moorings were deployed at 23°S and 25°S at about 20 nm off the coast. All hydrographic data are also used as background data in other EVAR subprojects, and as complementary data set in the Namibian environmental monitoring program, that samples the same cross shelf transects up to five times a year.

5.2.1 Equipment

CTD

The CTD-system "SBE 911plus" (SEABIRD-ELECTRONICS, USA) was used to measure the variables: pressure, temperature (2x SBE 3), conductivity (2x SBE 4), oxygen concentration (2x SBE 43), chlorophyll-a fluorescence (683nm), turbidity, PAR and SPAR. To minimize salinity spiking, temperature- (SBE 3), conductivity (SBE 4) and oxygen sensors (SBE 43) are arranged within a tube system, where seawater is pumped through with constant velocity. The CTD was equipped with a redundant sensor system sensor system for temperature, conductivity and oxygen. The temperature is given in ITS-90 temperature scale. Salinity is calculated from the Practical Salinity Scale (1978) equations. Fluorescence and turbidity are measured with a downward looking WET Labs fluorimeter. Pressure is determined with a Paroscientific Digiquartz pressure sensor.

Data were monitored during the casts and stored on hard disk with Seasave Version 7. For each station a configuration file (stationname.xmlcon) was written which contains the complete parameter set, especially sensor coefficients used for the conversion of raw data (frequencies) to standard output format.

Additionally, the CTD-probe was equipped with a Rosette water sampler with 21 Free Flow bottles of 10 l volume each. This design allows for closing of bottles automatically at predefined depths during down-casts. Closing depth and sensor values are aligned by appropriate choice of parameters of the CTD software generating the “bottle files”. The CTD was attached to winch 2 of the R/V METEOR.

Table 5.2.1 Type and serial numbers of mounted CTD sensors

Sensor	Type	SN	Last calibration
Pressure	Digiquartz	1072	10.10.2011
Temperature 0	SBE 3	4451	06.05.2019
Temperature 1	SBE 3	5261	06.05.2019
Conductivity 0	SBE 4	3722	06.05.2019
Conductivity 1	SBE 4	2936	06.05.2019
Oxygen 0	SBE 43	0644	15.06.2018
Oxygen 1	SBE 43	1732	15.11.2018
Chl-a fluorescence / Turbidity	WET Labs - FLNTURTD	3274	27.09.2013
PAR sensor	Biospherical Licor Chelsea	4381	06.09.1994
SPAR	SPAR/Surface Irradiance	6321	unknown

Pump-CTD

At the key stations a Pump-CTD system, equipped with a high pressure pump and connected to a special pump cable was used. The system based on a CTD "SBE 911 plus" (SEABIRD-ELECTRONICS, USA), measuring the parameters pressure, temperature, conductivity, and oxygen. The CTD-probe was mounted to a SeaBird Rosette water sampler with 7 Free Flow bottles (IOW/HydroBIOS) of 5 l volume, and 6 AFIS bottles. Data are monitored and stored to hard disk with Seasave software Version 7.

Water sampling is carried out with the 13 bottles and a continuous water stream of approximately 3,2 l per minute from the CTD through cable and winch into the analytics labs. The system consists of the submersible CTD-, Rosette-, pump probe unit, a special pump cable and a computer controlled winch. It allows the measurement of vertical profiles of the CTD parameters given above in combination with sophisticated online water sampling down to a depth of 400 m.

On 25.08. after the fourth deployment of the Pump-CTD the pump cable was damaged during the recovery of the device. The cable could be terminated again. The device was then used on the 25°S transect as planned.

ScanFish Towed CTD

High resolution hydrographic transects with the ScanFish towed CTD (SF) were performed along the cross shelf transects at 23°S, 17.3°S and 25°S.

The ScanFish consists of a Seabird 911+ CTD mounted on a wing shaped body undulating between sea surface and about 130 m depth when towed behind the ship. Additionally to the usual CTD sensors, the probe is equipped with sensors for dissolved oxygen concentration, turbidity and Chlorophyll-a fluorescence. The details of the used sensors are given in Table 5.2.2. Hydrographic data are transmitted via a multi-conductor cable and stored in the lab on a computer disc. The instrument was deployed over the stern of the ship. The cable was operated from a separate winch mounted at the aft deck. The cable is guided by a pulley block mounted below the A-crane. The A-crane will be used for deployment and recovery. The device is towed with 5-7 knots, the undulation depth is steered from the lab. Control commands are transmitted via the cable.

Due to failure of electrical wires in the ScanFish tow cable termination the SF transect at 23°S had to be untimely stopped before the end of the transect was reached. The same error occurred again during the following operation on the 18°S transect. This Transect was therefore also aborted

untimely. The cable was terminated again. The next operation on the 25°S transect could be carried out as planned.

Table 5.2.2 Type and serial numbers of CTD sensors mounted on ScanFish

Sensor	Type	SN	Last calibration
Pressure	Digiquartz	76058	11.10.2006
Temperature 0	SBE 3	5213	04.07.2018
Conductivity 0	SBE 4	4497	04.07.2018
Oxygen 0	SBE 43	0016	17.10.2018
Chl-a fluorescence / Turbidity	WET Labs - FLNTURTD	1223	10.12.2008

VMADCP's 38kHz and 76kHz

Two vessel mounted Acoustic Doppler Current Profilers (ADCP) Ocean Surveyor (frequencies 38 and 76 kHz, beam angle 30 deg), manufactured by RD-Instruments, were mounted downward looking at the ship hull. The data output of the ADCPs were merged online with the corresponding navigation data and stored on the hard disc using the program VMDAS. Current data are collected in beam coordinates to apply all corrections during post processing. The ADCPs were operated continuously during the entire cruise. Post-processing of the ADCP data was carried out using the Matlab® ADCP toolbox of IOW. The final profiles are 120 s and 300 s averages of the single ping profiles. At sections where bottom tracking was available the heading bias of the instrument was calculated. Heading bias and the local magnetic deviation were applied during post processing.

Moorings

During the cruise M157 the moorings of the Northern Benguela Mooring array were maintained. The array consists of three long term moorings at about 130 m depth along the northern Namibian shelf, and is operated in frame of the EVAR and BANINO projects in close collaboration with the NatMIRC institute, Swakopmund. The particular recovery and deployment times and positions of all moorings of the Northern Benguela Mooring array are summarized in Table 5.2.9.

Microstructure Profiler (MSS)

The MSS 90-S (Serial number 055) is an instrument for simultaneous microstructure and precision measurements of physical parameters in marine waters. The MSS profiler was equipped with 2 velocity microstructure shear sensors (for turbulence measurements), a microstructure temperature sensor, standard CTD sensors for precision measurements, a turbidity sensor, a micro oxygen optode and a vibration control sensor.

All sensors are mounted at the measuring head of the profiler, the microstructure ones being placed about 150 mm in front of the CTD sensors. The sampling rate for all sensors was 1024 samples per second. The profiler was balanced with negative buoyancy, which gave it a sinking velocity of about 0,6 m/s. It was deployed with a power block winch. The profiler was operated from the stern of R/V METEOR. Disturbing effects caused by cable tension (vibrations) and the ship's movement were excluded by a slack in the cable. After the deployment the sensors were flushed with pure water to prevent fouling.

The dissipation rate of turbulent kinetic energy was calculated by fitting the shear spectrum to the theoretical Nasmyth spectrum in a variable wave number range from 2 to maximum 30 cycles per

meter (cpm). The low wave number cut off at 2 cpm is to eliminate contributions from low frequent tumbling motions of the profiler. The MSS sensors were calibrated before the cruise in the IOW calibration lab.

During the cruise an in situ calibration of the MSS was performed on CTD profile 34H01. The calculated slope and offset of particular MSS sensors are given in Table 5.2.3.

Table 5.2.3 Calibration coefficients for particular MSS sensors.

MSS sensor	Slope	Offset
Temperature PT100	1.0024	-0.032814 K
Temperature NTC	1.0025	-0.022688 K
Conductivity	1.0032	-0.18243 mS/cm
Fast Oxygen optode	1.031	-9.4401 µmol/kg

TRIOS Radiation Measurement System

During the entire cruise a TRIOS radiation measurement system was used to gather reflectance data. The system was mounted at the bow of the ship. It consists of three spectrometers measuring the incoming global radiation, the forward incoming radiation and the reflectance of the sea surface. The data are stored in an ACCESS data base. No additional validation or preprocessing was performed during the cruise.

Underway Measurements

The R/V METEOR is equipped with numerous sensors, which continuously provide important environmental and navigation parameters. The available data set consists of weather parameters, surface water properties, navigation information, rope length, winch speed and more. The data are collected by a data acquisition system DSHIP3 manufactured by WERUM. All data are stored in a data base and can be extracted by a web interface. A description of all collected parameters is given in the ship specific DSHIP3 manual. All data are snapshots taken and stored every second. After the cruise the full data set was extracted. During the cruise a subset of the parameters was processed.

5.2.2 Preliminary Results

The results presented in the following section are preliminary and not comprehensive, since they are based in most cases on unevaluated raw data! The aim of this section is to give a first impression on the collected data set, using the examples of the equatorial transect and the Walvis Bay transect. An advanced data analysis will follow after all validated data sets are available.

Sea Surface Temperature and Salinity

Sea surface temperature and surface salinity distributions in the investigation area were compiled from data gathered with the ships thermosalinograph. The distributions shown in Fig are based on unvalidated data. The SST was between 12 and 16°C, according to the season. The cold temperatures on the coast at Walvis Bay and at 25°S are an indicator for upwelling water. The SSS shows an analogous distribution to the SST with low salinity in the upwelling water and higher salinity in the north of the study area.

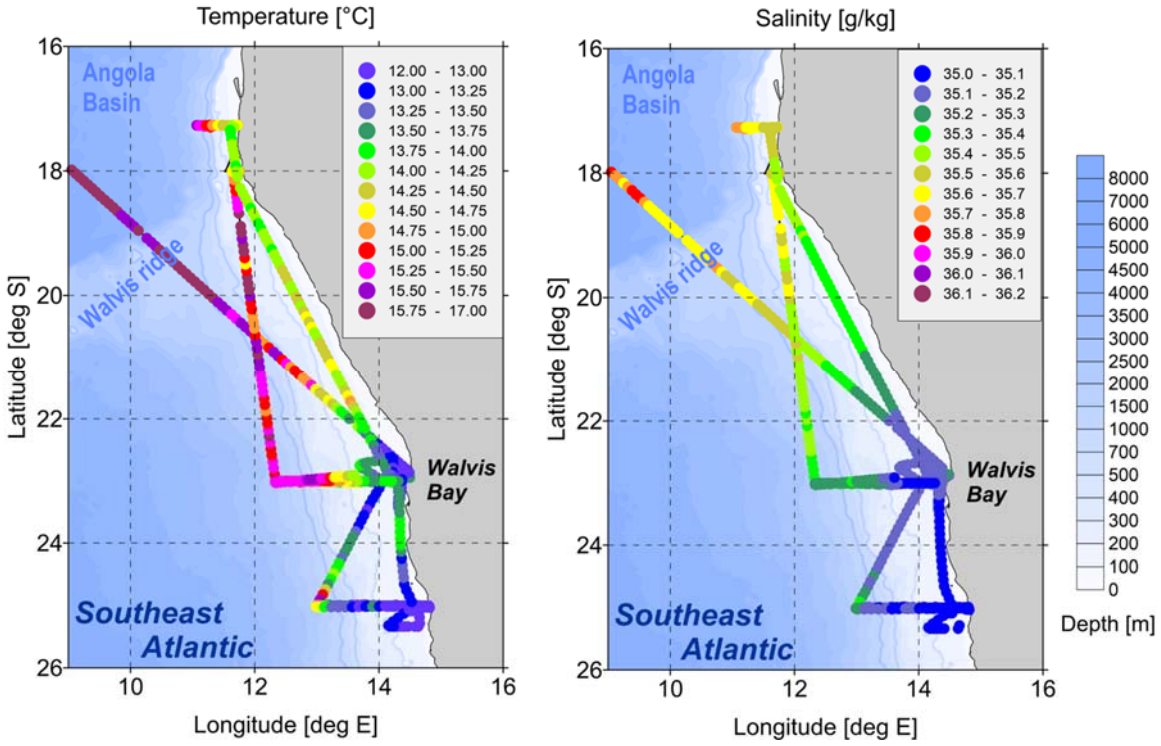

Fig. 5.2.1 Surface temperature (left) and surface salinity distribution (right) along the cruise track of M157 (30 min averaged values).

Equatorial Transect

On the transit from Mindelo to Walvis Bay only a station for device tests was performed. The observations along the transect were made with both VMADCP's and the ship thermosalinograph. The transect crossed the equatorial current system and the Angola Basin and supplied information about the current field for the upper 800 m.

The area north of 7°S is controlled by the equatorial current system. The most intensive eastward directed current is the equatorial under current (EUC) at the equator (Fig). The EUC is accompanied by several zonal current bands, namely the south equatorial under current (SEUC) at 2°S and the south equatorial counter current (SECC) near 5°S. Between the EUC and the SECC the westward flowing south equatorial current (SEC) is embedded. The meridional currents in the equatorial area were mainly northward directed and depicted a lower intensity (Fig. 5.2.3).

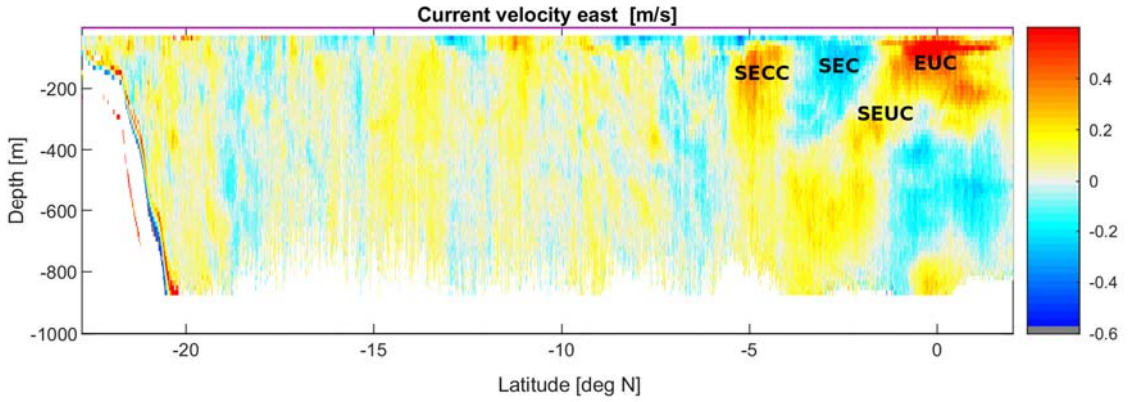

Fig. 5.2.2 East component of current velocity along the equatorial transect of the cruise M157. The data were gathered with the 38kHz Vessel mounted ADCP (8.08. – 17.08.2019). The abbreviations indicate zonal components of the equatorial current system.

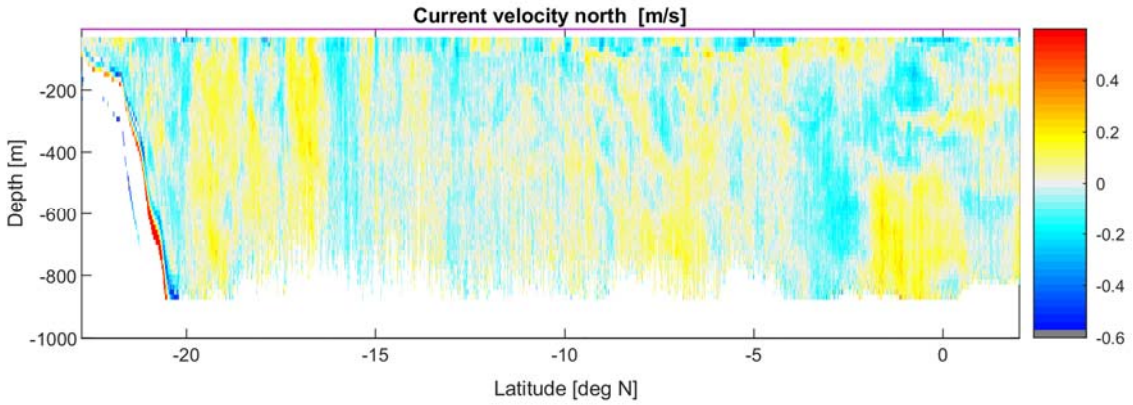

Fig. 5.2.3 North component of current velocity along the equatorial transect of the cruise M157. The data were gathered with the 38kHz Vessel mounted ADCP (8.08. – 17.08.2019).

In the Angola Gyre between 7°S to about 16°S the currents in the upper ocean are generally weak. This causes a long residence time of central water in the area and weak lateral ventilation. At the continental slope off southwest Africa weak southward directed currents were observed.

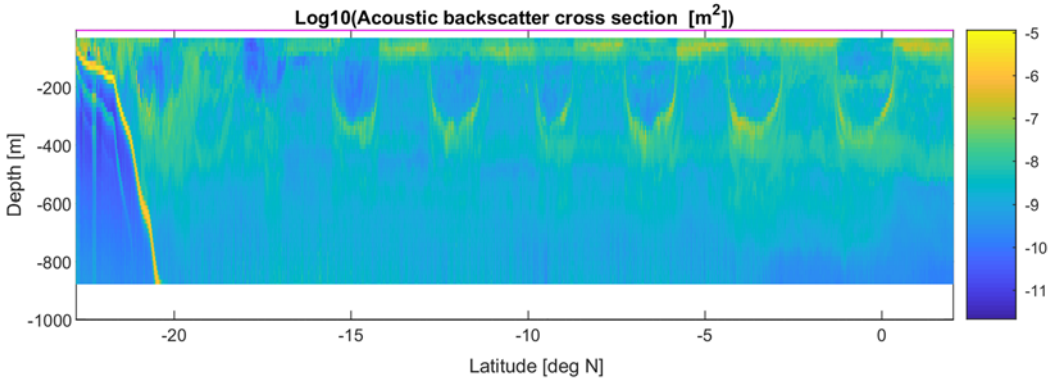

Fig. 5.2.4 Patterns of acoustic backscatter cross section along the equatorial transect of the cruise M157. The data were gathered with the 38kHz Vessel mounted ADCP (8.08. – 17.08.2019).

Additionally to the current velocity, the backscattering signal of the vessel mounted ADCPs provided an indirect measure of the vertical zooplankton distribution. Along the tropical part transect, north of 17°S, a pronounced signal diurnal vertical migration of zooplankton was observed. The timing of upward and downward movement coincides with dusk and down. During the night a larger part of the zooplankton seems to feed near the surface, whereas they rest during the daytime mainly in depth of 300 to 400 m, which confines to the depth layer of minimum oxygen concentration. Second scattering layers were observed throughout the time at 200 and 400 m. The depth of the lower scattering layer was increasing towards the equator to about 500 m. The vertical migration is also visible in the subtropical part of the transect south of 17°S, but less pronounced. Since no sampling was performed along the transect, no information about the zooplankton is available.

Walvis Bay Transect at 23°S

The majority of the stations worked during the cruise M157 was carried out along cross shelf transects. The main transect was off Walvis Bay at 23°. The ScanFish was used first to get synoptic information about the upper layer properties. Unfortunately, the ScanFish measurements had to be stopped untimely after a failure of the tow cable. However, the ScanFish transect could be repeated during the second half of the cruise. Afterwards MSS and CTD stations were performed.

The temperature distribution along the section shows a typical upwelling pattern with cold and low saline surface water on the coast. With increasing coastal distance the surface temperature rises. The mixed layer depth is offshore at about 50 to 70 m. Above the outer shelf edge the vertical displacement of the isotherms points to internal waves. The salinity structure is more complex and shows the influence of lateral transport processes along the shelf.

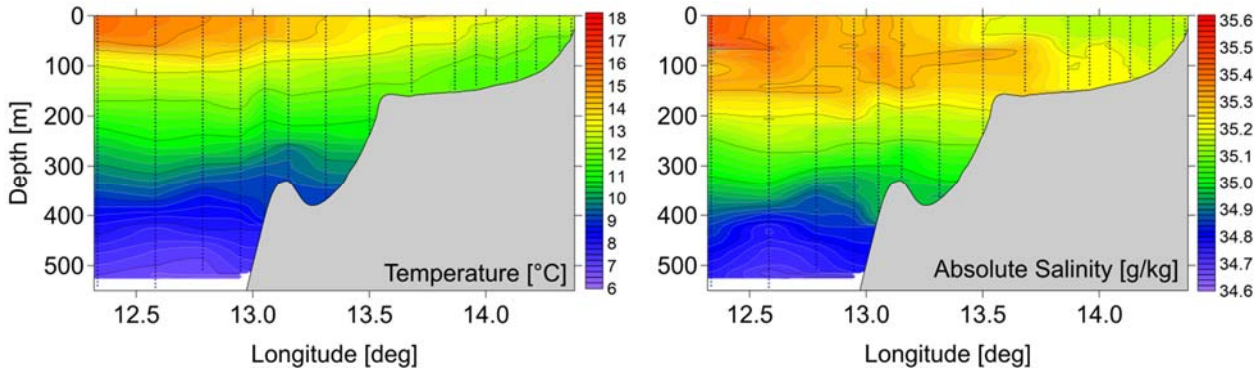

Fig. 5.2.5 Distribution of temperature (left) and salinity (right) along the cross shelf transect at 23°S. The figure is based on the preliminary MSS data gathered from 19.08. - 21.08.2019.

Due to the exchange with the atmosphere the surface layer was well ventilated. Below the mixed surface layer the oxygen content decreases strongly. Off the shelf the core of the OMZ was observed at about 300 m. On the shelf, the oxygen demand of the sediments caused a further reduction of oxygen content in the bottom water. However, no anoxic areas were observed.

The high turbidity was found in the surface water due to high phytoplankton abundance and in the bottom layer on the inner shelf where the camera of the Pump-CTD depicted thick layers of marine snow.

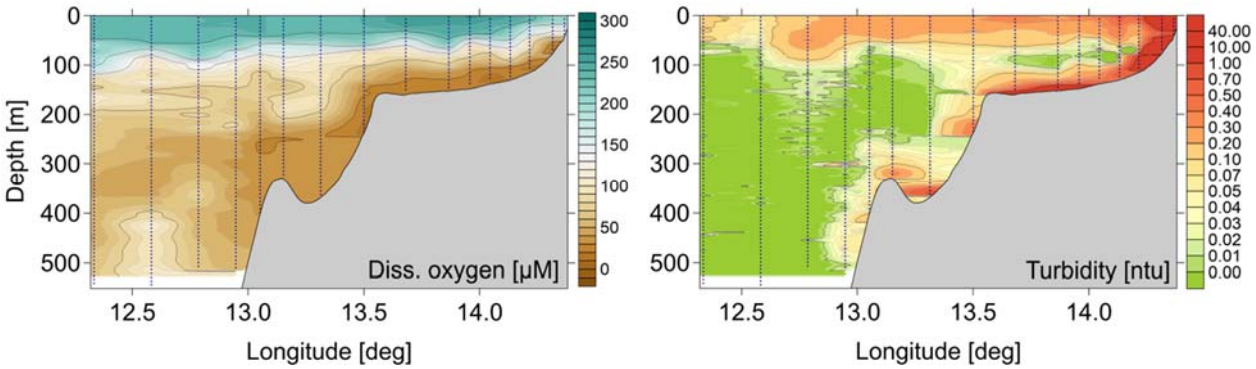

Fig. 5.2.6 Distribution of dissolved oxygen concentration (left) and turbidity (right) along the cross shelf transect at 23°S. The figure is based on the preliminary MSS data gathered from 19.08. - 21.08.2019.

The water mass distribution on the 23°S transect depicted a maximum SACW fraction (>40%) at the shelf edge in depths below 150 m. The inner shelf was covered nearly completely by ESACW. Its high oxygen content prevented the establishment of anoxic conditions in the bottom layer. Using the water mass definitions of SACW and ESACW the Apparent Oxygen Utilisation was calculeted. The higest oxygen demand was observed in the deep layers of the inner shelf where the surface sediments contain a high concentration of organic carbon.

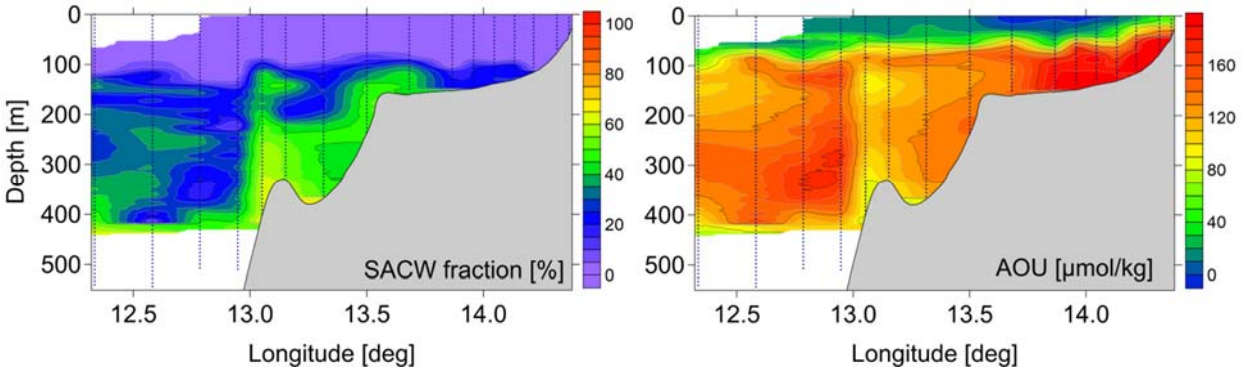

Fig. 5.2.7 Distribution of SACW fraction (left) and Apparent Oxygen Utilisation (right) along the cross shelf transect at 23°S. The figure is based on the preliminary MSS data gathered from 19.08. - 21.08.2019.

The dissipation rate of turbulent kinetic energy (TKE) is depicted in Fig 5.2.8. Hot spots of mixing are surface layer due to wind forcing, and the primary and secondary shelf breaks. Here internal waves interact with the topography and lead to break events of internal waves. This process resuspends settled material, which is then redistributed by the bottom currents.

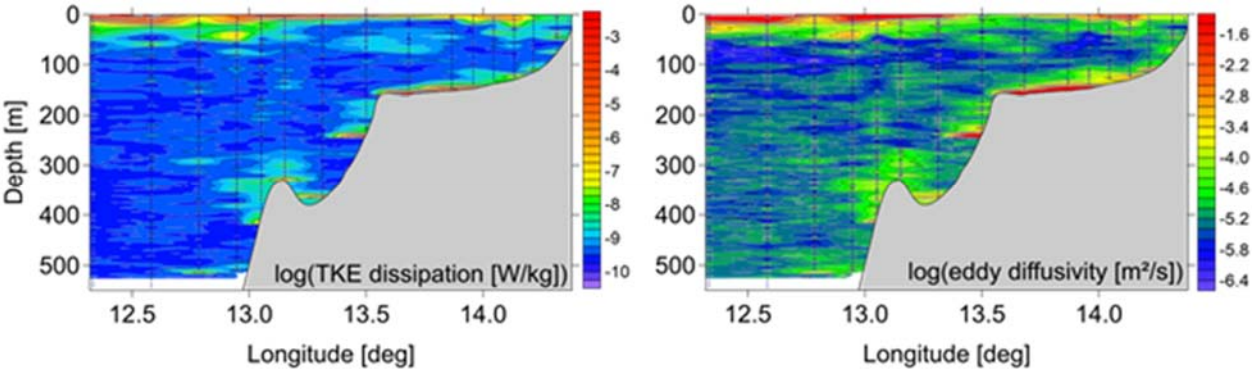

Fig. 5.2.8 Distribution of TKE dissipation (left) and eddy diffusivity (right) along the cross shelf transect at 23°S. The figure is based on the preliminary MSS data gathered from 19.08. - 21.08.2019.

Table 5.2.4: List of CTD stations, LADCP and AC-S casts

Station No.	Station name	DateTime	Latitude	Longitude	Water Depth	CTD	LADCP	AC-S
Meteor	NatMIRC	[UTC]			[m]	cast	cast	cast
M157_1-1		12.08.2019 12:25	09° 26.71'S	000° 25.53'E	5446.0	V0001F01	-	-
M157_6-1	N23110	19.08.2019 18:57	23° 00.00'S	012° 20.00'E	2070.0	V0002F01	001	000
M157_12-2	N23030	21.08.2019 06:25	23° 00.00'S	013° 51.99'E	151.0	V0003H01	002	001
M157_14-2	N23020	21.08.2019 20:15	23° 00.01'S	014° 02.80'E	138.0	V0004H01	003	002
M157_16-3	N23010	22.08.2019 18:12	23° 00.00'S	014° 12.94'E	119.0	V0005H01	004	003
M157_15-14	N23015	23.08.2019 21:41	23° 00.00'S	014° 08.08'E	133.0	V0006H01	005	004
M157_17-2	N23005	23.08.2019 23:48	23° 00.01'S	014° 19.00'E	76.0	V0007H01	-	*(005)*
M157_2-8	N23002	24.08.2019 05:07	23° 00.01'S	014° 22.00'E	46.0	V0008H01	-	*(006)*
M157_16-14	N23010	24.08.2019 13:03	23° 00.04'S	014° 12.94'E	118.0	V0009H01	-	-
M157_14-14	N23020	24.08.2019 14:44	22° 60.00'S	014° 03.20'E	138.0	V0010H01	-	-
M157_12-21	N23030	25.08.2019 03:42	22° 60.00'S	013° 52.00'E	150.0	V0011H01	006	-
M157_10-7	N23050	25.08.2019 09:46	22° 60.00'S	013° 30.01'E	241.0	V0012H01	007	*(007)*
M157_9-2	N23060	25.08.2019 21:04	23° 00.00'S	013° 19.01'E	362.0	V0013H01	008	008
M157_11-4	N23040	26.08.2019 03:59	22° 59.99'S	013° 40.99'E	154.0	V0014_01	009	009
M157_16-24	N23010	28.08.2019 13:36	22° 59.99'S	014° 12.97'E	113.0	V0015H01	*(010)*	-
M157_8-2	N23070	28.08.2019 22:32	22° 59.96'S	013° 08.97'E	321.0	V0016H01	011	010
M157_24-1		31.08.2019 02:26	17° 16.02'S	011° 43.45'E	33.0	V0017H01	-	*(011)*
M157_25-1		31.08.2019 14:55	17° 16.02'S	011° 04.00'E	1515.0	V0018_01	012	*(012)*
M157_25-3		31.08.2019 17:00	17° 16.02'S	011° 04.01'E	1516.0	V0019H01	013	-
M157_26-2		31.08.2019 22:42	17° 16.02'S	011° 09.00'E	1101.0	V0020H01	014	*(013)*

Station No.	Station name	DateTime	Latitude	Longitude	Water Depth	CTD	LADCP	AC-S
Meteor	NatMIRC	[UTC]			[m]	cast	cast	cast
M157_27-1		01.09.2019 01:31	17° 16.01'S	011° 16.49'E	508.0	V0021H01	015	*(014)*
M157_28-1		01.09.2019 06:12	17° 16.02'S	011° 30.06'E	151.0	V0022H01	016	*(015)*
M157_29-1		01.09.2019 11:27	17° 15.72'S	011° 43.03'E	42.0	V0023H01	-	*(016)*
M157_30-1		01.09.2019 15:38	17° 20.39'S	011° 36.12'E	117.0	V0024H01	-	*(017)*
M157_16-25	N23010	03.09.2019 04:33	22° 60.00'S	014° 13.01'E	114.0	V0025H01	-	-
M157_14-18	N23020	03.09.2019 06:22	23° 00.02'S	014° 03.01'E	140.0	V0026H01	-	-
M157_31-1	N25100	03.09.2019 20:03	25° 00.00'S	012° 59.84'E	1802.0	V0027H01	017	*(018)*
M157_43-2	N25015	05.09.2019 19:48	25° 00.00'S	014° 33.66'E	107.0	V0028H01	-	022
M157_44-2	N25010	06.09.2019 13:03	24° 60.00'S	014° 39.17'E	89.0	V0029_01	-	023
M157_34-4	N25070	06.09.2019 23:17	24° 59.99'S	013° 32.93'E	625.0	V0030H01	018	024
M157_36-2	N25060	07.09.2019 03:52	25° 00.00'S	013° 43.97'E	317.0	V0031H01	019	025
M157_38-2	N25050	07.09.2019 19:34	24° 60.00'S	013° 55.01'E	186.0	V0032H01	020	026
M157_39-2	N25040	07.09.2019 23:04	25° 00.01'S	014° 06.16'E	172.0	V0033H01	021	027
M157_41-14	N25025	09.09.2019 12:20	24° 60.00'S	014° 22.65'E	139.0	V0034H01	022	028
M157_40-2	N25030	10.09.2019 03:54	24° 59.99'S	014° 17.13'E	163.0	V0035_01	023	029
M157_42-2	N25020	10.09.2019 14:07	24° 59.98'S	014° 28.16'E	123.0	V0036_01	024	030
M157_43-19	N25015	10.09.2019 16:28	25° 00.00'S	014° 33.67'E	103.0	V0037H01	-	-
M157_45-2	N25005	10.09.2019 18:15	25° 00.01'S	014° 44.68'E	54.0	V0038H01	-	031
M157_46-3	N25002	10.09.2019 20:56	25° 00.00'S	014° 48.01'E	32.0	V0039H01	-	032
M157_49-3	LTCN	11.09.2019 11:20	25° 05.02'S	014° 32.09'E	113.0	V0040H01	-	033
M157_17-16	N23005	12.09.2019 19:47	23° 00.01'S	014° 19.01'E	75.0	V0041H01	-	034
M157_16-26	N23010	13.09.2019 03:55	22° 60.00'S	014° 13.00'E	114.0	V0042_01	-	035
M157_2-9	N23002	13.09.2019 11:15	22° 59.99'S	014° 22.01'E	46.0	V0043_01	-	*(036)*

Table 5.2.5: List of Pump-CTD casts

Station No.	Station name	DateTime	Latitude	Longitude	Water Depth	PCTD	Remarks
Meteor	NatMIRC	[UTC]			[m]	cast	
M157_1-3		12.08.2019 13:59	09° 26.72'S	000° 25.53'E	5443.0		Test deployment
M157_14-4	N23020	22.08.2019 00:30	23° 00.00'S	014° 02.84'E	140.0	P0001_01	Nutrients
M157_14-4	N23020	22.08.2019 03:45	23° 00.00'S	014° 02.84'E	137.0	P0001_02	Trace gas
M157_14-4	N23020	22.08.2019 05:55	23° 00.00'S	014° 02.84'E	139.0	P0001F03	AFIS
M157_16-6	N23010	22.08.2019 22:46	23° 00.00'S	014° 12.94'E	114.0	P0002F01	Nutrients
M157_16-6	N23010	23.08.2019 03:19	22° 60.00'S	014° 12.94'E	115.0	P0002F02	Trace gas
M157_16-6	N23010	23.08.2019 04:31	22° 60.00'S	014° 12.94'E	113.0	P0002F03	AFIS
M157_14-15	N23020	24.08.2019 16:32	22° 60.00'S	014° 03.19'E	139.0	P0003F01	Nutrients
M157_12-20	N23030	25.08.2019 03:00	22° 60.00'S	013° 52.00'E	149.0	P0004F01 P0004F02	Nutrients Trace gas
M157_43-4	N25015	06.09.2019 00:00	25° 00.00'S	014° 33.66'E	105.0	P0005_02	Nutrients
M157_43-5	N25015	06.09.2019 04:13	25° 00.00'S	014° 33.66'E	104.0	P0005_03	Trace gas
M157_43-6	N25015	06.09.2019 05:34	25° 00.00'S	014° 33.66'E	106.0	P0005_04	AFIS
M157_41-19	N25025	10.09.2019 02:11	24° 60.00'S	014° 22.71'E	139.0	P0006F02 P0006F03	Nutrients Trace gas
M157_44-9	N25010	11.09.2019 20:36	25° 00.01'S	014° 39.16'E	83.0	P0007_01 P0007_02	Nutrients Trace gas
M157_17-18	N23005	13.09.2019 02:14	23° 00.01'S	014° 19.01'E	77.0	P0008F01 P0008F02	Nutrients Trace gas
M157_2-11	N23002	13.09.2019 14:03	22° 59.99'S	014° 22.01'E	47.0	P0009_01 P0009_02	Trace gas Nutrients

Table 5.2.6: List of MSS stations and casts

Station No.	Station name	DateTime	Latitude	Longitude	Water Depth	Cast	Remarks
Meteor	NatMIRC	[UTC]			[m]	[count]	
M157_1-4		12.08.2019 14:28	09° 27.05'S	000° 25.73'E	5589.0	001-005	Test station
M157_3-1	N23080	19.08.2019 11:30	23° 00.77'S	012° 56.93'E	610.0	006-008	
M157_4-1	N23090	19.08.2019 13:19	23° 00.70'S	012° 47.31'E	943.0	009-010	
M157_5-1	N23100	19.08.2019 15:35	23° 00.72'S	012° 35.18'E	1429.0	011-012	

Station No.	Station name	DateTime	Latitude	Longitude	Water Depth	Cast	Remarks
Meteor	NatMIRC	[UTC]			[m]	[count]	
M157_6-3	N23110	19.08.2019 20:31	23° 00.84'S	012° 20.16'E	2054.0	014-015	013 no data
M157_7-1	N23075	20.08.2019 06:35	23° 00.83'S	013° 03.32'E	410.0	016-018	
M157_8-1	N23070	20.08.2019 08:26	23° 00.97'S	013° 09.35'E	331.0	019-023	020 no data
M157_9-1	N23060	20.08.2019 11:16	23° 00.88'S	013° 18.66'E	364.0	024-026	
M157_10-1	N23050	20.08.2019 14:05	23° 00.64'S	013° 30.01'E	241.0	027-029	
M157_11-1	N23040	20.08.2019 16:01	23° 00.77'S	013° 40.79'E	156.0	030-035	
M157_12-1	N23030	20.08.2019 17:57	23° 00.75'S	013° 51.98'E	152.0	036-041	
M157_13-1	N23025	20.08.2019 19:38	23° 00.61'S	013° 57.48'E	146.0	042-047	
M157_14-1	N23020	20.08.2019 21:16	23° 00.63'S	014° 02.75'E	140.0	048-053	
M157_15-1	N23015	20.08.2019 23:27	23° 00.63'S	014° 07.97'E	134.0	054-058	
M157_16-1	N23010	21.08.2019 00:55	23° 00.50'S	014° 12.87'E	114.0	059-063	
M157_17-1	N23005	21.08.2019 02:21	23° 00.52'S	014° 18.86'E	2535.0	064-069	
M157_2-2	N23002	21.08.2019 03:23	23° 00.37'S	014° 21.99'E	2052.0	070-076	
M157_16-5	N23010	22.08.2019 19:35	23° 00.16'S	014° 12.93'E	118.0	077-082	PCTD cast
M157_12-19	N23030	24.08.2019 18:47	23° 00.79'S	013° 52.07'E	147.0	083-088	PCTD cast
M157_17-10	N23005	26.08.2019 20:39	22° 59.25'S	014° 19.04'E	77.0	089-094	
M157_19-1	N18002	30.08.2019 14:42	18° 00.31'S	011° 45.91'E	60.0	095-100	
M157_20-1	N18005	30.08.2019 15:56	18° 00.55'S	011° 43.01'E	95.0	101-106	
M157_21-1	N18010	30.08.2019 17:18	18° 00.56'S	011° 38.12'E	130.0	107-111	
M157_22-1	N18013	30.08.2019 18:46	18° 00.72'S	011° 35.21'E	182.0	112-115	
M157_23-1	N18017	30.08.2019 20:07	18° 00.63'S	011° 31.19'E	235.0	116-118	
M157_31-3	N25100	03.09.2019 21:21	25° 00.50'S	012° 59.52'E	1833.0	119-120	
M157_32-1	N25090	04.09.2019 00:09	25° 00.25'S	013° 10.71'E	1444.0	121-123	
M157_33-1	N25080	04.09.2019 03:37	25° 00.16'S	013° 21.79'E	1015.0	124-125	
M157_34-1	N25070	04.09.2019 07:00	24° 59.89'S	013° 33.01'E	624.0	126-128	127 no data
M157_35-1	N25065	04.09.2019 11:40	24° 59.67'S	013° 38.59'E	446.0	129-130	
M157_36-1	N25060	04.09.2019 13:45	24° 59.59'S	013° 43.90'E	318.0	131	
M157_37-1	N25055	04.09.2019 16:55	25° 00.67'S	013° 49.63'E	235.0	132-134	
M157_38-1	N25050	04.09.2019 18:52	25° 00.04'S	013° 55.00'E	186.0	135-139	
M157_39-1	N25040	04.09.2019 20:48	25° 00.14'S	014° 06.18'E	177.0	140-144	
M157_40-1	N25030	04.09.2019 22:44	24° 59.96'S	014° 17.12'E	162.0	145-149	
M157_41-1	N25025	05.09.2019 00:22	24° 59.93'S	014° 22.68'E	141.0	150-155	
M157_42-1	N25020	05.09.2019 02:11	25° 00.24'S	014° 28.19'E	124.0	157-162	156 no data
M157_43-1	N25015	05.09.2019 03:36	24° 60.00'S	014° 33.73'E	109.0	163-168	
M157_44-1	N25010	05.09.2019 04:51	25° 00.02'S	014° 39.15'E	85.0	169-174	
M157_45-1	N25005	05.09.2019 06:05	25° 00.08'S	014° 44.59'E	54.0	175-181	180 no data
M157_46-1	N25002	05.09.2019 07:04	24° 59.69'S	014° 47.98'E	32.0	182-187	
M157_47	N25025	05.09.2019 14:50	24° 59.93'S	014° 22.68'E	141.0	188	Test
M157_43-5	N25015	05.09.2019 23:18	25° 00.00'S	014° 33.66'E	109.0	189-196	PCTD 5
M157_41-15	N25025	09.09.2019 12:20	25° 00.00'S	014° 22.65'E	139.0	197-199	calibration
M157_41-20	N25025	09.09.2019 19:02	25° 00.00'S	014° 22.71'E	140.0	200-207	PCTD 6
M157_49-1		11.09.2019 09:08	25° 05.01'S	014° 30.98'E	119.0	208-210	LTCN mooring
M157_44-10	N25010	11.09.2019 15:16	25° 00.01'S	014° 39.16'E	84.0	211-218	PCTD 7
M157_17-19	N23005	12.09.2019 21:14	23° 00.01'S	014° 19.01'E	77.0	219-226	PCTD 8
M157_2-12	N23002	13.09.2019 15:20	22° 59.99'S	014° 22.01'E	47.0	227-239	PCTD 9

Table 5.2.7: List of SCF transects during the cruise M157

Name	Latitude	Longitude	Deployed	Recovered	Depth	Remarks
			[UTC]	[UTC]	[m]	
M157_1-5 (test)	09° 28.15'S	000° 26.39'E	12.08.2019 15:06	12.08.2019 15:57	5428.0	Device test, no data
	09° 32.25'S	000° 28.95'E			5215.0	
M157_2-1 (transect 1)	23° 00.51'S	014° 21.94'E	18.08.2019 18:10	19.08.2019 09:07	46.0	Transect finished untimely due to failed cable connection
	23° 00.00'S	012° 56.73'E			605.0	
M157_24-9 (transect 2)	17° 16.15'S	011° 41.84'E	31.08.2019 07:54	31.08.2019 11:31	62.0	Transect finished untimely due to failed cable connection
	17° 16.04'S	011° 19.08'E			419.0	
M157_46-2 (transect 3)	25° 00.00'S	014° 47.95'E	08.09.2019 12:12	09.09.2019 04:30	34.0	Full length
	25° 00.00'S	012° 59.84'E			1802.0	
M157_2-13	23° 00.00'S	014° 22.67'E	13.09.2019 16:24	14.09.2019 11:09	47.0	Full length
	23° 00.00'S	012° 19.99'E			2069.0	

Table 5.2.8 List of VMADCP deployments during the cruise M157

ADCP	Deployment name	Start time	End time	STA Ens.	Bin size	Remarks
		[UTC]	[UTC]	No.	[m]	
VMADCP Ocean surveyor 38kHz	m157os38001 m157os38003	08.08.2019 18:46:31 12.08.2019 12:35:34	12.08.2019 11:59:34 17.08.2019 06:13:36	5354 6819	16	Equatorial section
	m157os38004 m157os38005 m157os38006	18.08.2019 18:10:14 22.08.2019 06:08:14 28.08.2019 12:19:34	21.08.2019 05:47:14 28.08.2019 12:14:16 29.08.2019 04:58:37	3578 9007 1000	16B	23°S transect 1
	m157os38007	29.08.2019 04:59:05	01.09.2019 18:22:36	5124	16B	Transit 23°S to 18°S and 18°S transect 2
	m157os38008	01.09.2019 18:23:22	03.09.2019 20:02:25	2980	16B	Transit 18°S to 25°S transect
	m157os38009	03.09.2019 20:03:09			16B	25°S transect 3
	m157os38010				16B	Transit 25°S to 23°S and 23°S transect 4
VMADCP Ocean surveyor 75kHz	m157os75001 m157os75003	08.08.2019 18:45:48 12.08.2019 12:04:13	12.08.2019 12:00:50 17.08.2019 06:13:14	5356 6850	8	Equatorial section
	m157os75004 m157os75006	18.08.2019 18:07:35 22.08.2019 06:12:14	21.08.2019 05:46:36 29.08.2019 04:58:14	3580 10007	4B	23°S transect 1
	m157os75007	29.08.2019 04:59:05	01.09.2019 18:22:05	5124	4B	Transit 23°S to 18°S and 18°S transect 2
	m157os75008	01.09.2019 18:22:58	03.09.2019 20:01:59	2980	4B	Transit 18°S to 25°S transect
	m157os75009	03.09.2019 20:02:41			4B	25°S transect 3
	m157os75010				4B	Transit 25°S to 23°S and 23°S transect 4

Table 5.2.9 List of mooring and drifter operations during the cruise M157

Name	Latitude	Longitude	Deployed	Recovered	Depth	Remarks
			[UTC]	[UTC]	[m]	
LTMB_19	23°00.010‘S	14°03.026‘E	*08.05.2019 14:59*	22.08.2019 07:00	130	Main release was successful.
LTMB_20	22°59.994‘S	14°02.992‘E	23.08.2019 14:48	23°00.274‘S	14°13.485‘E	Successful deployed during calm conditions.
LTMS_03	23°00.274‘S	14°13.485‘E	*08.05.2019 02:20*	24.08.2019 07:15	107	Mooring successful recovered, calm conditions.
Drifter 1	22° 59.93'S	13° 51.95'E	27.08.2019 13:36	-	150	Successful deployed, but no GPS messages received
Drifter 1	22° 59.73'S	13° 51.54'E	-	27.08.2019 15:43	146	Recovered since GPS messages delivered bad positions
LTKC_09	18°00.009’S	11°39.006’E	*05.07.2018 10:47*	30.08.2019 10:51	127	Release not successful, morring recovered with igel, second trial
LTKC_10	18° 00.00'S	011° 39.01'E	30.08.2019 13:04	*Planned for May 2020*	131	Successful deployed during rough conditions.
LTCN_01	25°05.00‘S	14°32.01‘E	11.09.2019 10:08	*Planned for May 2020*	111	Successful deployed during calm conditions

5.3 Marine Chemistry – Trace Gas Distribution in the Benguela Upwelling System

(B. Sabbaghzadeh, M. Glockzin, S. Otto)

The high surface productivity triggered by nutrient-rich Benguela upwelled waters results in significant fluxes of organic carbon to sub-surface waters. Hence, microbial O_2-consuming processes are promoted, driving oxygen depletion that favors trace gases i.e. N_2O and CH_4 production at relatively shallow depths. During upwelling, N_2O and CH_4-rich subsurface waters are also transported towards the surface waters, enhancing trace gas sea-air fluxes. We investigate the seasonal cycle of these fluxes by continuous surface trace gas measurement and by measuring the trace gases in discrete samples from the water column profiles.

Surface water concentrations of CH_4, N_2O and CO_2 were measured with IOW's self-built Mobile Equilibrator Sensor System (MESS). The system consists of two laser absorption spectroscopy gas analysers i.e. CH_4 / CO_2 analyser and N_2O / CO analyser. A custom-built equilibrator (shower-head type with additional air pump, water flow rate ~5 L min^{-1}, airflow rate ~4 L min^{-1}) was installed in line with the two analysers (Fig. 5.3.1).

Fig. 5.3.1 Mobile Equilibrator Sensor System (MESS), (M157 cruise R/V Meteor (Namibia))

Seawater was supplied by a deep-well pump installed in the moonpool of R/V METEOR at a water depth of about 5,6 m. The two LGR-analysers use the method of off-axis integrated cavity output spectroscopy (ICOS) that combines a highly specific infrared band laser with a set of strongly reflective mirrors to obtain an effective laser pathlength of several kilometers. It allows the detection of trace gases in the equilibrated gas phase with high precision and frequency (e.g. Gülzow et al. 2011). One standard gas was used to calibrate the sensors at the beginning of the cruise. Two more standard gases and one zero gas were then measured frequently as targets throughout the whole cruise, and the results were used for final recalibration of the measurements.

To estimate sea-air gas fluxes, the concentrations of trace gases in the ambient air were carried out at several locations during the cruise. For this purpose, tubing was installed on the starboard side, shortly below the bridge. All other related parameters such as temperatures (in-situ & equilibrator), the flow rate of seawater, flow into the equilibrator and etc. were also combined with information of the ships' position, meteorological data and thermosalinograph measurements (i.e. inlet at 3,3 m water depth) via UTC. All data was delivered by an NMEA string from R/V METEOR's data distributor system and used for the final calculation of in-situ concentrations of the trace gases. Hence, analyser and DSHIP data were combined in one-minute mean values, used for further analysis and mapping. Some preliminary results are displayed in Fig. 5.3.2.

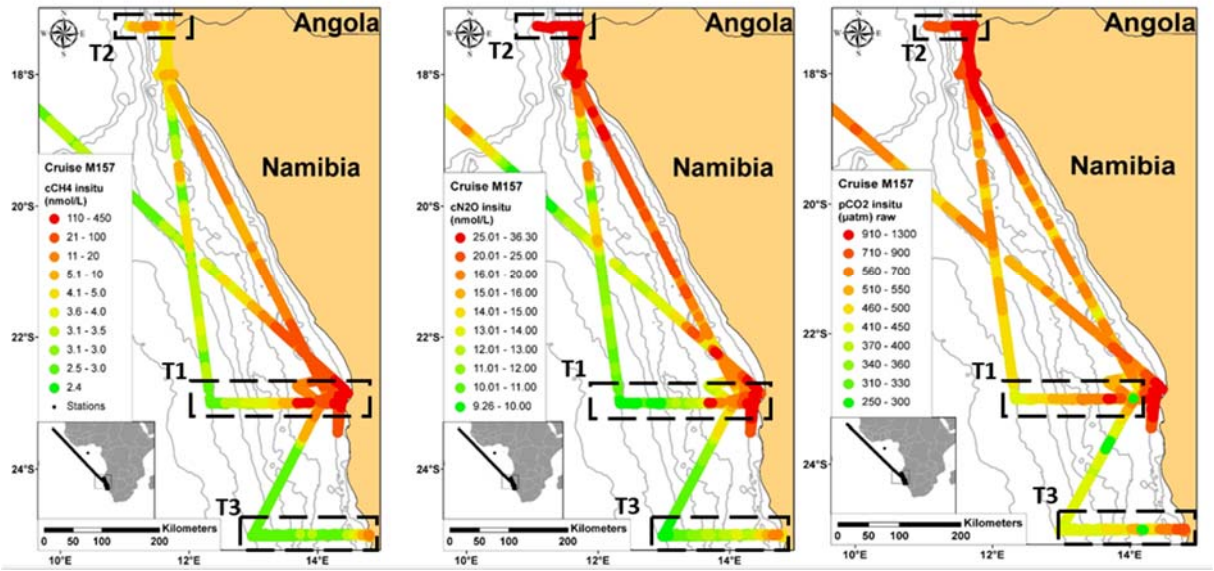

Fig. 5.3.2 Surface trace gas distribution in the African Eastern Boundary

To achieve the high resolution of water column profile and also a better understanding of the source or sink of trace gases within the depth profile, a Pump-CTD was in operation in line with MESS at few main stations. Some preliminary results are displayed (Fig. 5.3.3).

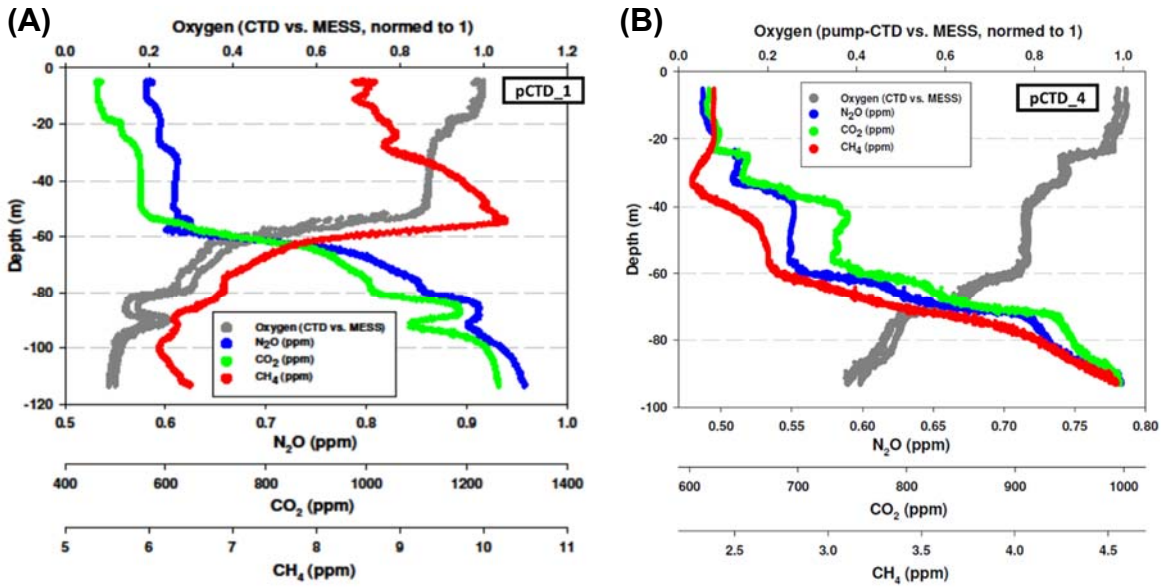

Fig. 5.3.3 Trace gas monitoring through the water column using pump CTD. (A) at 23°S, 14.03°E and (B) at 25°S, 14.33°E.

The two oxygen probes of MESS and pump CTD showed very parallel oxygen measurement through the water column ranged between >0.2 and 1 nm L^{-1} (Fig. 5.3.5). CH_4 oxic production in underlying waters between 25–50 m was present at 23°S. The production near sediment as the result of methanogenesis was also observed (Fig. 5.3.3 (A)). CH_4 consumption through the deeper waters was also found on this transect. On 25°S transect, the CH_4 profile showed a comparable pattern to N_2O and CO_2 with less concentration in upper waters while gradually increased through the water column. So, the source of CH_4 in sediment (i.e. methanogenesis) and consumption through the water column with the minimum in surface waters are suggested.

5.3.1 N_2O and CH_4 Depth Profiles

Nearly 300 discrete water samples were collected for the determination of trace gas concentrations within the water column at 30 selected stations. The in-house designed purge and trap system (P&T) determines CH_4 and N_2O concentrations in seawater samples using a dynamic headspace method. After desorption of volatile compounds with an inert ultrahigh pure carrier gas (Helium 99,999 % using purifier), the gases were analyzed by a gas chromatograph (GC) (Agilent 7890 B), equipped with a Flame Ionization Detector (FID) for CH_4 measurements and an Electron Capture Detector (ECD) for N_2O measurements (Fig. 5.3.4).

Fig. 5.3.4 The purge and trap system (IOW, Chemistry department). The system consists of four main components: A; the trap in the heating or cooling bath, B; Sample injection unit, C; Purge chamber with integrated frit and D; gas chromatograph.

The analytical system consists of four main components: a trap (stainless steel, 700 mm x 1/8", U-shaped) filled with HayeSep D (60/80 mesh, CS Chromatographie Service GmbH, Langerwehe, Germany) to enrich the relevant gas compounds, an injection unit, a purge chamber (200 x 24 mm) with integrated frit (porosity 2, Erich Eydam KG, Kiel, Germany) to purge 10 ml seawater with helium to displaced dissolved gases and a GC to separate CH_4 and N_2O with a special column circuit to operate in a FID and ECD-mode. The GC is run isothermally at 45°C with a Helium flow of 25 ml/min and is equipped with two columns (HP-Plot/Q+PT, ID 530 µm, film 40 µm, length 30 or 15 m). In FID-mode, CH_4 is detected during the first 5 minutes. After 5,5 minutes the GC system is switched to the ECD-mode and N_2O is detected (i.e. 7 min. in total runtime). The FID works at 200°C and the ECD at 345°C using a makeup gas i.e.10 % CO_2 in Nitrogen.

Nearly 10 ml of each discrete sample was flushed by Helium and the compounds in the gas phase were trapped in a column. The compounds were being held in the cooling bath over 10 minutes to be concentrated. The trap was then transferred to a heating bath and the gas phase compounds were released to the GC. To ensure accuracy of the measurements, the calibration standards were measured daily before and after water samples (a composition of 1991,2 ppb (± 5 %) N_2O and 9,257 ppm (± 2 %) CH_4 in synthetic air; all from Linde Group, Berlin, Germany). The calibration

range was chosen in a way that the samples are within the limits of the calibration. The standards followed the same time sequence and pathway as the samples.

The contribution of underlying water will help to explain surface oversaturation, equilibrium concentrations or undersaturation of the trace gases of interest (Fig. 5.3.5).

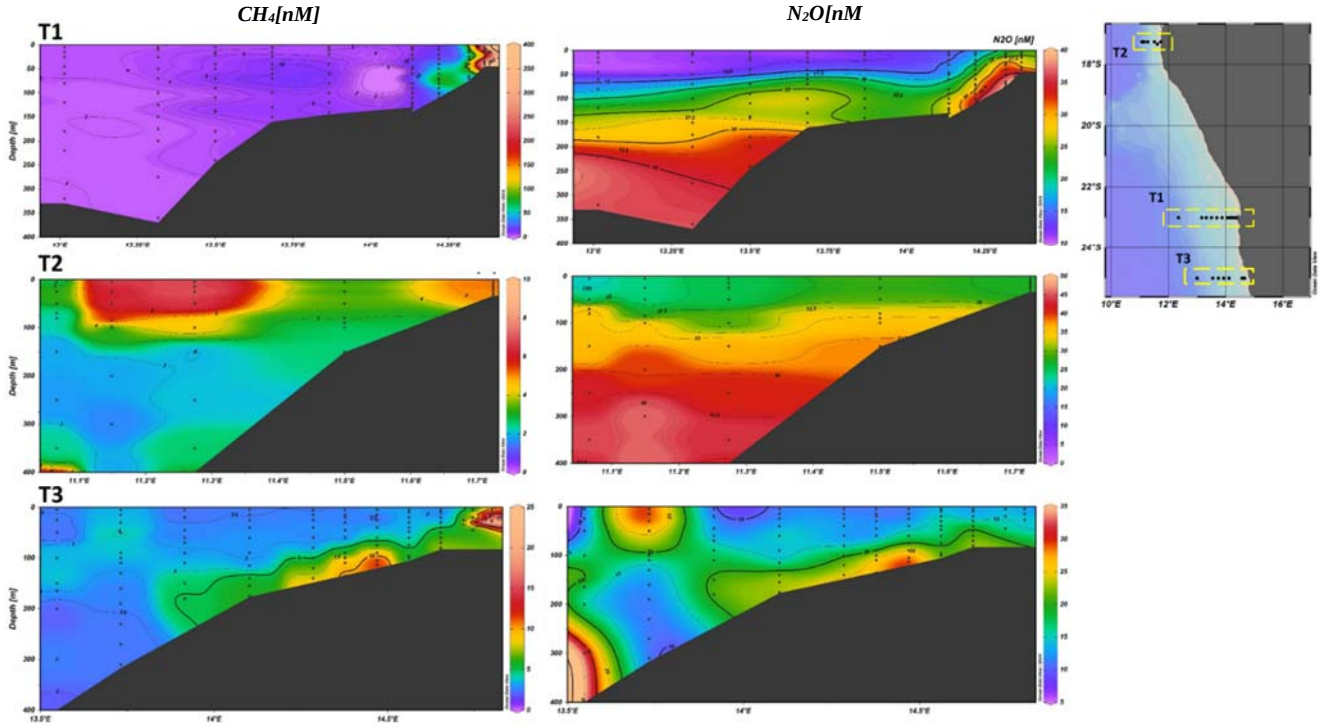

Fig. 5.3.5 Water column profiles of trace gases along M157 transects

The preliminary results showed very high concentrations of CH_4 i.e. about 360 nM in the coastal areas of T1 (23°S) while the concentrations decreased as the transect proceeded offshore to about 2 nM. N_2O maxima on mud belt and deeper waters in more offshore stations were also found. On T2 transect (17,3°S), the high concentration of CH_4 was found near the shore with one clear hotspot in the top 100 m in more offshore waters. N_2O pattern, however, was quite distinct on T2 transect with elevated concentrations towards the deeper waters. On T3 transect (25°S), CH_4 maxima were found nearshore and also at bottom waters with the suggestion of methanogenesis as the source of CH_4. N_2O was also found higher in deep waters except for one hotspot of N_2O found in the top 100 m water at one profile (Fig. 5.3.5).

5.3.2 Dissolved Inorganic Carbon (DIC) and pH Measurement

The sample size corresponded to CH_4 and N_2O measurements. The evaluations are currently in progress however the analytical procedure is briefly presented here. Automated Infra-Red Inorganic Carbon Analyzer (AIRICA) system (company Marianda e.K., 24145 Kiel) was used to measure the total carbonate (C_T) in seawater (Fig. 5.3.6).

C_T also known as Dissolved Inorganic Carbon (DIC), is one of the four parameters measured to determine the marine carbonate system. A discrete sample firstly is acidified and generates CO_2. The carbon is then released out of the water with the help of a carrier gas that streams through the acidified probe. The gas flows through a NAFION dryer and Peltier cooler to dry the gas stream. The system then measures the CO_2 concentration by using an infrared detector (LICOR 7000). Once in the LICOR detector, the CO_2 generates a peak which the area is directly proportional to the

carbon released, allowing DIC concentration to be calculated when the exact amount of the sample is known. With the help of certified reference materials, unnoticed blank impurities can be fixed, leading to more precise measurements and more valuable data.

The values of pH were also determined by adding an indicator (*m*-cresol purple) dye to seawater. The pH value was then detected by the VIS absorption spectrometry system. The determination was carried out by the changes in the colour of the indicator, depending on the sample pH value. For the whole procedure, the automatic flow "CONTROS HydroFIA® pH system was used. Buffer solutions were also measured for quality control.

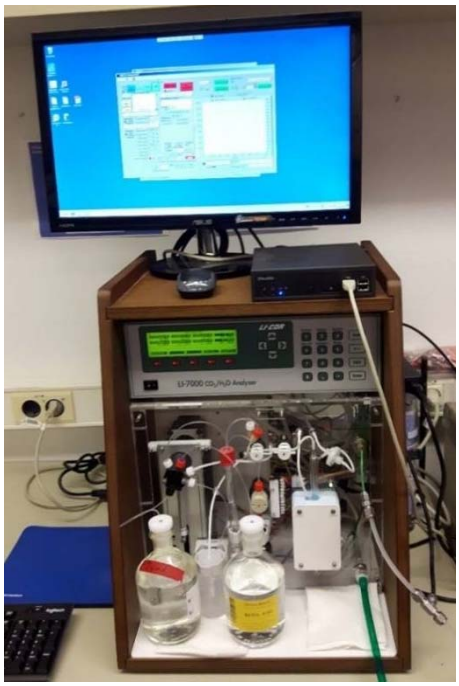

Fig. 5.3.6 Automated Infra-Red Inorganic Carbon Analyzer (AIRICA), IOW, Chemistry department.

5.4 Microbial Ecology

(J. Wäge, G. Dangl, C. Meeske, H. Langeloh)

The goal of this project part is the investigation of biogeochemical processes that are occurring in the water column and sediment, which especially show low oxygen concentrations. Until know there is only little information available on the temporal and special variability of microbial response to fluctuating oxygen conditions. Metagenomics and Metatranscriptomics will allow us to get an overview of the whole metabolic network of microorganisms and their reaction on changing environmental parameters. One of our key question is: "Which microbial mediated biogeochemical processes are taking place in the water column and sediment during different degrees of oxygen depletion and how fast are the microorganisms adapting to physical-chemical factors". To answer this question microbial communities were sampled in water depths of critical oxygen concentrations or where unusual concentrations in trace gases were found in CTD and Pump-CTD profiles. For this purpose, the CTD rosette was equipped with AFIS bottles, comprising an in-situ fixation system with a phenol/ethanol fixative (Feike et al., 2012), and samples were collected for metatranscriptomic analyses, which provides a picture of all expressed functional genes as indicators for localization of specific processes. Parallel free flow bottles were closed at the same water depths for nutrient analyses, microbial abundance (flow cytometry), enumeration of specific prokaryotic taxa (CARD-FISH) and collection of DNA/RNA for diversity analyses (based on 16S rRNA genes). In addition to the water column sampling, sediment surface samples for microbial abundance, enumeration, diversity analyses and expressed functional genes were collected also by two landers systems (see below).

Upwelling enhances the release of the greenhouse gases methane (CH_4), nitrous oxide (N_2O) and carbon dioxide (CO_2) into the atmosphere. Especially studies on N_2O production in the Benguela Upwelling System (BUS) are rare. In order to understand the mechanisms of trace gas production,

another important part of our works is to link the trace gas formation to the microbial key players and their activities. The main question is: "How are seasonal greenhouse gas fluxes between ocean and atmosphere related to the variability of physical drivers and microbiological processes?" Incubation experiments with nitrogen stable isotope tracers ($^{15}NH_4^+$, $^{15}NO_2^-$, $^{15}NO_3^-$) were used in order to identify N_2O production pathways. All results will be used to improve the biogeochemical model of the BUS.

5.4.1 Water column sampling

The water column was analysed by using a the SBE 911plus CTD system (Seabird Electronics, USA) equipped with temperature and conductivity sensors, and an oxygen sensor to choose the most interesting depth according to the oxygen concentration. At the depths of interest, water samples for microbial community analysis were collected on polycarbonate filters (1 L on 0,22 µm). For some stations also two size fractions (3 µm and 0,22 µm) were collected, in order to account for particle-associated microbes. Water samples for metatranscriptomic analysis were collected from Niskin bottles attached to the Pump-CTD, which were equipped with the Automatic Flow Injection Sampler (AFIS). AFIS is a modified water bottle with an integrated injection device for spraying and dispensing solutions into the sample right after closure of the bottle. This has the advantage that the water sample is fixed immediately and keeps the nucleic acids and proteins at their actual physiological state. This works even for microorganisms from deeper waters. For metagenomic analysis, larger volumes of water were filtered on Sterivex™ Filter units to highly concentrate the bacteria and archaea. All filters were snap frozen in liquid nitrogen and stored at -80°C. Additionally, samples for cell counts (fixation with a final concentration of 0,5 % Glutaraldehyde) and enumeration of specific prokaryotic taxa (fixation with a final concentration 2 % formaldehyde) were collected. CTD casts were performed along all three transects (17,3°S, 23°S, and 25°S). For detailed sampling see Table 1. Especially stations with low oxygen concentrations were of interest. Of the two possible OMZ forms, mid-water and above sediments (Fig. 5.4.1), only the latter was detected once, whereas no intermediate OM layer was encountered during the cruise.

5.4.2 Sediment core sampling

Using a multiple corer (MC) equipped with six core liners (length ~60 cm, inner diameter 10 cm) was used to obtain sediment cores. The cores were then brought to the laboratory for incubation experiments or were immediately sampled. Sampling included: water and sediment samples for N_2O/CH_4 concentrations, nutrient analyses, microbial abundance (flow cytometry), enumeration of specific prokaryotic taxa (CARD-FISH) and collection of DNA/RNA for diversity analyses.

Table 5.4.1 Summary of stations where microbial samples were collected and the type of sample. Grey boxes indicate sampled parameters for each station.

Transect	Station	Date	DNA filter	Flow Cytometer	CARD-FISH	MC	AFIS	^{15}N Incubation
23°S	M157_6	19.08.19	X	X	X			
23°S	M157_12	21.08.19	X	X	X	X		
23°S	M157_14	21.08.19	X	X	X		failed	
23°S	M157_16	22.08.19	X	X	X		Ok	X
23°S	M157_15	22.08.19	X	X	X			
23°S	M157_17	24.08.19	X	X	X			
23°S	M157_2	24.08.19	X	X	X			

Transect	Station	Date	DNA filter	Flow Cytometer	CARD-FISH	MUC	AFIS	^{15}N Incubation
23°S	M157_16	24.08.19	X					
23°S	M157_14	24.08.19	X				3 depths	X
23°S	M157_10	25.08.19	X	X	X	X		
23°S	M157_9	25.08.19	X	X	X			
23°S	M157_11	26.08.19	X	X	X			
23°S	M157_14	28.08.19				X		
23°S	M157_16	29.08.19				X		
23°S	M157_17	29.08.19				X		
17°S	M157_24	31.08.19	X	X	X			
17°S	M157_25	31.08.19	X	X	X			
17°S	M157_28	01.09.19	X	X	X			
17°S	M157_16	03.09.19	X	X	X			X
17°S	M157_31	03.09.19	X	X	X			
17°S	M157_41	03.09.19				X		X
25°S	M157_43	05.09.19	X	X	X		5 depths	X
25°S	M157_44	06.09.19	X	X	X			
25°S	M157_34	07.09.19	X	X	X			
25°S	M157_36	07.09.19	X	X	X			
25°S	M157_38	07.09.19	X	X	X			
25°S	M157_39	08.09.19	X	X	X			
25°S	M157_41	09.09.19	X	X	X			
25°S	M157_40	10.09.19	X	X	X			
25°S	M157_42	10.09.19	X	X	X			
25°S	M157_45	10.09.19	X	X	X			
25°S	M157_43	10.09.19	+STERIVEX					
25°S	M157_46	10.09.19	X	X	X			
25°S	M157_49	11.09.19	X	X	X			
23°S	M157_17	12.09.19	X	X	X			X
23°S	M157_16	13.09.19	+STERIVEX	X	X			
23°S	M157_2	13.09.19	X	X	X			X

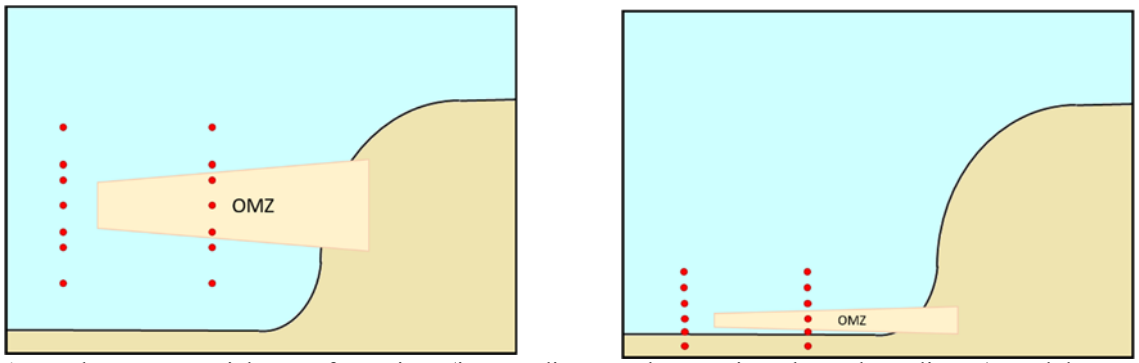

Fig. 5.4.1 The two potential OMZ formations (intermediate OM layer or just above the sediment). Red dots represent potential sampling depths.

5.4.3 Sediment Incubation Experiment

The aim of this experiment was to investigate how low oxygen concentrations affect the expression of selected genes (e.g., related to S and N transformations) and how the gene expression recovery is affected by this. The main questions are: Are specific microorganisms able to cope better with the change in oxygen, and how do the functional microbial profiles change with decreasing or increasing oxygen concentration? To look at these questions six sediment cores were taken by the multi corer (station 41) and the cores were closed with a special lid. The lid was equipped with two ducts for a temperature and oxygen sensor, a septum, a valve for releasing air bubbles and a tube for water sampling. Inside each core was a plastic ring which holds a magnetic cross. A spinning magnet

attached to a transformer was placed in the middle of all cores to allow slow stirring of the water column above the sediment (see Fig. 5.4.2).

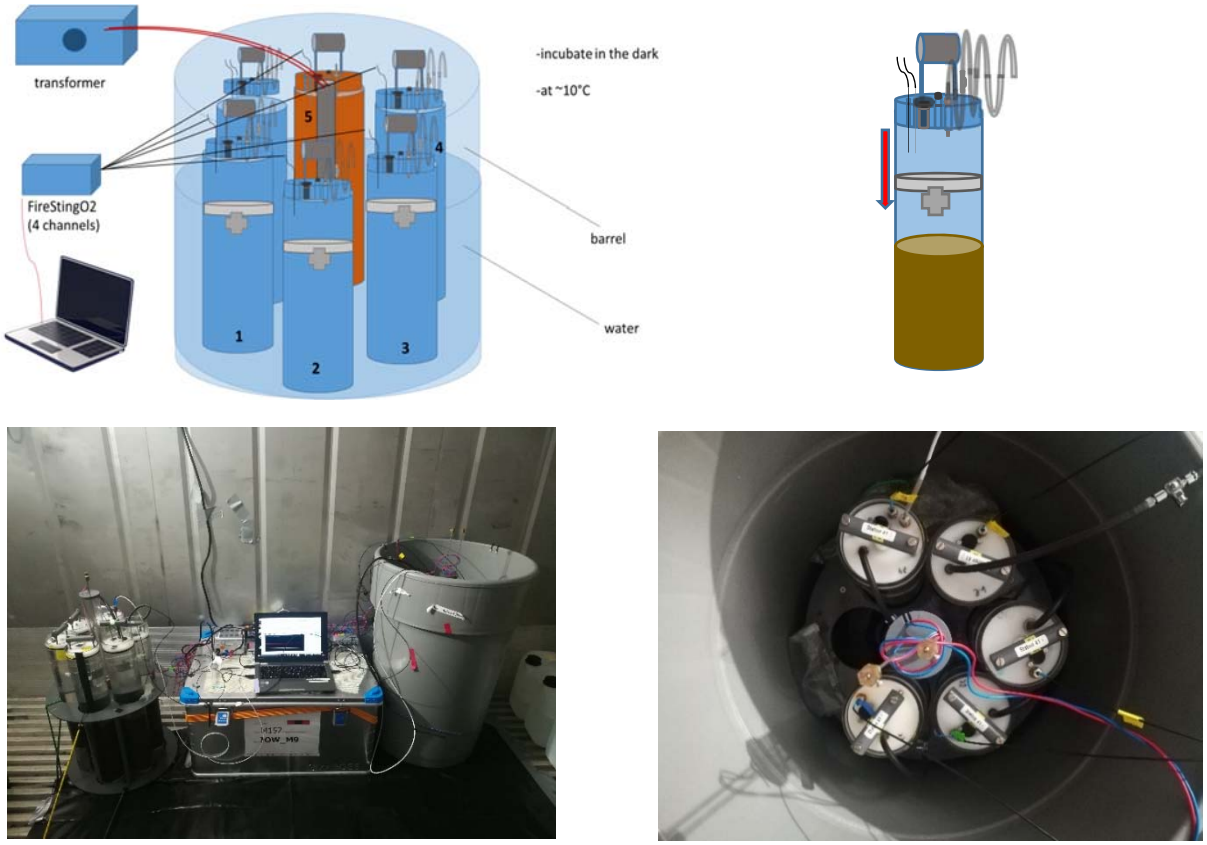

Fig. 5.4.2 Schematic diagram of the incubation setup and a sediment core. Pictures of the actual incubation setup in the cooling container.

All cores were closed to allow no oxygen to enter and the development of anoxic conditions. The experiment was carried out in a temperature-controlled container at darkness. Three of the six cores were sampled after different in situ low oxygen periods (Core 4, Core 3, and Core 6) and the other three cores were reoxygenated by bubbling with air (Core 1, Core 5, and Core 2). The following samples were taken: DNA/RNA, microbial abundance, enumeration of specific prokaryotic taxa, N_20/CH_4 gas samples, nutrients and for selected cores isotope paring was performed.

5.4.4 Microbial Sampling from the Lander System: Biogeochemical Observatory (BIGO)

The BIGO is used to measure in situ fluxes and biogeochemical effects on the seabed and carries two round flow chambers. From both chambers microbial samples were taken from the sediment for microbial diversity analyses and enumeration of specific prokaryotic taxa. For the diversity analyses 15 mL of sediment was collected in a Falcon™ tube and snap frozen in liquid nitrogen. For the enumeration of specific prokaryotic taxa 0,5 cm^3 sediment was fixed with 4 % formaldehyde solution and frozen at -20°C. Unfortunately, from all deployed BIGO's only one chamber could be sampled for microbial diversity in the water column. Thus, only at station M157_43 1 L of water was filtered on a 0,2 µm polycarbonate filter and snap frozen in liquid nitrogen for further analysis.

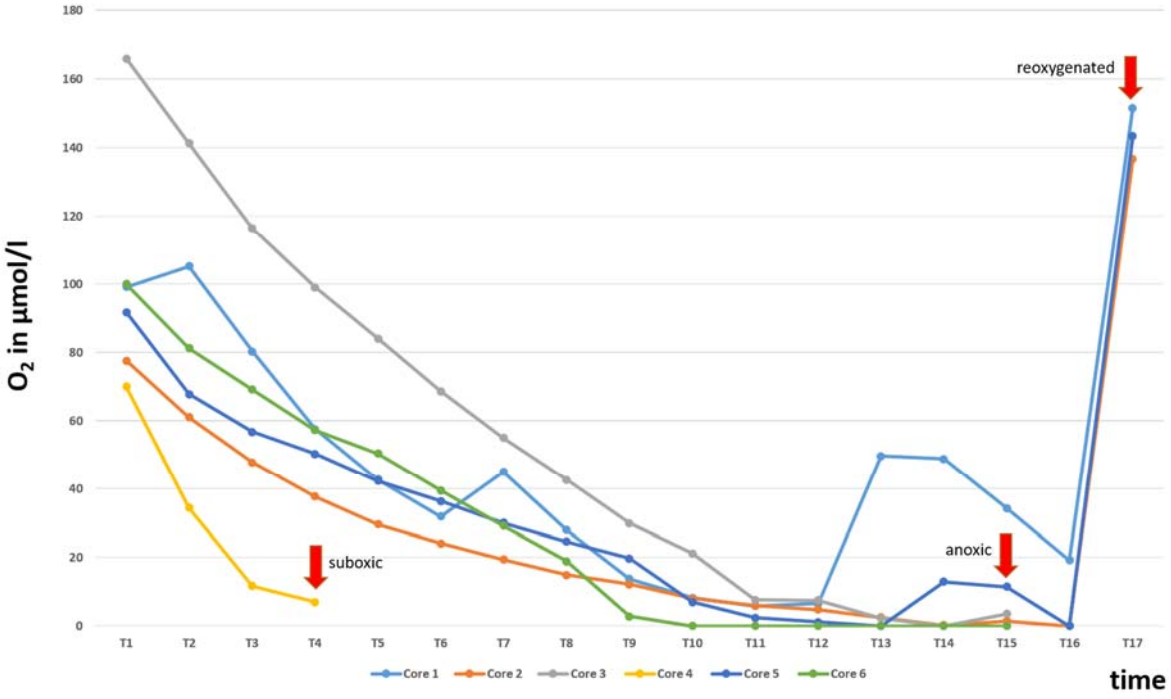

Fig. 5.4.3 Oxygen concentration in µmol L^{-1} measured inside six sediment cores (Core 1-6). Red arrows indicate sampling point of the whole core at different oxygen concentrations. Three cores were reoxygenated by bubbling with air.

5.4.5 ^{15}N Incubation Experiments for N_2O Production

Oxygen depleted areas are major sources of nitrous oxide (N_2O). The production of N_2O is usually ascribed to denitrifying and ammonia oxidizing microorganisms. In order to investigate N_2O production rates and their distribution, incubation experiments using stable isotope ^{15}N tracers were performed in the water column and in sediment cores which became anoxic over the time. Nitrogen stable isotope (^{15}N) incubation experiments were targeted at depths where oxygen concentrations were very low (2,0–9,0 µmol L^{-1}). Seawater was sampled into 120 mL serum bottles and processed immediately. Three suites of ^{15}N tracer solutions ($^{15}NH_4^+ + {}^{14}NO_2^-$, $^{15}NO_2^- + {}^{14}NH_4^+$ and $^{15}NO_3^- + {}^{14}NH_4^+ + {}^{14}NO_2^-$) were added and incubated in the dark. Incubations lasted between 0 and 48 hours in a temperature controlled environment close to in situ temperatures (~12°C) and were terminated after four time points by adding saturated $HgCl_2$ solution. Samples will be analyzed by isotope ratio mass spectrometry (IRMS) at the University of Basel in cooperation with Claudia Frey (Switzerland; Department of Environmental Sciences, Biogeochemistry Group).

Table 5.4.1 Summary of stations and depths where samples for nitrogen stable isotope (^{15}N) incubation experiments were taken. Grey boxes indicate which tracer was used.

Transect	Station	Date	Depths [m]	$^{15}NH_4^+$	$^{15}NO_3^-$	$^{15}NO_2^-$
23°S	M157_16*	23.08.19	10, 40, 70, 90, 100	X		X
23°S	M157_16	22.08.19	90, 100, 105		X	
23°S	M157_14	24.08.19	10, 30, 50, 90, 127	X	X	X
23°S	M157_16	03.09.19	10, 40, 70, 90, 100	X	X	X
25°S	M157_43	05.09.19	100	X	X	X
			100 (H_2S added before incubation)		X	X
17°S	M157_41	09.09.19	130	X	X	X
			130 (H_2S added before incubation)	X	X	X

Transect	Station	Date	Depths [m]	$^{15}NH_4^+$	$^{15}NO_3^-$	$^{15}NO_2^-$
23°S	M157_17	12.09.19	50, 56, 59, 63, 68	X	X	X
23°S	M157_2	13.09.19	35, 38, 41	X	X	X

*sampled from the PumpCTD

Table 5.4.3 Summary of stations where samples from anoxic sediment cores were taken for nitrogen stable isotope (^{15}N) incubation experiments. Grey boxes indicate which tracer was used.

Transect	Station	Date	Material	$^{15}NH_4^+$	$^{15}NO_3^-$	$^{15}NO_2^-$
23°S	M157_16	31.08.19	Water	X	X	X
			Sediment	X	X	X
17°S	M157_41	09.09.19	Water	X	X	X
			Sediment	X	X	X
25°S	M157_43	13.09.19	Water	X	X	X
			Sediment	X	X	X

5.4.6 ^{13}C labelled Sodium Bicarbonate Incubation for Determination of Chemolithoautotrophic Bacteria

To identify bacterial taxa that are using chemolithoautotrophic metabolic pathways, water samples from nearly anoxic CTD stations or from the anoxic/suboxic sediment incubations were taken. For each station or core, three serum bottles of 60 mL each were filled with sampling water and closed airtight so that no oxygen could enter the bottles. Afterwards the bottles were incubated with ^{13}C labelled Sodium Bicarbonate at concentrations of 110 µmol L^{-1} and 220 mmol L^{-1} which display in situ concentration and half of in situ concentration, respectively. The third bottle remained untreated and was used as a control. Incubation took place at in situ temperature (~12 °C) for a period of 24 hours before each sample was fixed with formaldehyde in a final concentration of 1,85% for 1–12 hours. Fixed samples were filtrated on 0,22 µm polycarbonate filters (1, 2 and 4 ml for each treatment) and stored at -20°C until further processing using CARD-FISH and NanoSims to determine bacterial taxa that used ^{13}C labelled Sodium Bicarbonate for chemolithoautotrophic metabolism.

Table 5.4.4 Stations with suboxic or anoxic conditions where ^{13}C incubation were conducted.

Transect	Station	MUC/CTD	Sampling date
23°S	M157_16	MC	29.08.19
17°S	M157_16	CTD	03.09.19
23°S	M157_16	MC	03.09.19
23°S	M157_16	CTD	13.09.19

5.5 Geomicrobiology

(H. Schulz-Vogt, C. Burmeister, J. Fabian, M. Tambo)

The overarching aim of this work package is to quantify sulfide oxidation rates under in situ conditions and under experimentally changed conditions, in order to evaluate the potential of sulfide oxidizing bacteria to detoxify sulfide under varying environmental conditions. This is combined with studies on the impact of sulfide oxidizing bacteria on the phosphorus cycle. For this study two cruises are planned, the current one under winter conditions with a mostly oxygenated water column and the following cruise under summer conditions with anoxic and possibly sulfidic bottom waters. The work package is closely related to the study on trace gases (s. Section 5.3) and to the study of microbial

distribution and gene expression (s. Section 5.4). For both related work packages nutrient profiles of the water column were determined concurrent with oxygen and sulfide profiles in order to put all observed bacterial activity into an environmental context.

5.5.1 Nutrient and Gas Profiles in the Water Column

For a detailed study of the water column Pump-CTD profiles were taken at 5 stations at the first transect at 23°S and 3 stations at the southern transect at 25°S. The Pump-CTD was lowered with a speed of 1-2 cm per second determining temperature, salinity, oxygen, chlorophyll and turbidity. The pumped water was lead directly into the laboratory where the water was split into two fractions, one connected to an autoanalyzer for determination of nitrate, nitrite, ammonia, phosphate and silicate and the other connected to a series of microelectrodes for the determination of oxygen, sulfide and hydrogen. As expected under winter conditions neither sulfide nor hydrogen were detectable. The oxygen microsensor (Unisense) in the laboratory gave a signal almost identical to the signal recorded by the Seabird oxygen sensor at the head of the Pump-CTD, indicating that the original stratification of the water column was conserved in spite of the pumping (Fig. 5.5.1A).

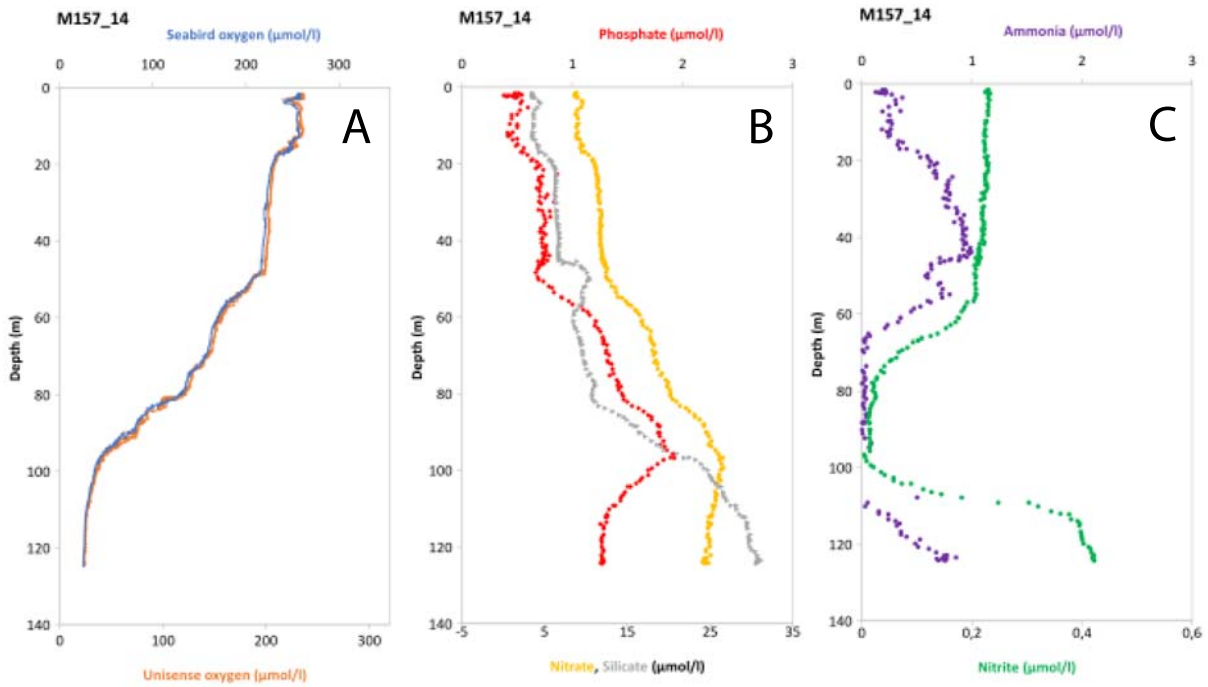

Fig. 5.5.1 Pump-CTD profiles at station 157_14: A, oxygen concentrations determined with the sensor at the head of the pump-CTD (Seabird, blue) and measured with a flow through microsensor at the outled of the pumped water (Unisense, orange). Profiles are almost identical indicating minimal mixing of water during pumping. B, profiles of nitrate (yellow), phosphate (red) and silicate (grey). C, profiles of ammonia (purple) and nitrite (green).

The nutrient profiles (Fig. 5.20 B and C) revealed strong changes in concentration for all measured compounds. Together with the assessment of the oceanographic situation (s. Section 5.2) it will be possible to determine, which of the changes in the profile reflect the origin of the water masses and which must be the result of microbial activity. None of the stations showed anoxia in the water column. In the water column sulfide oxidation was not measurable, even when water samples were deoxygenated.

5.5.2 Sulfide Oxidizing Bacteria in the Sediment

At one main station along the 23°S transect M157_16 the biovolume of *Thiomargarita* cells and the internal nitrate concentration was determined in triplicates. At the second main station M157_12 no *Thiomargarita* cells could be detected. Additionally, biovolume and internal nitrate concentrations were determined at two additional stations along this transect (M157_14 and M157_17) in single measurements (Table 5.15). In general there was a trend for higher biovolumes and nitrate concentrations towards the coast. This observation was verified by labeling active *Thiomargarita* and *Beggiatoa* cells with the BONCAT method, which shows the build-up of new proteins. Again a tendency for stronger labelling towards the coast could be observed (Fig. 5.5.2). At the transect along the 25°S biovolume and internal nitrate concentration were determined at the two main stations M157_41 and M157_43 in triplicates. Both stations showed much higher biovolumes compared to the transect at 25°S. This finding was supported by BONCAT labelling and by the observation of many cells in division.

Table 5.5.1 Biovolume of *Thiomargarita* and internal nitrate concentrations. At station 16, 41 and 43 the average of 3 measurements is given. At station 14 and 17 both values werde dtermined only once.

Station	Biovolume (µl ml^{-1})	+/-	internal NO_3^- (mmol l^{-1})	+/-
M157_16	0.6	0.6	128	64
M157_14	0.2		445	
M157_17	0.4		585	
M157_41	2.5	2.5	188	80
M157_43	1.2	1.2	521	227

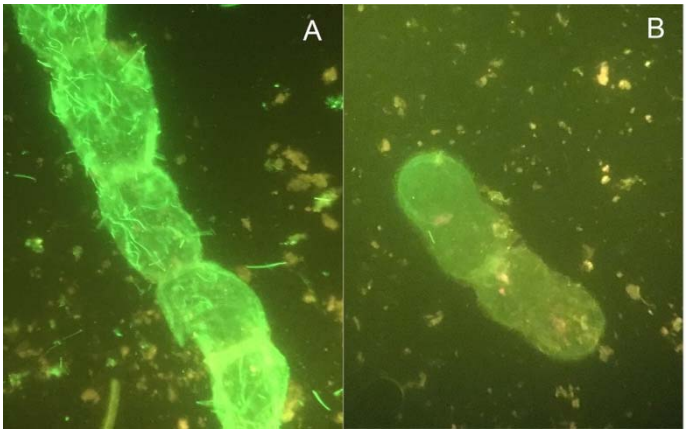

Fig. 5.5.2 Examples for *Thiomargarita* cells labelled with the BONCAT method to show growth by the incorporation of labelled amino acids. A, strongly labelled cells from station M157_17. B, Weakly labelled cells from station M157_14.

At all four main stations sulfide oxidation rates were determined and showed a high activity of sulfide oxidizing bacteria with higher values at the southern transect at 25°S.

In the northern transect *Thiomargarita* cells were not observed but at a single station M157_30 a so far unknown population of *Marithioploca* was discovered and sampled for sequencing of the 16S rRNA gene to determine its phylogenetic relation to *Marithioploca* from the Humboldt upwelling system.

5.6 Macrobenthic Ecology

(M.L. Zettler, K. Amorim, M. Tambo)

Low oxygen environments can be found in various marine settings – from shallow-water estuaries to open ocean continental shelves. Persistent low oxygen concentrations result in so-called oxygen minimum zones (OMZ) where bottom-water oxygen concentrations on the seafloor are per definition permanently <0,5 ml l^{-1}. In the Benguela upwelling system large sulphide-oxidizing bacteria (LSB) belonging to the Beggiatoceae fuel their metabolism with H_2S (Schulz & Jorgensen 2001) converting H_2S into non-toxic sulphur that accumulates as distinctive shiny white micro-granules in their cytoplasm. During anoxic conditions, nitrate stored in large vacuoles is used as the electron acceptor for anaerobic oxidation of sulphide. With the broad distribution of macrozoobenthic species, their presence in sulphidic areas is considered not directly related to H_2S, but possibly due to a detoxified habitat niche provided by the bacteria (Currie et al. 2018).

The core areas of OMZs have been subject to studies concerning ecological consequences of permanent low oxygen (e.g. Diaz & Rosenberg 2008, Stramma et al. 2012). The boundaries of OMZs, however, have not been considered as intensely even though they gain more and more importance with climate change having the potential to expand OMZs (Helly & Levin 2004). There have been numerous investigations focusing on benthic macrofaunal diversity, community structure and adaptation mechanisms (e.g. Diaz & Rosenberg 1995, Levin 2003, Zettler et al. 2009, Zettler & Pollehne 2013, Zettler et al. 2013, Eisenbarth & Zettler 2016). However, investigations of OMZ boundary communities have rather been part of comprehensive sampling strategies that have been conducted in order to investigate changes in macrobenthic community structure across oxygen gradients. These and other studies came to the conclusion that organisms that are able to cope with on the one hand potentially long-lasting hypoxia periods and on the other hand intense oxygen input e.g. by upwelling events can benefit from abundant food supply and build up high densities and biomass (Levin 2003, Gallardo et al. 2004). Dominant macrofaunal species of OMZ boundaries have been studied rather selectively. The main aim of our subgroup was the (1) comparison of macrobenthic diversity in the core area of the OMZ and on its edges and (2) to find out which living strategies allow surviving in this harsh environment. For the last point it is of special interest to focus on the behaviour of the animals, its metabolisms, morphological adaptations and symbionts.

5.6.1 Preliminary Results

During the cruise we sampled at all three transects: 7 stations on transect 17.3°S, 9 stations on transect 23°S and 10 stations on transect 25°S. In water depths up to 350 m at each station 3 Van-Veen-grabs (1000 cm^2) and 1 dredge haul were used for sampling the benthic diversity (Fig. 5.6.1). The material was sieved on-board. In addition at some stations we carried out sampling with MC (3-6 cores). The cores were used in experiments for oxygen demand, observation of species behaviour and for sediment analysis. In deeper waters (>350 m) a single box corer (2500 cm^2) were deployed (Fig. 5.6.1). The depth of the casts ranged between 500 and 2000 m. In cooperation with the Biochemistry Group (Section 5.7) especially in the oxygen minimum zones and their margins the lander was exposed. The sediment material sampled by the lander was later prepared (sieved) for further analysis. In the core area of the OMZ the dominant occurrence of *Lucinoma capensis* and *Nassarius vinctus* was obvious (Fig. 5.6.2). In the mud belt of the northern transect the bivalve *Lembulus bicuspidatus* occurred in high densities (Fig. 5.6.3).

In order to estimate nutrients and oxygen fluxes between water\sediment surfaces and further explore their relationship with soft sediment macrofauna diversity, we have performed incubations of sediment cores from seven different stations (Fig. 5.6.4). The incubations included triplicates of cores and blank vials containing water from the sediment cores surface. The concentrations of NO_2, NO_3, NH_4, SiO_2, PO_4 and oxygen were, at least, daily measured. Descriptions of animals' behaviour were additionally made with measurements. When possible, incubations were performed until, at least, one of the triplicates reach anoxia. By the end of the incubations, the cores were sieved and the macrofauna was fixed for further species identification. In parallel to the core incubations, 3 macrobenthic species were separately placed in gas tight vials filled with water from the bottom bottle of CTD from the station, or neighbour station, where the animals were collected, in order to estimate respiration rates and nutrient fluxes.

Selected species (*Lucinoma capensis, Lembulus bicuspidatus* and *Nassarius vinctus*) mainly from the dredge material at our main stations were stored in small incubation chambers to measure respiration rates or to expose to anoxic conditions for 40 hours. In order to analyse the metabolism mode utilized by two key species of macrofauna under contrasting oxygenation conditions, experiments with bivalves were performed by exposing individual to air saturated water, nitrogen saturated water, and/or reoxygenation. The gills and the labium were dissected before and after the incubation. Animal tissues were fixed by shock freezing or by placing tissues in RNA later, for further identification of metabolites present in the tissues. This material will be used to analyse metabolism pathways and to detect chemolithotrophic endosymbionts.

Regarding the biodiversity the analysis of the samples will take place in the laboratory about 3 months after the cruise and will probably needs more than a year. However, it is most obvious that the core area of the OMZ along the 23°S or 25° transects (40 to 120 m depth) shows a low diversity and density. Only very few species were found during this cruise. Only few ten meters deeper (>150 m) the diversity increased constantly down to 1000 m.

Fig. 5.6.1
The Van-Veen Grab was used in water depths down to 350 m, in deeper waters the heavy box corer was deployed.

Fig. 5.6.2 The edges of the core area along the 23°S and 25°S transects were dominated by the bivalve *Lucinoma capensis* (in the image however only few are alive) and the gastropod *Nassarius vinctus*.

Fig. 5.6.3 Although most of the shells are dead, *Lembulus bicuspidatus* belongs to the dominant species at the 17.3°S transect in water depths between 30 and 150 m. For the analysis of metabolism activities during and after the incubation we dissected the gills and labium of *L. bicuspidatus*.

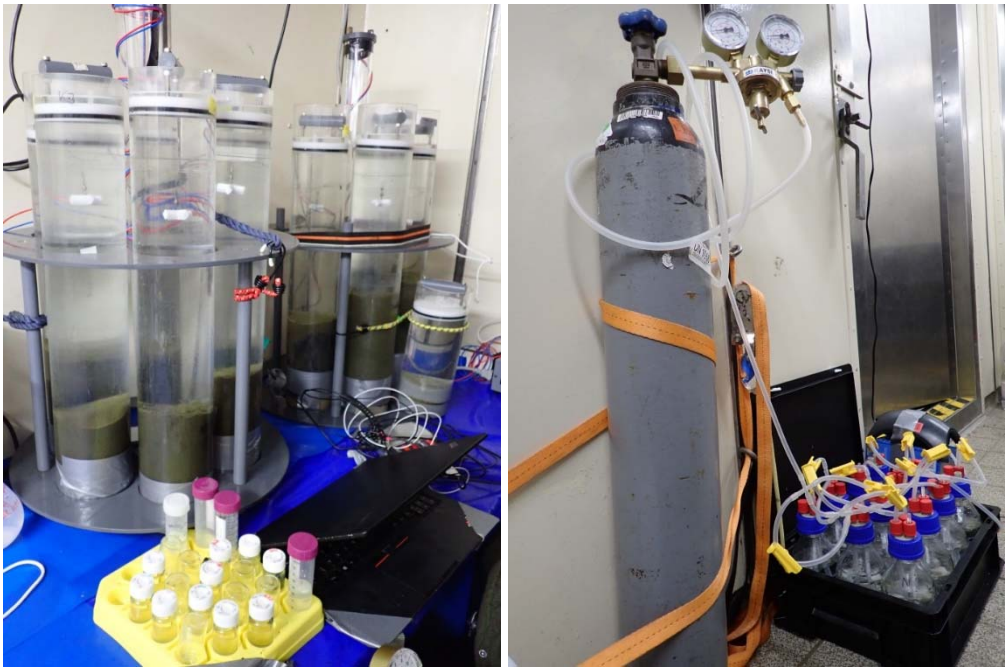

Fig. 5.6.4 Incubation for measurement of nutrient fluxes (left) and for study the metabolism pathways (right).

5.7 In Situ Flux Measurements and Experiments

(S. Sommer, A. Dale, H. Schulz-Vogt, M. Zettler, A. Beck, I. Mekelnburg, G. Nolte, M. Türk)

Central question of the work-package AP6 of the EVAR project is how benthic communities (bacteria and macrobenthos) respond to fluctuating redox-conditions characterized by the availability of oxygen (O_2) and nitrate (NO_3^-) in the bottom water and how this is reflected by benthic turnover rates and fluxes of O_2, the greenhouse gases methane (CH_4) and carbon dioxide (CO_2), as well as dissolved inorganic carbon, nutrients, sulfide, silicate and iron with particular respect to threshold levels, their magnitude and timing.

In cooperation with other work-packages, the interpretation of benthic biogeochemical flux and turnover measurements will help to address the following overarching aims of EVAR, i. to constrain key processes involved in benthic element cycling under variable bottom water redox conditions, ii. to resolve whether specific environmental conditions induce positive or negative feedbacks leading to overall regime shift in eastern boundary upwelling ecosystems, and iii. to recognize tipping points in biogeochemical element cycling in relation to upwelling variability and intensity.

5.7.1 Method

To best possibly address the questions mentioned above, we measured natural solute fluxes of the benthic environment. Moreover, in an experimental approach fluxes were measured, where the availability of O_2 and NO_3^- in the bottom water was manipulated directly at the seafloor. Two similar BIGO type Lander (Biogeochemical Observatory) were deployed, which independently from the ship enable the incubation of the seafloor and bottom water in two flux chambers for an extended time period of up to several days (Fig. 5.7.1).

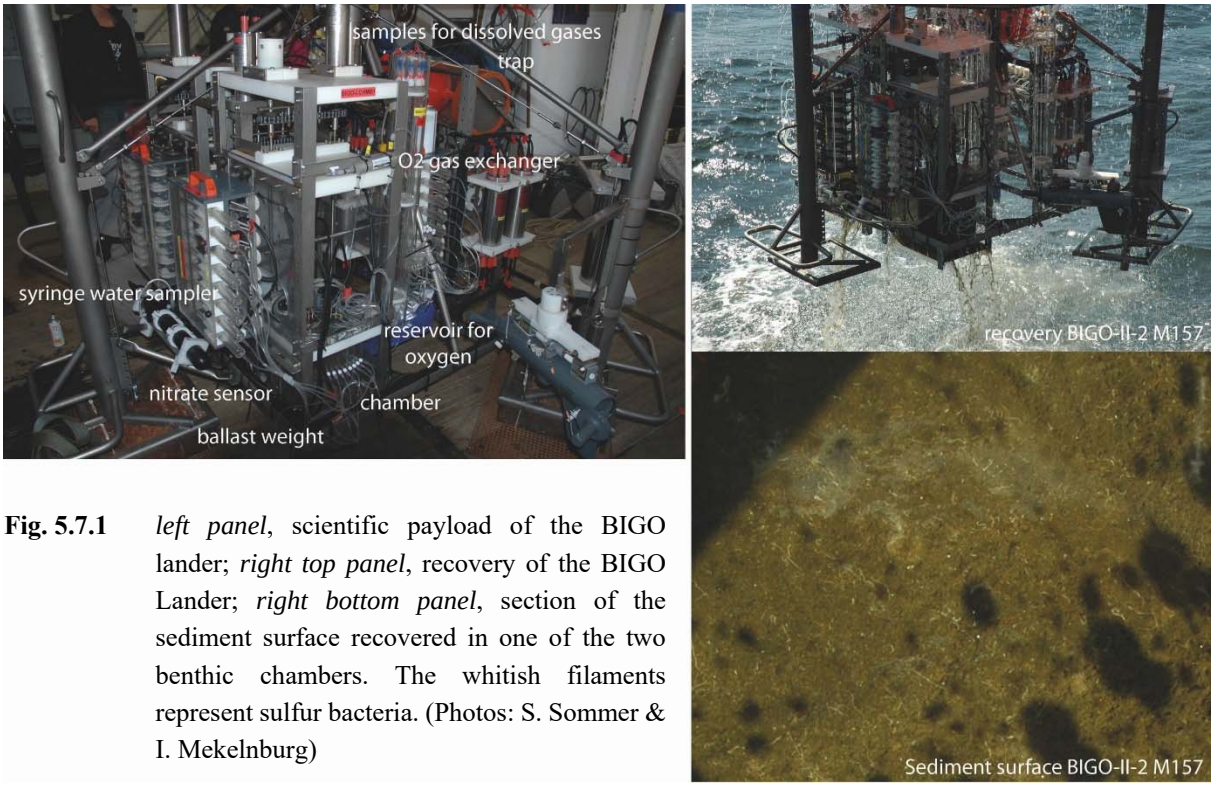

Fig. 5.7.1 *left panel*, scientific payload of the BIGO lander; *right top panel*, recovery of the BIGO Lander; *right bottom panel*, section of the sediment surface recovered in one of the two benthic chambers. The whitish filaments represent sulfur bacteria. (Photos: S. Sommer & I. Mekelnburg)

The BIGO type lander is described in detail by Pfannkuche and Linke (2003) and Sommer et al. (2009, 2016). In brief, the BIGO contained two circular flux chambers (internal diameter 28,8 cm, area 651,4 cm^2), herein referred to as chamber 1 (C1) and chamber 2 (C2). Typically, a TV-guided launching system allows smooth emplacement of the observatories at selected sites on the sea floor. However, during the cruise the bottom water was very turbid, hence we approached the seafloor using the launcher, but the lander was released without camera control in a distance of a few meters from the seafloor. Once, the observatories were placed on the sea floor the sediment was allowed to settle for several hours. Subsequently, the chambers were slowly driven into the sediment (~30 cm h^{-1}). During this initial time period, the water inside the flux chamber was periodically replaced with ambient bottom water. After the chamber was fully driven into the sediment, the water enclosed in the flux chambers was again replaced with ambient bottom water to flush out solutes that might have been released from the sediment during chamber insertion. The water volume enclosed by the benthic chambers was difficult to determine and needs careful assessment. The sediment was very soft and watery. In some cases, it was lost from the flux chambers when the lander was recovered on deck.

To determine the solute fluxes, eight sequential water samples were removed periodically with glass syringes (volume of each syringe ~46–47 ml). The syringes were connected to the chamber using 1 m long Vygon tubes with a dead volume of 6,9 ml. Prior to deployment, these tubes were filled with distilled water and care was taken to avoid enclosure of air bubbles. An additional syringe water sampler (8 sequential samples) was used to monitor the ambient bottom water. The sampling ports for ambient bottom water were positioned about 100 cm above the sediment-water interface. A subset of these syringe samples has been provided to the working group of G. Rehder (AP4, IOW, Warnemünde) for methane and DIC measurements.

For the measurement of dissolved gases (CH_4, pCO_2, sulfide) and dissolved inorganic carbon (DIC) water samples were pumped in to 750 mm long glass tubes with an internal diameter of 4,6 mm (volume ~12,5 ml) using a self-constructed 40 channel underwater peristaltic pump. Prior to deployment each glass tube was filled with distilled water, which was completely replaced by the sample without dilution. Eight tubes were used to sample each chamber and the ambient bottom water.

The incubations were conducted for time periods of 31,5 h to 34,7 h, defined by the time between the chamber was pushed into the sediment and the last syringe water sample was taken. Immediately after retrieval of the observatories, the water samples were transferred to the onboard cool room (10–12°C) for further sample processing. Due to limited space in the cool-room, during two BIGO deployments sampling took place on deck at air temperatures of about 12–14°C.

The O_2 concentration in each chamber and in the ambient bottom water was measured using optodes (Aanderaa Systems, Tengberg et al., 2006). As a novelty for our working group, two SUNA Sensors (Seabird Scientific) were used to measure NO_3^- inside chamber C2 of each BIGO. During BIGO deployments at the central mud belt station at 23°S the SUNA sensor was found to display a strong cross-sensitivity with sulfide levels higher than about 5–10 µmol l^{-1}. During the deployments BIGO-I-3 and BIGO-II-4 a prototype optical pH sensor (Pyroscience) was used in the ambient bottom water and in C2 respectively.

An oxygen gas exchange was used during some deployments to keep the O_2 level inside chamber 1 at a constant level. In principle, the system follows the system described by (Sommer et al. 2008). A reservoir of deionized water (MQ) was kept in a multilayer gastight bag which was prior to deployment bubbled with pure O_2 yielding a dissolved O_2 concentration of ~1350 µmol l^{-1}. The O_2

concentration inside the chamber was set to a distinct value and a pump was providing this solution to a gas exchanger (PDMSXA2500 or a smaller version) where gas exchange with the O_2 depleted chamber water took place. Between the chamber- and the reservoir circuit there was no exchange of water. Metadata (e.g. including position, depth, sampling intervals) of each lander deployment can be requested from S. Sommer (ssommer@geomar.de).

Geochemical parameters measured in the retrieved water samples (syringes, glass tubes) include: CH_4, pCO_2, O_2, DIC, phosphate, NO_3^-, NO_2^-, NH_4^+, sulfide, total alkalinity, Si, as well as IC and ICP MS data. Furthermore, where possible sediments were subsampled for microbial and macrobenthic analyses.

Additionally, the BIGO contained a trap for catching crustaceans in the benthic boundary layer using different fish baits (cf. Section 5.6).

5.7.2 Experimental Setup

At each main site, different experimental conditions were used:

- "control" treatment: One chamber was used for control flux measurements. These flux measurements are typically considered as fluxes of the natural system. During these incubations, the chambers were not manipulated in any way.
- During the "anoxia/NO_3" treatment NO_3^- was added to chamber C2 and tried to kept constant at the initial NO_3^- level at the beginning of the incubation or was set to a distinct value. This treatment addressed the effect of sustained ambient NO_3^- levels on the pathways of benthic nitrogen cycling during anoxia. It will be further determined to what extent sulfur bacteria make use of their internal NO_3^- storage or whether they use ambient NO_3^- for sulfide oxidation keeping their internal storage as a reserve for more adverse environmental conditions.
- During the oxic treatment the O_2 level in C1 was set to a distinct value. It was tried to maintain this O_2 level over the entire time period of the incubation. Whereas, the NO_3^- concentration was allowed to become depleted. This configuration was used to investigate the element turnover of the enclosed sediment system and the contribution of macro-benthic communities on the overall solute flux under conditions of ambient O_2 and NO_3^- levels for the entire duration of the incubation.

5.7.3 Preliminary Results

A total of 8 lander deployments were conducted at 4 main stations at the zonal transects at 23°S and 25°S (Table 5.7.1). At each site 2 deployments were carried out to apply all experimental treatments described above in a total of 4 chambers. The "anoxia/NO_3" treatment was conducted twice.

In the following, examples of in situ incubations at the center and the edge of the mud-belt along the 23°S transect are given. The sediments at both sites were extremely soft and watery. Similar conditions were encountered at the southern transect at 25°S. Upon recovery of the lander back on deck of R/V METEOR the chambers were not tight enough to prevent the water enclosed in the flux chambers to leak out. Hence sediment samples for geochemical porewater analyses were not taken. Remaining sediments were sampled for macrobenthos and occasionally for microbial analyses, please see respective reports. In some cases, upon recovery the overlying water body inside the flux chambers was turbid. Yet, the water sampled by the syringes were always clear indicating undisturbed conditions during the incubation at the seafloor.

Table 5.7.1 Station list of in situ flux measurements using BIGO I and BIGO II. MB: Mudbelt

Gear	Station	Date	Lat. S	Long. E	Depth (m)	Habitat
BIGO-I-1	M157_16	22.08.19	23°00’	014°13’	118	Center MB
BIGO-II-2	M157_16	26.08.19	23°00’	014°13’	113	Center MB
BIGO-II-1	M157_12	25.08.19	23°00’	013°52’	147	Edge MB
BIGO-I-2	M157_12	25.08.19	23°00’	013°52’	149	Edge MB
BIGO-I-3	M157_41	05.09.19	25°00’	014°23’	139	Center MB
BIGO-II-4	M157_41	09.09.19	25°00’	014°23’	139	Center MB
BIGO-I-4	M157_43	10.09.19	25°00’	014°34’	105	Edge MB
BIGO-II-3	M157_43	06.09.19	25°00’	014°34’	109	Edge MB

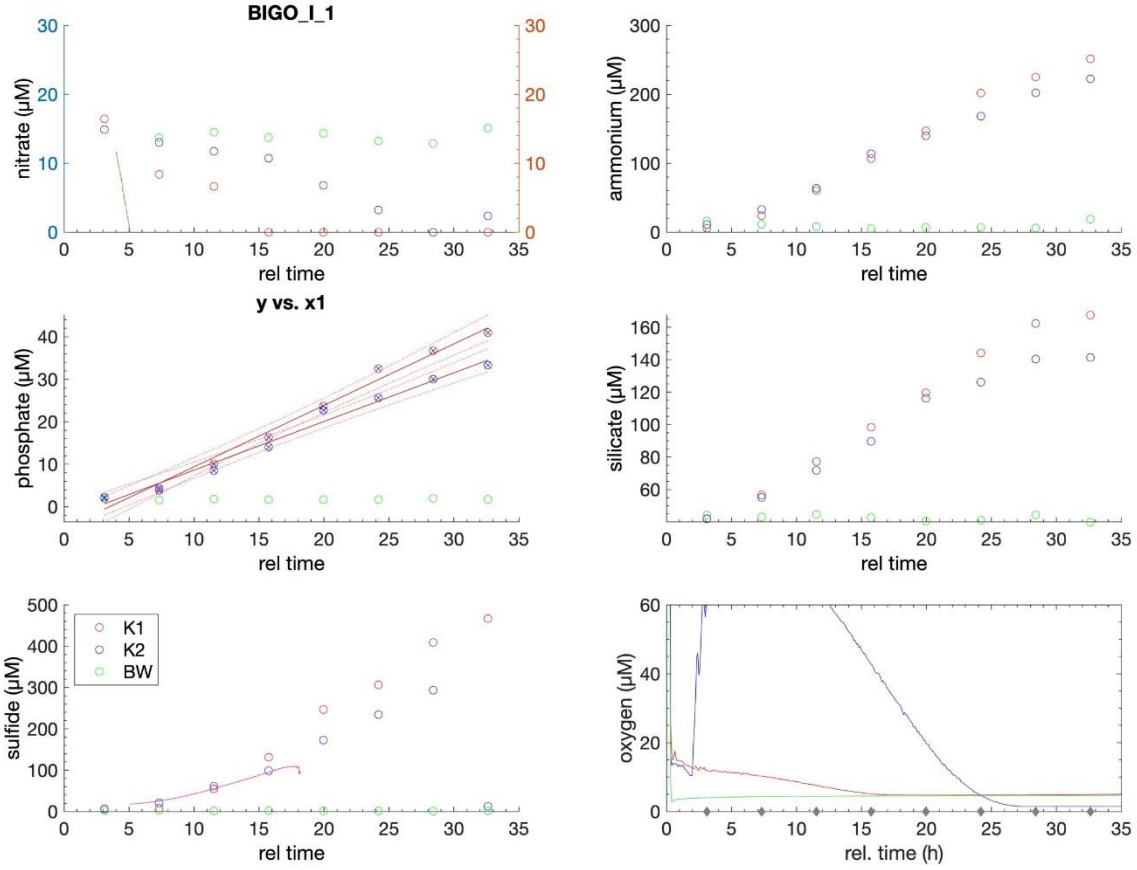

Fig. 5.7.1 Time course of solute concentrations in chamber 1 (K1, red circles), chamber 2 (K2, blue circles) and the ambient bottom water (BW, green circles) during the incubation BIGO-I-1 at the center of the mud-belt at 23°S. Continuous measurements of oxygen are depicted in the lower right panel using the same color code.

At the station M157_16 (BIGO-I-1) in the center of the mudbelt, the sediment surface was densely populated by sulfur bacteria. O_2 and NO_3^-, whose initial concentrations were low, were rapidly consumed (Fig. 5.7.1). Apparently, the degradation of organic matter predominantly takes place through bacterial sulfate respiration releasing high amounts of toxic sulfide into the pore water. With decreasing O_2 and NO_3^- levels, sulfide oxidation in the surface sediment was not sufficient to prevent seafloor sulfide emission. Concurrently with the release of sulfide high amounts of ammonium (NH_4^+) and phosphate (PO_4^{3-}) were emitted into the bottom water. Both fluxes are very high and cannot explained by organic matter degradation alone. During this deployment NO_3^- was added from a stock solution (200 µmol l^{-1}) into C2. However, this was not sufficient to compensate for its

enormous demand by the enclosed microbial community. For subsequent lander deployments, the concentration of the NO_3^- stock solution was then increased to 400 µmol l^{-1}. For the last two BIGO deployments the concentration of the NO_3^- stock solution was set to 1000 µmol l^{-1} using ^{15}N-NO_3^-. The high O_2 concentration in C2 likely results from the dissolution of small air bubbles, which became trapped in the pump circuit supplying the chamber water to the SUNA sensor. This was avoided during the subsequent deployments.

In contrast, the organic matter degradation at the fringe of the mud belt (M157_12, BIGO-II-2) was sustained by O_2 and NO_3^-, which were only slowly consumed (Fig. 5.7.2). NH_4^+, which mainly is released during organic matter degradation (ammonification), started to accumulate inside the flux chamber only after the concentrations of O_2 and NO_3^- became lower during the time course of the incubation. PO_4^{3-} was even slowly taken up by the seafloor. Sulfide was not detected at this rather inactive site.

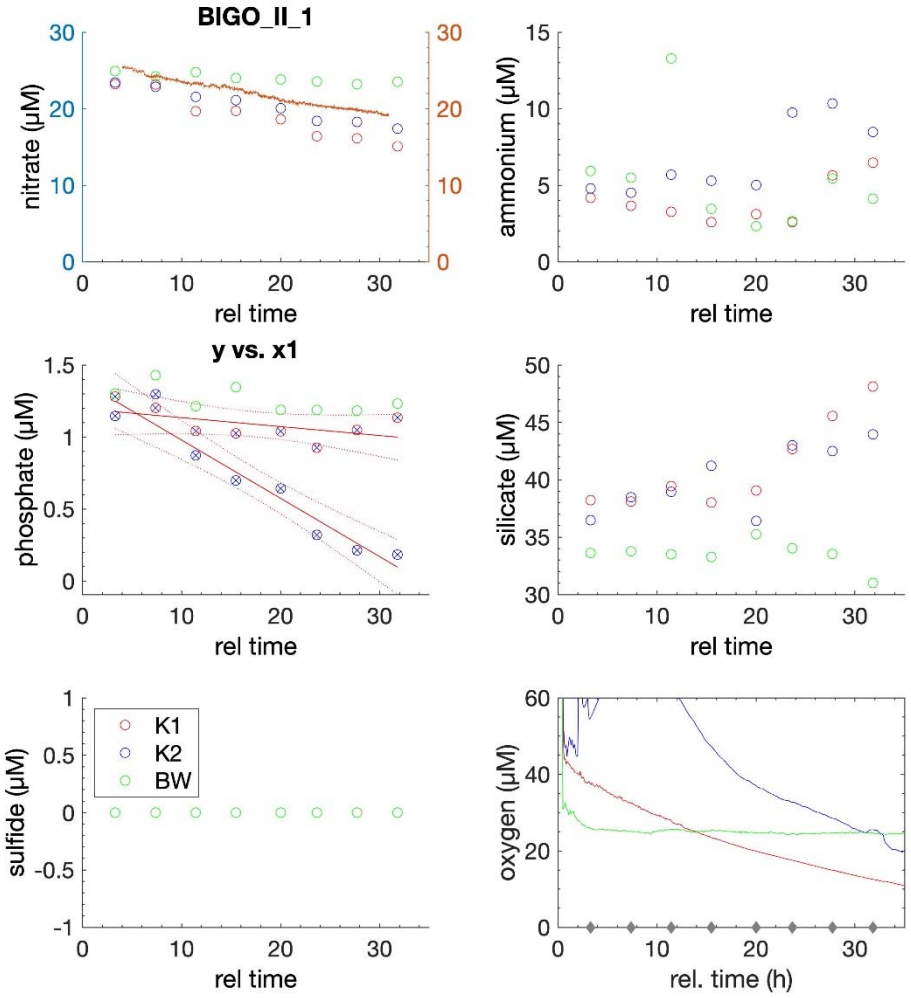

Fig. 5.7.2: Time course of solute concentrations in chamber 1 (K1, red circles), chamber 2 (K2, blue circels) and the ambient bottomwater (BW, green circles) during the incubation BIGO-II-1 at the fringe of the mud-belt at 23°S. Continuous measurements of oxygen are depicted in the lower right panel using the same color code. The brownish line shown in the upper left panel depicts continuous NO_3^- measurements using a Seabird Scientific SUNA sensor.

In cooperation with other working groups of the EVAR project further investigations about the micro- and macrobenthos as well as the release of trace gases were conducted.

5.7.5 Expected Results

After analysis and interpretation of the data we expect to quantitatively better understand the effect of variable availability of oxidants on the fluxes of particularly sulfide, NH_4^+, PO_4^{3-} as well as trace gases. This help us to couple the magnitude of these fluxes to variable physical and geochemical bottom water conditions and to gain a better up-scaling and predictive capability of benthic-pelagic coupling in the Benguela upwelling zone at seasonal and inter-annual time scales. We further hope to better constrain the role of sulfur bacteria, particularly *Thiomargarita namibiensis* in the cycling of sulfur, nitrate, ammonium and phosphate and to get better insight into the dynamics of sulfidic events.

5.8 Sediment Geochemistry

(F. Scholz, C. Anderson, M. Kossack, M. Zabel)

The coring device suited best for the sampling of undisturbed surface sediments, including overlying bottom water is the multicorer (MC; Fig. 5.8.1). The MC used during the cruise was equipped with six large plastic liners, each of 60 cm length and 10 cm in diameter. At most stations the MC was deployed multiple times to fulfill all scientific inquiries. In total the MC was deployed for pore water investigations at 8 times with great success. Depending on the sediment composition, the recovery of the MC cores varied between 25 and 55 cm. Depending on sediment characteristics, the hive and veer velocities varied from 0,3 to 0,5 ms^{-1}. Due to the very fluffy character of sediments in the Namibian mud belt, modifications to the MUC were necessary to prevent over-penetration into the sediment. Wooden planks were added to the coring device (Fig. 5.8.1).

Fig. 5.8.1:
Modified Multicorer (MUC). Wooden planks were added to prevent over-penetration of the device in the very fluffy sediments in the Namibian mud belt (courtesy M. Zabel).

To compliment expedition goals, longer sediment cores were retrieved with a classical gravity corer (GC). The GC consists of a 1,5 t head weight, steel pipes of 6–12 m length with internal, exchangeable plastic liners and a core catcher. The hive and veer velocities varied between 0,8 and 1,0 ms^{-1}. With 10 deployments in total, we could recover long sediment cores from 7 sites. Gravity cores recovered

during M157 varied in length from 2,1 to 9,8 m. The total length of all sediment cores recovered during expedition M157 is 34,2 m.

5.8.1 Work at Sea

Upon recovery on deck, all cores were stored in a refrigerated lab at a temperature of approximately 4°C after recovery to prevent warming of the sediments on board. The cores from the MC were processed within a few hours for pore water analysis, while the gravity cores were subsampled for pore water within 3 days of recovery.

Various analytical methods were used to characterize organic carbon and nutrient turnover in surface (MC) and subsurface (GC) sediments. Onboard investigations focused on pore waters, but sediment samples were also taken for subsequent analyses in our home labs. An overview about the types of analyses conducted and subsamples taken from each core is given in Table 5.8.1.

Table 5.8.1 Stations where pore extraction and analyses as well as sediment sampling were carried out for geochemical investigations

Gear	Station	Transect	Lat. S	Long. E	Water Depth (m)	GC Recovery (cm)
MC + GC	M157_12	23°S	23°00’	13°52,0’	151	526
MC + GC	M157_14	23°S	23°00’	14°02,9’	138	365
MC + GC	M157_16	23°S	23°00’	14°13,0’	119	437
MC + GC	M157_17	23°S	23°00’	14°19,0’	78	620
MC + GC	M157_34	25°S	25°00’	13°32,9’	626	984
MC + GC	M157_41	25°S	25°00’	14°22,6’	140	210
MC + GC	M157_43	25°S	25°00’	14°33,9’	107	280
MC	M157_48	25°S	25°00’	14°12,4’	173	---

Bottom water of the MC cores was siphoned with a plastic tube and filtered for subsequent analyses. To prevent oxidation of reduced substances, MC cores were subsampled in a glove bag under argon atmosphere at maximum resolution of 1–4 cm. A defined volume of sediment was sampled into pre-weighed plastic cups for the determination of water content and porosity. Pore water was collected by centrifuging sediment samples in cooled centrifuge for 20 minutes at 4000 rpm. The supernatant pore water samples were filtered (0,2 nm cellulose-acetate filters) under argon atmosphere in a second glove bag. Sediment samples in centrifuge tubes were kept for shore-based analyses of the solid phase.

GCs were immediately sectioned into one meter segments on deck after recovery. A defined sediment volume of 5 cm^3 was sampled into glass vials containing a saturated NaCl solution for methane and hydrocarbon isotope headspace analyses. In addition, sediment samples were taken for radiocarbon dating as well as water content and porosity at section cuts (see above). Pore waters from GCs were recovered using Rhizon micro suction samplers (RSS, 5 cm, 0,2 µm porous polymer, Rhizosphere Research) at a resolution of 15–40 cm. The first ml extracted by the Rhizons was discarded to prevent oxidation artifacts.

Dissolved iron (Fe^{2+}) and phosphate (PO_4^{3-}) concentrations were determined photometrically (Hach Lange DR 5000 photometer) at 565 nm and 880 nm wavelengths. An iron sensitive color complex was formed by adding 1 mL of acidified sample (20 µL of 1% ascorbic acid) to 50 µL of a ferrospectral receiver in disposable polystyrene cuvettes. Phosphate concentrations were determined by application of the Molybdenum Blue method (Grasshoff et al. 1999). About 1 mL of sample was

mixed with 50 µL of an ammonium molybdate solution in a disposable polysterene cuvette and spiked with 50 µL of an ascorbic acid solution. The phosphomolybdate complex was thus reduced to molybdenum blue. Highly sulfidic samples were spiked with 20 µL of 30% HCl and bubbled with argon for one minute to remove sulfide interference during PO_4^{3-} analysis.

Ammonium (NH_4^+) was detected onboard with a flow injection Teflon-tape gas separator technique after Hall & Aller (1992). Approximately 200–300 µL of plain sample was injected into the analytical line by an auto sampler, and mixed with an alkaline solution (0,01 M NaOH + 0,2 M Na citrate) to form gaseous NH_3. The gaseous phase passed through a PTFE membrane and caused a conductivity signal in a receiving acid solution (0,001 M HCl, 34 µS cm1). The resulting conductivity was determined using a temperature compensated conductivity meter with flow-through-cell (Amber Science 1056 and 529) and recorded electronically.

In addition to the aliquots used for onboard analyses of the parameters mentioned above, we collected the following sample splits for onshore laboratory analyses when allowed by available pore water volume: 1,8 mL of sample each for DIC and NPOC, 0,1 mL diluted with 1,9 ml Milli-Q water for onshore anion analysis, 0,5 mL of sample diluted with 4,5 mL of 1 M HNO_3 for cation analysis, 1 mL of sample preserved with 0,5 mL zinc acetate solution for onshore H_2S analysis, 2 ml for the nitrogen isotope composition of NH_4^+ (lander stations only), and 8 ml for the analyses of trace metal concentration and isotope ratios (MC cores only). The remaining sample was stored without the addition of preservatives.

5.8.2 Preliminary results

The sediment geochemistry group focused on the two offshore transects at 23°S and 25°S. Examples of pore water profiles of Fe^{2+}, PO_4^{3-} and NH_4^+ at two MC stations within (M157-16) and at the outer rim (M157-12) of the mud belt at 23°S are given in Fig. 5.8.2.

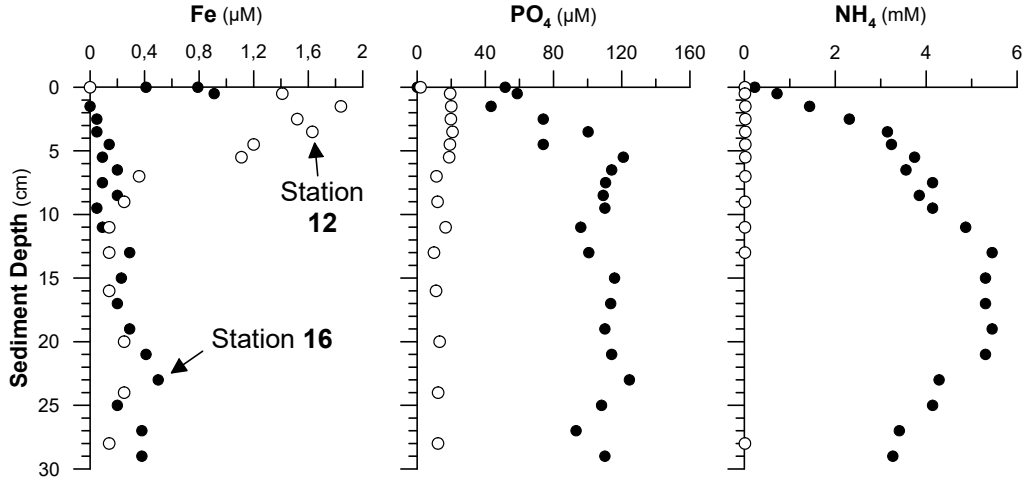

Fig. 5.8.2: Examples of pore water profiles of Fe^{2+}, PO_4^{3-} and NH_4^+ at two station within (Station 16; 119 m wd) and at the outer rim (Station 12; 151 m wd) of the mud belt at 23°S.

Pore water Fe^{2+} profiles at Stations 12 and 16 are characterized by a peak within the uppermost 10 cm of the sediment. Increasing Fe^{2+} concentrations across the sediment-water interface indicate an upward directed diffusive benthic flux. Iron concentrations at station 16 are lower and the gradient across the sediment-water interface is less pronounced. This observation can be explained by more reducing conditions and, thus, higher H_2S concentrations in surface sediments within the mud belt.

Due to sulfidic conditions within the surface sediment, a higher proportion of the sedimentary reactive Fe can be retained and buried as Fe sulfide mineral. In contrast to Fe^{2+}, pore water PO_4^{3-} and NH_4^+ concentrations increase from the outer rim to the center of the mud belt. Phosphate and NH_4^+ are primarily released from organic material that is decomposed within the sediment. Therefore, increasing PO_4^{3-} and NH_4^+ concentrations from Station 12 to Station 16 reflect increasing organic carbon rain and degradation rates between these two sites.

A GC was retrieved at 7 of the 8 MC stations. Examples of pore water profiles of PO_4^{3-} and NH_4^+ in the MC and GC at Station 17 are given in Fig. 5.8.3. The offset between pore water profiles in MCs and GCs was used to determine how much surface sediment was lost during the recovery of the GC. In this case the data may indicate that the upper 32 cm of the GC sediment core have been lost. Ammonia concentration increase throughout the recovered depth interval, which is indicative of intense organic matter degradation in subsurface sediments. Simultaneous release of phosphate from decaying organic matter is not reflected by the pore water profiles. Instead, PO_4^{3-} concentrations are constant throughout the GC. This observation suggests that pore water PO_4^{3-} is in equilibrium with authigenic phosphate minerals that have precipitated during early diagenesis (i.e., carbonate fluorapatite, CFA).

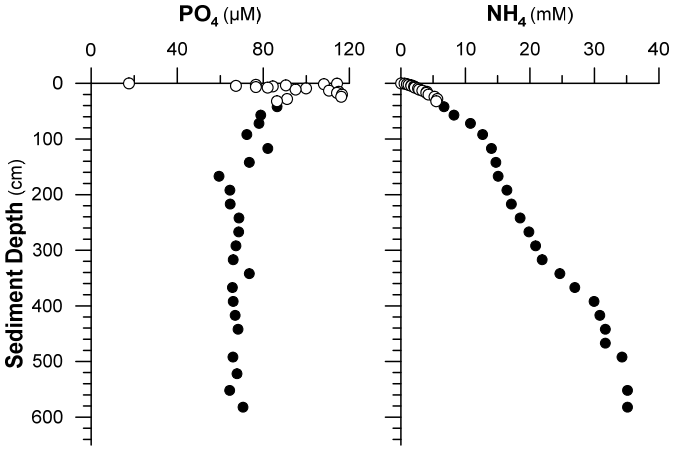

Fig. 5.8.3: Pore water profiles of PO_4^{3-} and NH_4^+ in a MC and GC at Station 17 within the mud belt at 23°S.

Ongoing work in home-based laboratories will focus on a quantification of benthic nutrient turnover and fluxes as well as a precise dating of the sedimentary records recovered with the GCs. The latter will be necessary to reconstruct oxygenation and element turnover in the OMZ off Namibia on millennial timescale across the Holocene.

6 Ship's Meteorological Station

(M. Stelzner)

On the fourth of August 2019 at 7 am, R/V METEOR departed from Mindelo (Sao Vicente, Cape Verde). The cruise begun with a two-week transit to Walvis Bay (Namibia). The weather in the cruise area was influenced by a northerly flow at the edge of a subtropical high with its centre area southwest of the Azores. The wind strength was between four to five Beaufort. The significant wave height was approx. 1,5 metre and composed mainly two swell components, one from the North and one from the South, latter increasing with time.

From the sixth to the eight of August 2019, R/V METEOR sailed in the area of the Intertropical Convergence Zone (ITCZ). The wind backed to west and further to southwest and increased to six Beaufort for one day, which was due to a small depression in the African coastal area. At the same time, the shower and thunderstorm activity in the vicinity of R/V METEOR increased.

Upon reaching the equator at noon on the 9th of August, the wind turned first to south and later to southeast. The now steady southeast trade wind mostly blew with four to five Beaufort. A persistent swell of 2 m height from southeast was observed. The further south R/V METEOR sailed the more the air temperature dropped with around 1°C per day. While 22°C were measured near the equator, the temperature had dropped to only 12°C at the approach of Walvis Bay. On the 17th of August 2019, R/V METEOR reached the harbour of Walvis Bay in dense fog. This fog remained while in port over the next 1,5 days during the stay of R/V METEOR.

On 18th August 2019 at 1800 hours, R/V METEOR left the harbour of Walvis Bay and the research cruise M157 commenced. The research cruise was divided into 3 research areas along the latitudes of 17.3°S, 23°S and 25°S. The first research area at 23°S was reached after a few hours travel from Walvis Bay. For ten days, research was carried out between 13°E and the coast of Namibia. The weather was influenced by a subtropical high with its centre over the south-eastern Atlantic. In a southerly to south-easterly flow the wind strength was mostly four to five Beaufort. The significant wave height was 2 to 2,5 metre.

From the 20th of August 2019, a trough extended far south along the African Atlantic coast, starting from the tropical low-pressure zone in the north. Small-scale pressure systems were embedded in this trough, which in the following days caused changeable, albeit mostly weak, wind conditions in the research area. The swell, mostly coming from southwest, rarely rose above 1,5 metre. In the night to the 22th of August 2019 fog formed, which lasted almost the whole day. The calm, but with about 13°C quite cool weather stayed until the 25th of August 2019.

On the 26th of August 2019 the subtropical high shifted a little to the east, which intensified the pressure difference along the whole southwest African coast. The wind was blowing again from a constant southern to south-eastern direction and increased to five to six Beaufort. One day later, a stronger swell reached the cruising area. Together with the slightly increased wind sea, the significant wave height now increased to 3 metre.

On the 29th of August 2019, the research at 23°S concluded and the transit to the second research area along 17,3°S began. With six Beaufort wind from south and an unchanged sea state the research area was reached already after one day due to following seas. Meanwhile the wind increased further: in the night to the 31th of August 2019, the wind speed peaked at eight Beaufort with gusts up to 48,3 kn (Beaufort 10).

After only two days research in the second area along 17,3°S, work concluded and the transit to the third section at 25°S began. At the same time, a new trough strengthened over the coastal area and spread again far south coming from the tropics. The wind decreased and mostly blew from southern directions, at times variable with less than four Beaufort. The significant wave height decreased to 1,5 to 2 metre. In the evening of the third of September 2019, R/V METEOR reached the research area at 25°S, again accompanied by dense fog, which only lasted until night. In the following days, the wind and the significant wave height barely changed at all.

In the night of the sixth of September 2019, the wind turned for two days to a northerly direction, it remained however very weak. The humid air led again to dense fog. Until shortly before the end of the cruise, the above mentioned south reaching trough dominated the weather condition around R/V METEOR. The wind came weakly from different directions; the significant wave height fell to less than 1 metre, on the ninth of September 2019 even to less than 0,5 metre and again fog fields formed.

On the last two days, the subtropical high was pushed north and northeast by a storm low situated in the middle latitudes. As a result, the now constant wind from south to southeast increased to five to six Beaufort. Due to a further swell field, the significant wave height increased again to 2 to 2,5 metre.

7 Station List 157

Station No.	Date 2019	Time (UTC)	Device	Action	Latitude (S)	Longitude (E)	Water Depth (m)
Transit from Mindelo to Walvis Bay							
M157_1-1	12.08.	12:16	CTD	max depth	09° 26,716'	000° 25,532'	5462
M157_1-2	12.08.	12:44	AC-S	max depth	09° 26,716'	000° 25,533'	5444
M157_1-3	12.08.	13:31	P-CTD	in water	09° 26,717'	000° 25,533'	5443
M157_1-4	12.08.	14:13	MSS	in water	09° 26,841'	000° 25,604'	5915
M157_1-5	12.08.	15:06	Scanfish	profile start	09° 28,146'	000° 26,392'	5428
Transect at 23°S							
M157_2-1	18.08.	18:10	Scanfish	profile start	23° 00,512'	014° 21,937'	46 / 605
M157_3-1	19.08.	10:19	MSS	in water	22° 59,898'	012° 56,764'	602
M157_4-1	19.08.	12:31	MSS	in water	23° 00,028'	012° 46,972'	948
M157_5-1	19.08.	14:42	MSS	in water	22° 59,991'	012° 34,815'	1441
M157_6-1	19.08.	18:02	CTD	max depth	23° 00,000'	012° 20,008'	2072
M157_6-2	19.08.	19:20	AC-S	max depth	23° 00,001'	012° 20,005'	2074
M157_6-3	19.08.	19:36	MSS	in water	23° 00,012'	012° 20,011'	2078
M157_6-4	19.08.	21:43	BC	on ground	23° 00,004'	012° 20,000'	2071
M157_4-2	20.08.	02:56	BC	on ground	22° 59,997'	012° 46,996'	946
M157_7-1	20.08.	05:37	MSS	in water	23° 00,007'	013° 02,989'	386
M157_8-1	20.08.	07:24	MSS	in water	22° 59,985'	013° 08,999'	322
M157_9-1	20.08.	10:22	MSS	in water	23° 00,030'	013° 18,991'	361
M157_10-1	20.08.	13:25	MSS	in water	22° 59,970'	013° 30,017'	240
M157_11-1	20.08.	15:14	MSS	in water	23° 00,017'	013° 41,004'	150
M157_12-1	20.08.	17:12	MSS	in water	23° 00,005'	013° 51,974'	152
M157_13-1	20.08.	18:55	MSS	in water	22° 59,963'	013° 57,477'	145
M157_14-1	20.08.	20:33	MSS	in water	22° 59,981'	014° 02,725'	140
M157_15-1	20.08.	22:06	MSS	in water	23° 00,062'	014° 07,962'	136
M157_16-1	21.08.	00:19	MSS	in water	23° 00,005'	014° 12,962'	112
M157_17-1	21.08.	01:53	MSS	in water	23° 00,062'	014° 18,952'	2704
M157_2-2	21.08.	02:59	MSS	in water	22° 59,988'	014° 21,996'	94
M157_12-2	21.08.	06:10	CTD	max depth	23° 00,003'	013° 51,997'	152
M157_12-3	21.08.	06:49	AC-S	max depth	23° 00,000'	013° 51,993'	151
M157_12-4	21.08.	08:28	OFOS	profile start	22° 59,994'	013° 52,142'	148
M157_12-5	21.08.	09:27	MC	on ground	22° 59,996'	013° 51,994'	151
M157_12-6	21.08.	10:03	MC	on ground	22° 59,995'	013° 51,995'	151
M157_12-7	21.08.	10:37	MC	on ground	22° 59,995'	013° 51,994'	150
M157_12-8	21.08.	11:04	MC	on ground	22° 59,995'	013° 51,994'	150
M157_12-9	21.08.	11:29	MC	on ground	22° 59,995'	013° 51,994'	151
M157_12-10	21.08.	18:09	Lander	deployed	23° 00,006'	013° 52,005'	148
M157_14-2	21.08.	20:00	CTD	max depth	23° 00,007'	014° 02,798'	138

Station No.	**Date** 2019	**Time** (UTC)	**Device**	**Action**	**Latitude** (S)	**Longitude** (E)	**Water Depth** (m)
M157_14-3	21.08.	20:32	AC-S	max depth	23° 00,008'	014° 02,800'	139
M157_14-4	21.08.	20:55	P-CTD	in water	23° 00,009'	014° 02,804'	138
M157_14-5	22.08.	07:39	Mooring	on deck	22° 59,944'	014° 02,956'	139
M157_14-6	22.08.	08:26	Dredge	on ground	23° 00,001'	014° 02,934'	140
M157_14-7	22.08.	09:46	OFOS	profile start	23° 00,253'	014° 02,937'	139
M157_14-8	22.08.	10:46	MC	on ground	22° 59,983'	014° 02,983'	137
M157_14-9	22.08.	11:12	MC	on ground	22° 59,984'	014° 02,983'	139
M157_14-10	22.08.	11:27	MC	on ground	22° 59,985'	014° 02,981'	139
M157_14-11	22.08.	11:45	MC	on ground	22° 59,984'	014° 02,982'	138
M157_14-12	22.08.	12:04	MC	on ground	22° 59,986'	014° 02,986'	137
M157_16-2	22.08.	17:11	Lander	deployed	23° 00,006'	014° 13,016'	118
M157_16-3	22.08.	17:53	CTD	max depth	23° 00,000'	014° 12,943'	119
M157_16-4	22.08.	18:27	AC-S	max depth	23° 00,000'	014° 12,942'	115
M157_16-5	22.08.	18:55	MSS	in water	22° 59,526'	014° 12,954'	114
M157_16-6	22.08.	19:51	P-CTD	in water	22° 59,991'	014° 12,932'	114
M157_12-11	23.08.	06:27	Lander	released	22° 59,844'	013° 51,881'	151
M157_12-12	23.08.	08:34	Dredge	on ground	23° 00,037'	013° 52,026'	150
M157_12-13	23.08.	09:53	VVG	on ground	23° 00,035'	013° 52,125'	151
M157_12-14	23.08.	10:15	VVG	on ground	23° 00,034'	013° 52,124'	152
M157_12-15	23.08.	10:35	VVG	on ground	23° 00,035'	013° 52,124'	151
M157_12-16	23.08.	10:46	VVG	on ground	23° 00,035'	013° 52,125'	151
M157_12-17	23.08.	11:26	MC	on ground	23° 00,035'	013° 52,123'	149
M157_12-18	23.08.	12:06	MC	on ground	23° 00,034'	013° 52,124'	150
M157_14-13	23.08.	15:05	Mooring	deployed	23° 00,019'	014° 03,061'	135
M157_15-2	23.08.	16:39	MC	on ground	23° 00,007'	014° 08,008'	136
M157_15-3	23.08.	16:55	MC	on ground	23° 00,009'	014° 08,009'	135
M157_15-4	23.08.	17:28	MC	on ground	23° 00,001'	014° 08,007'	140
M157_15-5	23.08.	17:56	MC	on ground	23° 00,002'	014° 08,007'	139
M157_15-6	23.08.	18:22	Dredge	on ground	23° 00,003'	014° 08,032'	140
M157_15-7	23.08.	19:02	MC	on ground	23° 00,002'	014° 08,079'	140
M157_15-8	23.08.	19:24	MC	on ground	23° 00,003'	014° 08,081'	139
M157_15-9	23.08.	19:46	VVG	on ground	23° 00,003'	014° 08,080'	139
M157_15-10	23.08.	20:00	VVG	on ground	23° 00,002'	014° 08,078'	136
M157_15-11	23.08.	20:14	VVG	on ground	23° 00,002'	014° 08,078'	138
M157_15-12	23.08.	20:33	VVG	on ground	23° 00,002'	014° 08,079'	138
M157_15-13	23.08.	20:46	VVG	on ground	23° 00,002'	014° 08,079'	133
M157_15-14	23.08.	21:22	CTD	max depth	23° 00,002'	014° 08,079'	138
M157_15-15	23.08.	22:00	AC-S	max depth	23° 00,002'	014° 08,081'	140
M157_17-2	23.08.	23:31	CTD	max depth	23° 00,009'	014° 18,999'	76
M157_17-3	24.08.	00:03	AC-S	max depth	23° 00,008'	014° 19,000'	80
M157_17-4	24.08.	00:16	VVG	on ground	23° 00,008'	014° 19,001'	79
M157_17-5	24.08.	00:27	VVG	on ground	23° 00,008'	014° 19,002'	77
M157_17-6	24.08.	00:38	VVG	on ground	23° 00,008'	014° 19,001'	77
M157_17-7	24.08.	00:43	VVG	on ground	23° 00,009'	014° 19,000'	76
M157_17-8	24.08.	00:49	VVG	on ground	23° 00,009'	014° 19,002'	77

Station No.	Date 2019	Time (UTC)	Device	Action	Latitude (S)	Longitude (E)	Water Depth (m)
M157_17-9	24.08.	01:21	Dredge	on ground	23° 00,040'	014° 19,105'	76
M157_2-3	24.08.	02:53	Dredge	on ground	23° 00,027'	014° 22,206'	85
M157_2-4	24.08.	03:45	VVG	on ground	23° 00,011'	014° 22,006'	45
M157_2-5	24.08.	03:55	VVG	on ground	23° 00,012'	014° 22,008'	46
M157_2-6	24.08.	04:06	VVG	on ground	23° 00,011'	014° 22,009'	46
M157_2-7	24.08.	04:28	AC-S	max depth	23° 00,011'	014° 22,008'	46
M157_2-8	24.08.	04:52	CTD	max depth	23° 00,010'	014° 22,005'	46
M157_16-7	24.08.	07:10	Mooring	recovered	23° 00,332'	014° 13,475'	112
M157_16-8	24.08.	08:04	Lander	recovered	23° 00,039'	014° 12,940'	113
M157_16-9	24.08.	19:27	MC	on ground	23° 00,039'	014° 12,942'	115
M157_16-10	24.08.	10:46	MC	on ground	23° 00,038'	014° 12,942'	114
M157_16-11	24.08.	11:05	MC	on ground	23° 00,039'	014° 12,941'	114
M157_16-12	24.08.	11:19	MC	on ground	23° 00,039'	014° 12,942'	113
M157_16-13	24.08.	11:34	MC	on ground	23° 00,038'	014° 12,942'	114
M157_16-14	24.08.	12:29	CTD	max depth	23° 00,037'	014° 12,942'	116
M157_14-14	24.08.	14:33	CTD	max depth	22° 59,999'	014° 03,196'	132
M157_14-15	24.08.	15:47	P-CTD	in water	22° 59,998'	014° 03,196'	139
M157_12-19	24.08.	17:59	MSS	in water	23° 00,021'	013° 52,006'	151
M157_12-20	24.08.	19:11	P-CTD	in water	22° 59,997'	013° 51,989'	152
M157_12-21	25.08.	03:35	CTD	max depth	22° 59,997'	013° 52,000'	150
M157_10-2	25.08.	06:02	VVG	on ground	22° 59,997'	013° 29,917'	242
M157_10-3	25.08.	06:32	VVG	on ground	22° 59,997'	013° 29,916'	242
M157_10-4	25.08.	07:00	VVG	on ground	22° 59,997'	013° 29,916'	242
M157_10-5	25.08.	07:38	Dredge	on ground	22° 59,997'	013° 30,023'	241
M157_10-6	25.08.	08:54	AC-S	max depth	22° 59,996'	013° 30,009'	240
M157_10-7	25.08.	09:15	CTD	max depth	22° 59,995'	013° 30,009'	241
M157_10-8	25.08.	10:01	MC	on ground	22° 59,995'	013° 30,010'	241
M157_10-9	25.08.	19:37	MC	on ground	22° 59,996'	013° 30,010'	241
M157_10-10	25.08.	11:06	MC	on ground	22° 59,995'	013° 30,010'	241
M157_10-11	25.08.	11:24	MC	on ground	22° 59,995'	013° 30,009'	241
M157_12-22	25.08.	17:10	Lander	deployed	22° 59,999'	013° 52,008'	149
M157_9-2	25.08.	20:43	CTD	max depth	22° 59,990'	013° 18,988'	361
M157_9-3	25.08.	21:20	AC-S	max depth	23° 00,004'	013° 19,004'	361
M157_9-4	25.08.	21:56	VVG	on ground	23° 00,004'	013° 19,002'	362
M157_9-5	25.08.	22:14	VVG	on ground	23° 00,004'	013° 19,004'	362
M157_9-6	25.08.	22:33	VVG	on ground	23° 00,003'		362
M157_9-7	25.08.	23:16	Dredge	on ground	23° 00,054'	013° 19,305'	360
M157_11-2	26.08.	02:21	VVG	on ground	22° 59,988'	013° 40,992'	154
M157_11-3	26.08.	02:40	VVG	on ground	22° 59,988'	013° 40,994'	154
M157_11-4	26.08.	03:36	CTD	max depth	22° 59,988'	013° 40,994'	158
M157_11-5	26.08.	04:20	AC-S	max depth	22° 59,987'	013° 40,994'	154
M157_16-15	26.08.	08:53	BTP	on ground	23° 00,001'	014° 12,992'	114
M157_16-16	26.08.	10:36	MC	on ground	23° 00,003'	014° 12,995'	114
M157_16-17	26.08.	11:03	MC	on ground	23° 00,002'	014° 12,998'	117
M157_16-18	26.08.	11:32	MC	on ground	23° 00,003'	014° 12,999'	114

Station No.	**Date** 2019	**Time** (UTC)	**Device**	**Action**	**Latitude** (S)	**Longitude** (E)	**Water Depth** (m)
M157_16-19	26.08.	11:46	MC	on ground	23° 00,004'	014° 12,999'	113
M157_16-20	26.08.	11:56	MC	on ground	23° 00,003'	014° 13,000'	114
M157_16-21	26.08.	17:06	Lander	released	23° 00,025'	014° 12,988'	114
M157_17-10	26.08.	20:11	MSS	in water	22° 58,796'	014° 19,110'	76
M157_12-23	27.08.	11:45	Lander	released	23° 00,029'	013° 52,089'	149
M157_12-24	27.08.	13:36	Drifter	deployed	22° 59,933'	013° 51,954'	150
M157_12-25	27.08.	14:33	GC	on ground	22° 59,935'	013° 51,980'	151
M157_14-16	27.08.	18:00	GC	on ground	22° 59,884'	014° 02,885'	138
M157_16-22	28.08.	06:52	GC	on ground	22° 59,825'	014° 12,970'	119
M157_17-11	28.08.	08:53	GC	on ground	22° 59,980'	014° 18,964'	77
M157_17-12	28.08.	09:34	GC	on ground	22° 59,994'	014° 18,986'	78
M157_17-13	28.08.	10:43	MC	on ground	23° 00,000'	014° 19,005'	77
M157_17-14	28.08.	11:12	MC	on ground	23° 00,000'	014° 19,000'	77
M157_17-15	28.08.	11:33	MC	on ground	22° 59,966'	014° 19,006'	79
M157_16-23	28.08.	12:42	Lander	released	23° 00,022'	014° 13,037'	114
M157_16-24	28.08.	13:25	CTD	max depth	22° 59,995'	014° 12,962'	113
M157_14-17	28.08.	15:25	MC	on ground	22° 59,989'	014° 03,011'	139
M157_12-26	28.08.	17:04	MC	on ground	22° 59,990'	013° 52,003'	149
M157_12-27	28.08.	17:28	MC	on ground	22° 59,968'	013° 52,007'	149
M157_8-2	28.08.	22:12	CTD	max depth	22° 59,963'	013° 08,967'	321
M157_8-3	28.08.	22:48	AC-S	max depth	22° 59,965'	013° 08,968'	321
Transect at 17,5°S							
M157_18-1	30.08.	00:54	Mooring	released	17° 59,863'	011° 39,199'	132
M157_18-2	30.08.	13:23	Mooring	deployed	18° 00,006'	011° 39,086'	131
M157_19-1	30.08.	13:47	MSS	in water	18° 00,250'	011° 41,803'	112
M157_20-1	30.08.	15:18	MSS	in water	17° 59,928'	011° 42,990'	93
M157_21-1	30.08.	16:39	MSS	in water	17° 59,936'	011° 37,947'	131
M157_22-1	30.08.	17:53	MSS	in water	17° 59,761'	011° 34,891'	187
M157_23-1	30.08.	19:22	MSS	in water	17° 59,938'	011° 30,898'	234
M157_24-1	31.08.	02:23	CTD	max depth	17° 16,023'	011° 43,445'	34
M157_24-2	31.08.	02:38	AC-S	max depth	17° 16,022'	011° 43,445'	34
M157_24-3	31.08.	03:25	VVG	on ground	17° 16,023'	011° 43,443'	33
M157_24-4	31.08.	03:36	VVG	on ground	17° 16,022'	011° 43,445'	33
M157_24-5	31.08.	03:52	VVG	on ground	17° 16,023'	011° 43,444'	34
M157_24-6	31.08.	04:19	Dredge	on ground	17° 16,014'	011° 43,552'	32
M157_24-7	31.08.	06:23	MC	on ground	17° 16,013'	011° 43,437'	33
M157_24-8	31.08.	06:42	MC	on ground	17° 16,014'	011° 43,436'	33
M157_24-9	31.08.	07:54	Scanfish	profile start	17° 16,155'	011° 41,841'	62 / 419
M157_25-1	31.08.	14:11	CTD	max depth	17° 16,017'	011° 04,006'	1520
M157_25-2	31.08.	15:14	AC-S	max depth	17° 16,017'	011° 04,004'	1515
M157_25-3	31.08.	16:29	CTD	max depth	17° 16,017'	011° 04,005'	1517
M157_25-4	31.08.	17:55	BC	on ground	17° 16,016'	011° 04,006'	1523
M157_26-1	31.08.	20:45	BC	on ground	17° 16,020'	011° 08,998'	1101
M157_26-2	31.08.	22:14	CTD	max depth	17° 16,020'	011° 08,999'	1105
M157_26-3	31.08.	23:00	AC-S	max depth	17° 16,020'	011° 09,000'	1102

Station No.	Date 2019	Time (UTC)	Device	Action	Latitude (S)	Longitude (E)	Water Depth (m)
M157_27-1	01.09.	01:07	CTD	max depth	17° 16,014'	011° 16,496'	507
M157_27-2	01.09.	01:47	AC-S	max depth	17° 16,014'	011° 16,497'	508
M157_27-3	01.09.	02:23	BC	on ground	17° 16,013'	011° 16,494'	508
M157_28-1	01.09.	05:56	CTD	max depth	17° 16,016'	011° 30,058'	151
M157_28-2	01.09.	06:41	AC-S	max depth	17° 16,017'	011° 30,058'	152
M157_28-3	01.09.	07:07	VVG	on ground	17° 16,017'	011° 30,059'	151
M157_28-4	01.09.	07:27	VVG	on ground	17° 16,017'	011° 30,059'	151
M157_28-5	01.09.	07:48	VVG	on ground	17° 16,017'	011° 30,059'	145
M157_28-6	01.09.	08:12	Dredge	in water	17° 16,017'	011° 30,091'	151
M157_28-7	01.09.	09:21	MC	on ground	17° 16,014'	011° 30,067'	150
M157_29-1	01.09.	11:24	CTD	max depth	17° 15,721'	011° 43,026'	41
M157_29-2	01.09.	11:37	AC-S	max depth	17° 15,722'	011° 43,026'	41
M157_29-3	01.09.	11:46	VVG	on ground	17° 15,721'	011° 43,026'	42
M157_29-4	01.09.	11:58	VVG	on ground	17° 15,721'	011° 43,025'	40
M157_29-5	01.09.	12:10	VVG	on ground	17° 15,721'	011° 43,025'	40
M157_29-6	01.09.	12:25	Dredge	in water	17° 15,725'	011° 43,034'	41
M157_29-7	01.09.	13:43	MC	on ground	17° 15,729'	011° 43,024'	41
M157_30-1	01.09.	15:33	CTD	max depth	17° 20,387'	011° 36,120'	117
M157_30-2	01.09.	15:55	AC-S	max depth	17° 20,389'	011° 36,121'	117
M157_30-3	01.09.	16:12	VVG	on ground	17° 20,389'	011° 36,121'	117
M157_30-4	01.09.	16:26	VVG	on ground	17° 20,390'	011° 36,122'	116
M157_30-5	01.09.	16:43	VVG	on ground	17° 20,389'	011° 36,121'	119
M157_30-5	01.09.	16:47	VVG	on ground	17° 20,388'	011° 36,122'	115
M157_30-6	01.09.	16:58	Dredge	in water	17° 20,390'	011° 36,129'	117
M157_30-7	01.09.	17:29	Dredge	in water	17° 20,524'	011° 36,300'	118
M157_30-8	01.09.	18:11	MC	on ground	17° 20,613'	011° 36,380'	116
Transect at 23°S							
M157_16-25	03.09.	04:16	CTD	max depth	22° 59,998'	014° 13,010'	114
M157_14-18	03.09.	06:15	CTD	max depth	23° 00,023'	014° 03,005'	140
Transect at 25°S							
M157_31-1	03.09.	19:18	CTD	max depth	25° 00,002'	012° 59,836'	1803
M157_31-2	03.09.	20:18	AC-S	max depth	25° 00,001'	012° 59,835'	1805
M157_31-3	03.09.	20:33	MSS	in water	25° 00,013'	012° 59,828'	1801
M157_32-1	03.09.	22:42	MSS	in water	24° 58,970'	013° 11,526'	1373
M157_33-1	04.09.	02:38	MSS	in water	24° 59,265'	013° 22,359'	985
M157_34-1	04.09.	06:12	MSS	in water	24° 59,184'	013° 33,370'	603
M157_34-2	04.09.	07:30	MC	on ground	25° 00,001'	013° 32,947'	627
M157_34-3	04.09.	08:51	GC	on ground	24° 59,999'	013° 32,948'	626
M157_35-1	04.09.	10:51	MSS	in water	24° 59,056'	013° 38,836'	436
M157_36-1	04.09.	13:09	MSS	in water	24° 59,060'	013° 43,604'	509
M157_37-1	04.09.	15:31	MSS	in water	24° 59,277'	013° 49,174'	243
M157_38-1	04.09.	18:04	MSS	in water	24° 59,322'	013° 54,960'	186
M157_39-1	04.09.	20:00	MSS	in water	24° 59,170'	014° 06,169'	176
M157_40-1	04.09.	21:54	MSS	in water	24° 59,123'	014° 17,154'	165
M157_41-1	04.09.	23:28	MSS	in water	24° 59,024'	014° 22,678'	142

Station No.	**Date** 2019	**Time** (UTC)	**Device**	**Action**	**Latitude** (S)	**Longitude** (E)	**Water Depth** (m)
M157_42-1	05.09.	01:04	MSS	in water	24° 59,117'	014° 28,125'	122
M157_43-1	05.09.	02:59	MSS	in water	24° 59,280'	014° 33,638'	109
M157_44-1	05.09.	04:18	MSS	in water	24° 59,268'	014° 39,194'	89
M157_45-1	05.09.	05:39	MSS	in water	24° 59,279'	014° 44,706'	54
M157_46-1	05.09.	06:46	MSS	in water	24° 59,281'	014° 47,938'	32
M157_41-2	05.09.	09:41	GC	on ground	25° 00,001'	014° 22,647'	139
M157_41-3	05.09.	10:47	MC	on ground	25° 00,003'	014° 22,649'	139
M157_41-4	05.09.	14:04	VVG	on ground	25° 00,003'	014° 22,648'	139
M157_41-5	05.09.	14:57	VVG	on ground	25° 00,003'	014° 22,649'	139
M157_41-6	05.09.	15:15	VVG	on ground	25° 00,004'	014° 22,649'	139
M157_41-7	05.09.	15:43	Dredge	in water	25° 00,112'	014° 22,887'	141
M157_41-8	05.09.	17:45	Lander	deployed	25° 00,002'	014° 22,652'	140
M157_43-2	05.09.	19:31	CTD	max depth	25° 00,002'	014° 33,662'	106
M157_43-3	05.09.	20:04	AC-S	max depth	25° 00,002'	014° 33,663'	110
M157_43-4	05.09.	20:24	P-CTD	in water	25° 00,003'	014° 33,664'	107
M157_43-5	05.09.	21:35	MSS	in water	25° 00,003'	014° 33,664'	108
M157_43-6	06.09.	05:00	P-CTD	in water	24° 59,999'	014° 33,662'	104
M157_43-7	06.09.	08:52	VVG	on ground	25° 00,003'	014° 33,663'	107
M157_43-8	06.09.	09:07	VVG	on ground	25° 00,003'	014° 33,663'	107
M157_43-9	06.09.	09:21	VVG	on ground	25° 00,001'	014° 33,665'	105
M157_43-10	06.09.	09:41	Dredge	in water	25° 00,002'	014° 33,712'	109
M157_43-11	06.09.	10:48	MC	on ground	25° 00,006'	014° 33,669'	106
M157_43-12	06.09.	11:13	MC	on ground	25° 00,007'	014° 33,670'	106
M157_44-2	06.09.	12:50	CTD	max depth	24° 59,999'	014° 39,171'	83
M157_44-3	06.09.	13:15	AC-S	max depth	24° 59,998'	014° 39,170'	88
M157_44-4	06.09.	13:30	VVG	on ground	24° 59,999'	014° 39,171'	85
M157_44-5	06.09.	13:50	VVG	on ground	24° 59,998'	014° 39,170'	83
M157_44-6	06.09.	14:05	VVG	on ground	24° 59,999'	014° 39,171'	88
M157_44-7	06.09.	14:21	Dredge	in water	25° 00,011'	014° 39,188'	87
M157_43-13	06.09.	16:51	Lander	deployed	25° 00,005'	014° 33,662'	108
M157_34-4	06.09.	22:55	CTD	max depth	24° 59,992'	013° 32,936'	633
M157_34-5	06.09.	23:31	AC-S	max depth	24° 59,994'	013° 32,934'	626
M157_34-6	07.09.	00:22	BC	on ground	24° 59,993'	013° 32,936'	627
M157_36-2	07.09.	03:23	CTD	max depth	25° 00,002'	013° 43,968'	317
M157_36-3	07.09.	04:09	AC-S	max depth	25° 00,002'	013° 43,968'	317
M157_36-4	07.09.	04:29	VVG	on ground	25° 00,002'	013° 43,968'	317
M157_36-5	07.09.	04:59	VVG	on ground	25° 00,002'	013° 43,968'	317
M157_36-6	07.09.	05:31	VVG	on ground	25° 00,002'	013° 43,969'	317
M157_36-7	07.09.	06:00	Dredge	in water	25° 00,003'	013° 43,884'	318
M157_41-9	07.09.	10:09	Lander	at surface	24° 59,988'	014° 22,468'	137
M157_41-10	07.09.	11:07	MC	on ground	25° 00,022'	014° 22,644'	140
M157_41-11	07.09.	11:28	MC	on ground	25° 00,022'	014° 22,644'	141
M157_41-12	07.09.	12:11	GC	on ground	25° 00,022'	014° 22,643'	140
M157_41-13	07.09.	12:34	GC	on ground	25° 00,022'	014° 22,644'	140
M157_43-14	07.09.	13:53	GC	on ground	25° 00,004'	014° 33,855'	107

Station No.	**Date** 2019	**Time** (UTC)	**Device**	**Action**	**Latitude** (S)	**Longitude** (E)	**Water Depth** (m)
M157_47-1	07.09.	16:00	GC	on ground	25° 00,181'	014° 17,771'	161
M157_38-2	07.09.	19:18	CTD	max depth	24° 59,998'	013° 55,003'	186
M157_38-3	07.09.	19:45	AC-S	max depth	24° 59,997'	013° 55,010'	186
M157_38-4	07.09.	20:06	VVG	on ground	24° 59,997'	013° 55,010'	187
M157_38-5	07.09.	20:26	Dredge	in water	24° 59,997'	013° 55,038'	186
M157_39-2	07.09.	22:50	CTD	max depth	25° 00,010'	014° 06,165'	177
M157_39-3	07.09.	23:18	AC-S	max depth	25° 00,013'	014° 06,163'	177
M157_39-4	07.09.	23:34	VVG	on ground	25° 00,015'	014° 06,164'	176
M157_39-5	07.09.	23:50	VVG	on ground	25° 00,014'	014° 06,164'	187
M157_39-6	08.09.	00:05	VVG	on ground	25° 00,019'	014° 06,160'	177
M157_39-7	08.09.	00:19	VVG	on ground	25° 00,018'	014° 06,151'	176
M157_39-8	08.09.	00:33	VVG	on ground	25° 00,018'	014° 06,150'	177
M157_39-9	08.09.	00:46	Dredge	in water	25° 00,034'	014° 06,167'	177
M157_43-15	08.09.	06:02	Lander	at surface	25° 00,039'	014° 33,604'	105
M157_43-16	08.09.	08:46	MC	on ground	25° 00,000'	014° 33,671'	108
M157_43-17	08.09.	09:08	MC	on ground	25° 00,002'	014° 33,670'	105
M157_46-2	08.09.	12:12	Scanfish	profile start	25° 00,004'	014° 47,946'	34 / 1802
M157_41-14	09.09.	11:54	CTD	max depth	24° 59,997'	014° 22,647'	140
M157_41-15	09.09.	11:39	MSS	in water	24° 59,997'	014° 22,645'	140
M157_41-16	09.09.	12:37	AC-S	max depth	24° 59,999'	014° 22,647'	141
M157_41-17	09.09.	13:54	Lander	released	24° 59,999'	014° 22,648'	140
M157_41-18	09.09.	16:24	BTP	max depth	24° 59,998'	014° 22,706'	139
M157_41-19	09.09.	17:40	P-CTD	in water	25° 00,000'	014° 22,710'	139
M157_41-20	09.09.	18:27	MSS	in water	24° 59,998'	014° 22,707'	140
M157_41-21	09.09.	19:42	MSS	in water	24° 59,998'	014° 22,707'	140
M157_40-2	10.09.	03:32	CTD	max depth	24° 59,992'	014° 17,133'	163
M157_40-3	10.09.	04:10	AC-S	max depth	24° 59,993'	014° 17,134'	162
M157_48-1	10.09.	06:02	VVG	on ground	25° 00,275'	014° 12,391'	173
M157_48-2	10.09.	06:22	VVG	on ground	25° 00,274'	014° 12,390'	172
M157_48-3	10.09.	06:42	VVG	on ground	25° 00,272'	014° 12,391'	172
M157_48-4	10.09.	07:00	Dredge	in water	25° 00,290'	014° 12,399'	175
M157_48-4	10.09.	07:32	Dredge	on deck			173
M157_48-5	10.09.	07:57	MC	on ground	25° 00,353'	014° 12,319'	173
M157_39-10	10.09.	09:20	OFOS	max depth	25° 00,008'	014° 06,173'	177
M157_39-11	10.09.	09:51	Dredge	in the water	25° 00,025'	014° 06,190'	177
M157_42-2	10.09.	13:41	CTD	max depth	24° 59,984'	014° 28,161'	124
M157_42-3	10.09.	14:24	AC-S	max depth	24° 59,984'	014° 28,161'	123
M157_43-18	10.09.	15:39	Lander	deployed	25° 00,003'	014° 33,666'	105
M157_43-19	10.09.	16:23	CTD	max depth	25° 00,001'	014° 33,666'	104
M157_45-2	10.09.	18:05	CTD	max depth	25° 00,005'	014° 44,677'	52
M157_45-3	10.09.	18:31	AC-S	max depth	25° 00,006'	014° 44,679'	53
M157_45-4	10.09.	18:38	VVG	on ground	25° 00,005'	014° 44,678'	54
M157_45-5	10.09.	18:54	VVG	on ground	25° 00,006'	014° 44,681'	56
M157_45-6	10.09.	19:08	VVG	on ground	25° 00,005'	014° 44,678'	54
M157_45-7	10.09.	19:22	Dredge	in water	25° 00,012'	014° 44,693'	53

Station No.	**Date** 2019	**Time** (UTC)	**Device**	**Action**	**Latitude** (S)	**Longitude** (E)	**Water Depth** (m)
M157_46-3	10.09.	20:49	CTD	max depth	25° 00,009'	014° 47,987'	33
M157_46-4	10.09.	21:08	AC-S	max depth	25° 00,001'	014° 48,011'	32
M157_46-5	10.09.	21:15	VVG	on ground	25° 00,001'	014° 48,011'	33
M157_46-6	10.09.	21:25	VVG	on ground	25° 00,002'	014° 48,011'	33
M157_46-7	10.09.	21:33	VVG	on ground	25° 00,002'	014° 48,011'	33
M157_46-8	10.09.	21:40	Dredge	in water	25° 00,015'	014° 48,026'	33
M157_41-22	11.09.	05:50	MC	on ground	24° 59,997'	014° 22,719'	140
M157_41-23	11.09.	06:11	MC	on ground	24° 59,995'	014° 22,718'	140
M157_41-24	11.09.	06:34	Lander	at surface	25° 00,023'	014° 22,689'	141
M157_49-1	11.09.	08:42	MSS	in water	25° 05,038'	014° 30,353'	121
M157_49-2	11.09.	10:09	Mooring	released	25° 05,019'	014° 31,987'	113
M157_49-3	11.09.	11:04	CTD	max depth	25° 05,017'	014° 32,086'	113
M157_49-4	11.09.	11:33	AC-S	max depth	25° 05,017'	014° 32,087'	113
M157_44-8	11.09.	12:48	MC	max depth	25° 00,007'	014° 39,160'	85
M157_44-9	11.09.	13:28	P-CTD	in water	25° 00,007'	014° 39,159'	84
M157_44-10	11.09.	14:08	MSS	in water	25° 00,007'	014° 39,160'	85
M157_43-20	12.09.	07:03	BTP	max depth	25° 00,042'	014° 33,701'	109
M157_43-21	12.09.	08:38	Lander	at surface	25° 00,042'	014° 33,700'	103
Transect at 23°S							
M157_17-16	12.09.	19:28	CTD	max depth	23° 00,007'	014° 19,005'	76
M157_17-17	12.09.	19:57	AC-S	max depth	23° 00,008'	014° 19,006'	76
M157_17-18	12.09.	20:12	P-CTD	in water	23° 00,007'	014° 19,007'	76
M157_17-19	12.09.	20:50	MSS	in water	23° 00,008'	014° 19,006'	76
M157_17-20	12.09.	21:38	MSS	in water	23° 00,008'	014° 19,005'	77
M157_16-26	13.09.	03:34	CTD	max depth	22° 59,993'	014° 12,977'	113
M157_16-27	13.09.	04:09	AC-S	max depth	22° 59,999'	014° 13,003'	113
M157_16-28	13.09.	06:10	MC	on ground	22° 59,999'	014° 13,001'	113
M157_16-29	13.09.	06:28	MC	on ground	22° 59,998'	014° 13,002'	114
M157_2-9	13.09.	10:49	CTD	max depth	22° 59,988'	014° 22,014'	46
M157_2-10	13.09.	11:25	AC-S	max depth	22° 59,988'	014° 22,012'	46
M157_2-11	13.09.	11:42	P-CTD	in water	22° 59,988'	014° 22,013'	46
M157_2-12	13.09.	14:40	MSS	in water	22° 59,988'	014° 22,013'	46
M157_2-13	14.09.	09:00	Scanfish	profile start	23° 00,002'	012° 34,482'	47 / 2069

Abbreviations

Water column

AC-S In situ absorption spectrophotometer
BTP Benthic Trace Profiler for sampling the benthic nepheloid layer
CTD water sampling rosette equipped with sensors
Drifter Drifting sensor string for surface observations
Mooring anchored sensor chains for long- and short-term deployments
MSS Microstructure profiler for turbulence and mixing study
OFOS Ocean Floor Observation System
P-CTD Pump-CTD for ultra-high-resolution sampling
Scanfish towed undulating CTD for the upper water column

Benthic interface and sediments

BC Box corer
Dredge Trawl of chains to sampling biota and coarse material at the sea floor
GC Gravity corer (6-12 m steel tubing)
Lander Biogeochemical Observatories (BIGO-1/-2) for benthic in-situ measurements and sampling
MC Multiple corer (8 tubes)
VVG Van-Veen-Grab sampler for sediment surface samples

8 Data and Sample Storage and Availability

The ship's station list and all metadata from sampling and observations, including ship tracks, will be stored in the WDC MARE data base PANGAEA within 8 months after the expedition ends. The storage of the samples for subsequent investigations can be guaranteed by the MARUM, IOW and GEOMAR. All scientific data retrieved from observations, measurements and on-shore analyses would also be submitted to PANGAEA as soon as the data are published and/or assessed for quality. After a protection period of three years after the end of the cruise, all data would be freely available for the scientific community under the international Creative Commons (CC) data license of type CC BY 4.0 (https://creativecommons.org/licenses/by/4.0/). In particularly justified cases the release could be earlier. Surplus samples (if existing) will be provided to the scientific community on request.

Additionally, all hydrographic data gathered was stored on a data repository in the IOW immediately after the cruise. The processed and validated data were stored in the ODIN data base (https://odin2.io-warnemuende.de). According to the IOW data policy and to facilitate the international exchange of data, all metadata will be made available under the international ISO 19115 standards for georeferenced metadata.

Table 8.1 Overview of data availability

Type	Databases	Available	Free Access	Contact
CTD/PCTD data	ODIN + PANGAEA	01.03.2020	01.10.2022	martin.kolbe@io-warnemuende.de
MSS/ACS data		01.03.2020	01.10.2022	volker.mohrholz@io-warnemuende.de
VMADCP data		01.03.2020	01.10.2022	toralf.heene@io-warnemuende.de
Mooring data		01.03.2020	01.10.2022	volker.mohrholz@io-warnemuende.de
Macrobenthic ecological data		01.10.2020	01.10.2022	michael.zettler@io-warnemuende.de
Geomicrobiol. data		01.10.2020	01.10.2022	heide.schulz-vogt@io-warnemuende.de
Chemical data		01.10.2020	01.10.2022	bita.sabbaghzadeh@io-warnemuende.de gregor.rehder@io-warnemuende.de heide.schulz-vogt@io-warnemuende.de
Pore water data	PANGAEA	01.10.2020	01.10.2022	mzabel@uni-bremen.de fscholz@geomar.de ssommer@geomar.de
Geochem. sediment data		01.10.2020	01.10.2022	mzabel@uni-bremen.de fscholz@geomar.de

9 Acknowledgements

The overall very successful course of this expedition needs to be attributed to the friendly cooperation and very efficient technical assistance of Captain Detlef Korte, his officers and the whole crew. It was always obvious that all people on board worked on a common task. We would like to thank everybody involved, last but not least the Leitstelle METEOR Hamburg, among other things, for help with the currently quite complex procedure for obtaining work permits. The expedition was funded by the Federal Ministry of Education and Research (BMBF; 03F0814).

10 References

Bakun, A. (1990) *Science* 247: 198-201.

Currie, B., Utne-Palm, A.C. & Salvanes, A.G.O. (2018) *Frontiers in Marine Science* 5: 341

Diaz, J.D. & Rosenberg, R. (1995) *Oceanogr. Mar. Biol. Annu. Rev.* 33: 245-303.

Diaz, R.J. & Rosenberg, R. (2008) *Science* 321: 926-929.

Eisenbarth, S. & Zettler, M.L. (2016) *Journal of Marine Systems* 155: 1-10.

Emeis, K.-C., Brüchert, V., Currie, B., Endler, R., Ferdelman, T., Kiesling, A., Leipe, T., Noli-Peard, K., Struck, U. & Vogt, T. (2004) *Cont. Shelf. Res.* 24: 627-642.

Feike, J., K. Jürgens, J. T. Hollibaugh, S. Krüger, G. Jost & Labrenz, M. (2012) *ISME J.* 6: 461-470

Gallardo, V.A., Palma, M., Carrasco, F.D., Gutiérrez, D., Levin, L.A. & Cañete, J.I. (2004) *Deep-Sea Res.* II 51: 2475-2490.

Gülzow, W., Rehder, G., Schneider, B., Schneider von Deimling, J. & Sadkowiak, B. (2011) *Limnol. Oceanogr. Methods* 9: 176-184.

Grasshoff, K., Kremling, K. & Ehrhardt, M. (Eds.) (1999) *Methods of seawater analysis*, 3rd edn. Wiley-VCH, Weinheim, New York.

Hall, P.O.J. & Aller, R.C. (1992) *Limnology and Oceanography* 37: 1113-1119.

Helly, J.J. & Levin, L.A. (2004) *Deep-Sea Res. I* 51: 1159-1168.

Junker, T., Mohrholz, V., Siegfried, L. & van der Plas, A. (2017) *J. Mar. Sys.* 165: 36-46.

Levin, L.A. (2003) *Mar. Biol. Annu. Rev.* 41: 1-45.

Little, M.G., Schneider, R.R., Kroon, D., Price, B., Bickert, T. & Wefer, G. (1997) *Palaeogeogr. Paleoclimat. Palaeocl.* 130:135-161.

Neumann, A. Lahajnar, N. & Emeis K.-C. (2016) *Continental Shelf Research* 113: 47-61.

Noffke, A., Hensen, C., Sommer, S., Scholz, F., Bohlen, L., Mosch, T., Graco, M. & Wallmann, K. (2012) *Limnol. Oceanogr.* 57: 851-867.

Pfannkuche, O. & Linke, P. (2003) *Sea Technology* 44, 50-55.

Rykaczewski, R.R., Dunne, J.P., Sydeman, W.J., Gracía-Reyes, M., Black, B.A. & Bograd, S.J. (2015) *Geophys. Res. Lett.* 42(15): 6424-6431.

Schulz, H.N. & Jorgensen, B.B. (2001) *Annu. Rev. Microbiol.* 55: 105-137.

Sommer, S., Gier, J., Treude, T., Lomnitz, U., Dengler, M., Cardich, J. & Dale, A.W. (2016) *Deep-Sea Research I* 112, 113-122.

Sommer, S., Linke, P., Pfannkuche, O., Schleicher, T., Schneider v. Deimling, J., Reitz, A., Haeckel, M., Flögel, S. & Hensen, C. (2009) *Marine Ecology Progress Series* 382, 69-86.

Sommer, S., Türk, M., Kriwanek, S. & Pfannkuche, O. (2008) *Limnol. Oceanogr.: Methods* 6, 23-33.

Stramma, L., Prince, E.D., Schmidtko, S., Jiangang, L., Hoolihan, J.P., Visbeck, M., Wallace, D.W.R., Brandt, P. & Körtzinger, A. (2012) *Nature Climate Change* 2: 33-37.

Tengberg, A., Hovdenes, J., Andersson, H.J., Brocandel, O., Diaz, R., Hebert, D., Arnerich, T., Huber, C., Körtzinger, K., Khripounoff, A., Rey, F., Rönning, C., Schimanski, J., Sommer, S. & Stangelmayer, A. (2006) *Limnol. Oceanogr.: Methods* 4, 7-17.

Zettler, M.L. & Pollehne, F. (2013) In: Williams E. Fischer & Adams B. Green (eds.) *Upwelling: Mechanisms, ecological effects and threats to biodiversity*. Nova Science Publishers, Hauppauge NY: 35-58.

Zettler, M.L., Bochert, R. & Pollehne, F. (2009) *Marine Biology* 156: 1949-1961.

Zettler, M.L., Bochert, R. & Pollehne, F. (2013) *African Journal of Marine Science* 35: 283-290.

11 Abbreviations

AC-S	In-situ absorption spectrophotometer
ADCP	Acoustic Doppler Current Profiler
AFIS	Automatic Flow Injection Sampler
AFRICA	Automated Infra-Red Inorganic Carbon Analyzer
BC	Boxcorer
BIGO	Bio-Geochemical Observatory (Lander System)
BTP	Bottom Trace Profiler
BUS	Benguela Upwelling System
CTD	cluster of sensors which measure Conductivity, Temperature, and Pressure
DIC	Dissolved Inorganic Carbon
ECD	Electron Capture Detector
ESACW	East South Atlantic Central Water
EUC	Equatorial Under Current
GC	Gravity Corer
ICOS	Integrated Cavity Output Spectroscopy
IRMS	Isotope Ration Mass Spectrometry
MC	Multicorer
MESS	Mobile Equilibrator Sensor System
MSS	Microstructure profiler
NPOC	Non-Purgeable Organic Carbon
OFOS	Ocean Floor Observation System
OMZ	Oxygen Minimum Zone
POPs	Persistent Organic Pollutants
SACW	South Atlantic Central Water
SEC	South Equatorial Current
SECC	South Equatorial Counter Current
SEUC	South Equatorial Under Current
SSS	Sea Surface Temperature
SST	Sea Surface Salinity
TKE	Turbulent Kinetic Energy